Dissertation submitted to the Combined Faculties for the Natural Sciences and for Mathematics of the Ruperto-Carola University of Heidelberg, Germany

for the degree of

Doctor of Natural Sciences

presented by

Mag. Robert Hermann

born in Vienna, Austria

Oral examination: 28.02.2014

Dissertation

Regulation of Neural Progenitor Proliferation by ANKHD1

Mag. Robert Hermann

Referees:

Prof. Dr. Ana Martin-Villalba

Prof. Dr. Anne Régnier-Vigouroux

Abstract

During mammalian neural development, a wide variety of neurons and glial cells differentiate from common neural progenitor cells (NPCs). Postnatally, some of these cells transform to adult neural stem/progenitor cells which reside in specialized niches where they continue to produce neurons. The mechanisms controlling NPC fate, however, are not fully understood. Microarray analysis of ribosome-enriched transcripts in NPCs revealed a preferential loading of ribosomes with transcripts important for neuronal differentiation. One preferentially loaded transcript is Ankyrin repeat and KH domain-containing protein 1 (ANKHD1). ANKHD1 is a 270 kDa protein that has been shown to play important roles in progenitor cell proliferation, differentiation, and survival. Moreover, it was found to be deregulated in several cancers, including some leukemias. Due to its apparent role in progenitor cell regulation, ANKHD1 may also be an important functional regulator in NPCs. However, no function for ANKHD1 in the mammalian brain has been described so far.

The present project aims at elucidating the role of ANKHD1 in embryonic and adult neural progenitor cells in mice. We show that ANKHD1 is expressed throughout murine embryonic brain development and in adult neural progenitor cells. Expression can be detected as early as E12.5 and is robust during the course of cortical development. Selective knockdown of ANKHD1 via *in utero* electroporation in the developing neocortex promotes apical and basal progenitor proliferation and inhibits differentiation into neurons. This phenotype could be rescued by simultaneous overexpression of human ANKHD1. Similar to NPCs during development, knockdown of ANKHD1 in primary neurosphere cultures of adult NPCs promotes their proliferation and inhibits neuronal differentiation. Deregulation of embryonic and adult neural progenitor cells can lead to the development of brain cancers, such as glioblastoma multiforme. Accordingly, deregulation of ANKHD1 in glioma initiating cells influences their proliferative capacity. Together, these results substantiate the relevance of ANKHD1 for controlling proliferation and differentiation of neural progenitors.

Zusammenfassung

Während der Entwicklung des Nervensystems von Säugetieren differenzieren eine Vielzahl von Neuronen und Gliazellen aus gemeinsamen neuralen Vorläuferzellen (NPCs). Einige NPCs werden postnatal zu adulten neuralen Stamm- / Vorläuferzellen, die sich in spezialisierten Nischen befinden und weiterhin Neuronen produzieren. Die Mechanismen, die das NPC Schicksal kontrollieren sind nicht vollständig verstanden. Microarray Analysen von Ribosom-angereicherten Transkripten in NPCs haben gezeigt, dass Ribosomen bevorzugt mit Transkripten geladen werden, die wichtig für neuronale Differenzierung sind. Ankyrin repeat and KH domain-containing protein 1 (ANKHD1) ist eines dieser vorrangig geladenen Transkripte. Es spielt wichtige Rollen in der Regulation von Proliferation, Differenzierung und dem Überleben von Vorläuferzellen und kann in mehreren Krebsarten dereguliert sein. Aufgrund der Rolle von ANKHD1 bei der Regulierung von Vorläuferzellen, könnte es auch ein wichtiger Regulator von NPCs sein. Allerdings ist bisher noch keine Funktion von ANKHD1 im Säugerhirn beschrieben.

Das vorliegende Projekt untersucht die Rolle von ANKHD1 in embryonalen und adulten neuralen Vorläuferzellen. Wir zeigen, dass ANKHD1 während der gesamten murinen embryonalen Entwicklung des Gehirns, als auch in adulten neuralen Vorläuferzellen exprimiert wird. Die Expression kann bereits am Tag E12.5 nachgewiesen werden und bleibt im Verlauf der kortikalen Entwicklung robust. Selektiver Knockdown von ANKHD1 durch *in utero* Elektroporation im sich entwickelden Neocortex fördert die Proliferation von apikalen und basalen Vorläuferzellen und hemmt ihre Differenzierung in Neuronen. Dieser Phänotyp kann durch die gleichzeitige Überexpression von humanem ANKHD1 gerettet werden. Ähnlich wie in NPCs während der Entwicklung, führt ein knockdown von ANKHD1 in Primärkulturen von adulten, als Neurosphären wachsenden NPCs zu stärkerer Proliferation und hemmt die neuronale Differenzierung. Deregulierung von embryonalen und adulten NPCs kann zur Entstehung von Gehirntumoren, wie z.B. Glioblastoma Multiforme, führen. Wir konnten zeigen, dass eine Deregulierung von ANKHD1 in Glioma initiierenden Zellen ihre Proliferation beeinflusst. Zusammengenommen belegen unsere Ergebnisse die Bedeutung von ANKHD1 für die Steuerung der Proliferation und Differenzierung von neuralen Vorläuferzellen.

Acknowledgements

Over the past four years I have received support and encouragement from a great number of individuals. Foremost, I would like to express my sincere gratitude to my advisor Ana Martin-Villalba for giving me the opportunity to pursue my thesis work in her lab at the German Cancer Research Center, her continuous support and guidance. The road we traveled together so far surely was a bumpy one, but in the end we are still seated safely and moving forward on track.

I would like to thank my thesis advisors committee members Anne Régnier-Vigouroux and Jochen Wittbrodt for their support and suggestions throughout my PhD time as well as my examiners Gislene Pereira and Stephan Frings.

Enric, you have been a great colleague, but more importantly a great friend over the past four years, and I want to thank you for all the scientific input (and corrections of my thesis), the activities outside the lab, the great food we shared—even if it tasted like chicken, the many times you listend to my complains and those times we couldn't stop laughing.

Si, in the one year we now spent together in the lab you have become an very important person in my life. Without your motivation and corrections my thesis would be very different and for sure not finished yet. I want to thank you for the great time we have.

I want to thank Damian, Pak Kin Wilson Joao el Pakino Wacau from Macau Slow Lou, Gonzalo Gonolino, Georgios Georg Kalamari Cabronakis, Avni and Liang for your help as well as all the fun in and outside the lab. Damian, also thanks for correcting my thesis.

Special thanks to you Steffi, Carina, Katrin, Melanie, Tim, Dewi, Milos, Ting, Cedric, Robert, Marcin, Andreas, and Desiree for your great help in the lab throughout the years. Thanks to N. who always saw it.

Thanks to everyone from the Brainbros, Mustolinos and MBS, as well as Karin, Adriane, Benny, Melli, and Chris for making my time outside the lab so wonderful.

Stephan and Kathi, you have been there for me for so many years now. I want to thank you for being great friends throughout the good and bad times I have had. It all would have been very different without you.

I owe my deepest gratitude to my mother Marcela and my sister Anna-Marie for their unflagging love and support; this work would not have been possible without you. Mom, there are no words that could describe how thankful I am for your continuous support and all the possibilities it has brought to me. Anna-Marie, you are much more of a motivation and inspiration for me than you can imagine.

Thank you.

Contents

List of Figures

List of Tables

Abbreviations

A	anterior
ºC	degree Celcius
AEP	anterior entopeduncular area
Ascl1	Achaete-scute like 1
ANK	ankyrin
ANKHD1	Ankyrin repeat and KH domain-containing protein 1
ANR/CoP	anterior neural ridge / commisural plate
AP	apical progenitor
bHLH	basic-helix-loop-helix
BLBP	brain lipid binding protein
BP	Basal Progenitor
BrdU	bromodeoxyuridine
CAG	CMV enhancer, beta-actin, beta-globin promoter
CD95	cluster of differentiation 95
CGE	caudal ganglionic eminences
CMV	cytomegalovirus
CNTF	ciliary neurotrophic factor
CP	cortical plate
CPN	callosal projection neurons
CSW	corkscrew
CThPN	corticothalamic projection neurons
Cxh	cortical hem
D	dorsal
DIV	day in vitro
DG	dentate gyrus
Dll1	Delta-like ligand 1
DNA	Deoxyribonucleic acid
DEPC	Diethyl pyrocarbonate
DTT	Dithiothreitol
E	embryonic day
EDTA	2,2′,2″,2‴-(ethane-1,2-diyldinitrilo)tetraacetic acid
EGF	epidermal growth factor

ERK	extra- cellular signal regulated
FACS	fluorescence-activated cell sorting
FGF	fibroblast growth factor
fwd	forward
GBM	glioblastoma multiforme
GFAP	glial fibrillary acidic protein
GFP	green fluorescent protein
GIC	glioma initiating cell
GLAST	glial fibrillary acidic protein
GN	granule neurons
GW	gestational week
HBS	HEPES buffered saline
HBSS	Hank's balanced salts solution
HEPES	4-(2-hydroxyethyl)-1-piperazineethanesulfonic acid
HCl	hydrochloric acid
HEK	human embrionic kidney
Hes	Hairy and Enhancer of split
HIV	human immunodeficiency virus
HRP	horseradish peroxidase
IL-6	Interleukin-6
INM	interkinetic nuclear migration
ISH	*in situ* hybridization
IUE	*in utero* electroporation
IP	immunoprecipitation
IZ	intermediate zone
KH	K homology
L	lateral
LGE	lateral ganglionic eminences
LIF	leukemia inhibitory factor
M	medial
MADM	Mosaic Analysis with Double Markers
MASK	multiple ankyrin repeats, single KH domain
MCS	multiple cloning site
MEK	mitogen-activated

MgCl2	magnesium chloride
MGE	medial ganglionic eminences
$MgSO_4$	magnesium sulfate
NaCl	sodium chloride
Ncx	neocortex
Ngn	Neurogenin
NICD	Notch intracellular domain
NLS	nuclear localization signal
OPC	oligodendrocyte progenitor cells
ORF	open reading frame
P	posterior
PBS	phosphate buffered saline
PCR	Polymerase chain reaction
PDGF	platelet-derived growth factor
PFA	paraformaldehyde
qRT	quantitative real time
rev	reverse
RG	radial glia
RNA	Ribonucleic acid
RTK	receptor tyrosine kinase
SDS	sodium dodecyl sulfate
SEV	sevenless
SHH	sonic hedgehog
SHP2	Src homology phosphatase 2
SVZ	subventricular zone
Tbr2	T-box brain protein 2
TBS	Tris buffered saline
TLX	tailless
TN-C	tenascin
TNFR	tumor necrosis factor receptor
Tris	2-Amino-2-hydroxymethyl-propane-1,3-diol
V	ventral
VZ	ventricular zone
YFP	yellow fluorescent protein

1 Introduction

1.1 Function of stem and progenitor cells during development and adulthood

Multicellular organisms develop from pluripotent stem cells that are capable of generating all cell types of the organism. Often, more restricted pluri- and uni-potent stem cells remain after development to maintain tissues throughout life. The regulation of stem / progenitor cell activity is the basis of sustainable life for many organisms, including mammals. During development, regulation of progenitor identity, symmetric and asymmetric divisions, and differentiation properties is essential to generate – at the right time and at the appropriate place – the correct amount of differentiated cells.

In adult organisms, some tissues need constant progenitor activity to maintain their integrity and function. Examples for such are the blood system and intestine, were mature cells have short average life spans. Without constant generation of newly differentiated cells, these tissues would degenerate and stop providing essential life functions. Other tissues contain few or no stem / progenitor cells, and these are often found to be restricted to certain regions in the organ. In many of these previously referred to as "quiescent tissues", stem / progenitor cells were discovered during the last two decades and shown to be functionally relevant. One example of such a tissue is the mammalian brain, were most of the cells are post mitotic and remain functional throughout life. However, stem cell niches and regions where new cells are added to the system or replace other cells have been identified in recent years (see section 1.4.1). Moreover, in some tissues, progenitor cells can react to certain stimuli (such as injury) and accordingly change their proliferation and differentiation programs. For instance, bronchioalveolar stem cells in the lung proliferate during epithelial cell renewal [46], and progenitors in the brain can be activated – and change the fate of their progenies – following insults such as stroke or ischemia (see Nakafuku M [61] for reviews). However, also non-injury / tissue damage related changes do occur in progenitor cells. For instance, increase of neuronal output after physical activity (running [96] and learning [32]) has been reported. Besides their tissue repair, maintenance, and other physiological functions, stem / progenitor cells have been also connected to disease development, e.g. in cancer (see 1.4.2).

In line with the scope of the presented thesis, the following sections will discuss mammalian brain development in more detail, followed by short introductions of adult neurogenesis and the relation of neural progenitor cells (NPCs) to cancers in the brain.

1.2 Mammalian brain development

The mammalian brain is a remarkable organ, endowed with enormous processing power and fascinating capabilities. An average human brain consists of approximately 86 billion neurons of many thousand different types [6], which form approximately 100-500 trillion synaptic connections between them [21]. The other major cell type found in the brain are glial cells (astrocytes and oligodendrocytes) which are similarly abundant as neurons in humans[1]. Other cell types residing in the brain include ependymal cells, choroid plexus cells (which are modified ependymal cells that generate the cerebral spinal fluid), and microglia ("macrophages of the brain"). Moreover, immune cells can infiltrate the brain after injury and other stimuli (reviewed in Rezai-Zadeh et al. [69]).

In the following sections, mammalian brain development will be explained based on the mouse as a model organism. While many steps in mouse and human brain development are very similar and many basic mechanisms seem to be identical, it is obvious that some differences must be present to explain features of the brain unique to humans. Some of these have been described and studied while others are still poorly understood. For instance, the differences in the ratio of neurons to glial cells have been described [6], and the evolvement of a gyrencephalic brain in humans (i.e. their cortical layers form folded structures as consequence of a tremendous expansion of cell numbers) versus the lissencephalic brain of mice are currently studied. Nonetheless, many mechanisms studied and discovered in mice hold true for human brain development and are used as foundation to understand human brain function and development of disease treatment.

Development of the brain begins around gestational day 7.5 to 9.5 (E 7.5 to E 9.5) in mice (gestational week (GW) three in humans) with the emergence of the neural plate, and is a protracted process not completed until late adolescents [86]. First,

[1] Mice and other rodents have more neurons then glia

neuroepithelial cells are generated from the ectoderm to form the neural plate and followed by the neural tube. The most anterior part of the neural tube forms the brain, while the remaining neural tube develops into the spinal column. Three vesicle-like structures, the prosencephalon, mesencephalon, and rhombencephalon arise from the most anterior part of the neural tube at E10.5 in mice and E28 in humans, representing the basic structures from which the brain develops [86]. The prosencephalon, the embryonic precursor of the forebrain, will further subdivide into the telencephalon and diencephalon. The rhombencephalon subdivides into the metencephalon and myelencephalon, while the mesencephalon does not further subdivide. These five vesicles, aligned along the rostral-caudal axis of the embryo represent the primary organization of the central nervous system (CNS) [85].

1.3 Neural development in the mammalian forebrain

As mentioned above, the forebrain develops from the telencephalon and diencephalon. From the diencephalon the more posterior forebrain structures are formed, including the thalamus, subthalamus, hypothalamus and epithalamus [42]. The telencephalon on the other hand develops into the cerebrum, which consists of the cerebral cortex, hippocampus, basal ganglia, and olfactory bulbs. Basal ganglia mainly consist of (amongst other groups of nuclei) the striatum, globus pallidus, substantia nigra, nucleus accumbens, and subthalamic nucleus.

Within the cerebrum, the cerebral cortex forms the neocortex, archicortex (Hippocampus) and paleocortex. The neocortex accounts for approximately three quarters of human brain volume and is responsible for higher functions, such as conscious thought, language, and sensory perception. Evolutionary, it is the newest part of the cerebral cortex. It is built up of a six layered structure that is lissencephalic (i.e. ”smooth”) in mice, rats, and many other rodents, but is folded (i.e. has sulci and gyri) in primates and some other mammals, due to the massive expansion of neural precursor cells in these animals. The neocortex is apparently a distinguishing feature of mammals, responsible for the highest neural functions, and is the most studied structure of the brain. The work with embryonic neural progenitors (eNPCs) in this thesis is focused on the developing neocortex.

The structural foundations of the developing telencephalon are established by early

patterning events. Diffusible morphogens, released from signaling centers in and around the telencephalon instruct the antero-posterior and later dorso-ventral patterning of the telencephalon. The main signaling centers are the anterior neural ridge (later commisural plate; ANR/CoP), the cortical hem, the anti-hem (or pallial-subpallial boundary (PSB)) and the ventral signaling center (see Fig. 1 for an illustration of signaling centers and patterning). The main signaling molecules include various FGF ligands, BMPs / Wnt, and Sonic Hedgehog (SHH). For instance, FGF8 is produced rostrally in the ANR/CoP, while BMPs and Wnt are expressed caudally and dorsally in the cortical hem. FGF7 and TGF-a are produced in the anti-hem and SHH expression defines the ventral signaling center (see Götz and Sommer [35] and Iwata and Hevner [41] for reviews).

Expression of these signaling molecules in defined areas establishes unique gradient patterns. According to these gradients, expression of transcription factors in neuroepithelial cells, such as Pax6, Emx2, Coup-Tf1, and Sp8 is induced and regulated (Figure 1 B). The combinations of these transcription factor gradients ultimately lead to formation of the prospective area boundaries [41].

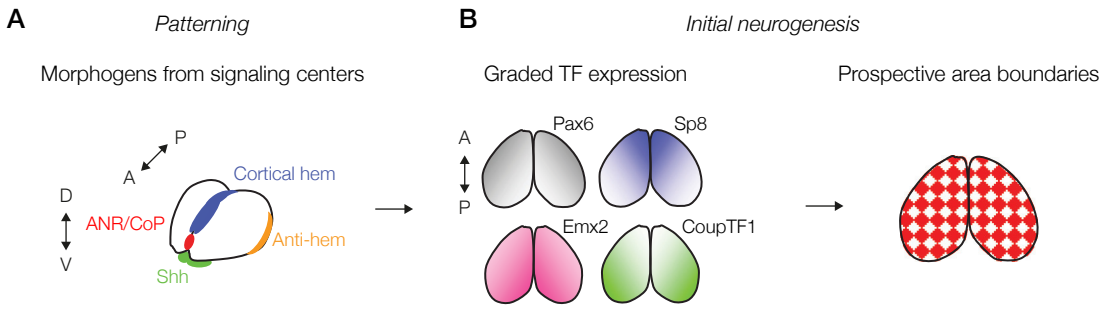

Figure 1: Patterning in the telencephalon. Modified from Iwata and Hevner [41]. Signaling centers (A) establish transcription factor (TF) gradients (B) which form prospective area boundaries. ANR/CoP = anterior neural ridge / commisural plate; Shh = Sonic Hedgehog; A = anterior; P = posterior; D = dorsal; V = ventral.

1.3.1 Neocortical development

At the onset of neocortical development, around E9-10 in the mouse [48], the entire ventricular zone (VZ) is a pseudostratified epithelium consisting exclusively of neuroepithelial cells [14]. These cells divide rapidly and symmetrically to expand their population pool, before their gradual transition into radial glia (RG) cells. RG cells

have their cell body located in the VZ, are in contact with the apical surface of the developing neocortex, and extend a radial fiber that reaches the pial surface [44]. RG start expressing astroglial markers, such as the astrocyte-specific glutamate transporter (GLAST), brain lipid-binding protein (BLBP), and Tenascin C (TN-C). Primate RG cells also express the intermediate filament protein, glial fibrillary acidic protein (GFAP), which, however, is absent in rodent and chick RG cells [10]. RG will give rise to all major cell types of the central nervous system, and are often referred to as the stem cells of the developing brain.

Neuroepithelial and radial glia cells display a complex mitotic behavior know as interkinetic nuclear migration (INM). INM is characterized by migration of the cell nucleus during the distinct phases of the cell cycle: Nuclei undergoing S phase form a layer away from the ventricle (still within the VZ, though), while nuclei in M phase are aligned at the ventricular surface [48]. The functional significance of this INM remains elusive.

RG cells divide mostly asymmetrically[2] to generate a wide variety of different neurons first, at later stages astrocytes and even later stages oligodendrocytes. Figure 2 shows a schematic representation of the temporary distinct, yet overlapping, phases of neuronal and glial differentiation in the mammalian neocortex. During each asymmetric division a RG cell produces a new RG cell (i.e. self renewal) and a neuron or basal progenitor (BP) cell[3], which can further divide symmetrically before final differentiation (Figure 3 illustrates symmetric and asymmetric divisions of RG and BPs during neocortical development). In this way, RG can specify during neocortical development to produce all the different neuronal subtypes, astrocytes, and oligodendrocytes. While fate-mapping and clonal experiments *in vitro* and *in vivo* [78] have revealed that RG cells can indeed be multipotent, more specified RG cells, giving rise to only neurons or glia, have also been observed [97] and it cannot be excluded that both types co-exist *in vivo*. Recent studies support the notion that RG cells might be heterogenous regarding their offspring producing capacities and fate potential. For instance, Franco et al. [28] identified Cux2 positive RG cells in the developing murine neocortex that are intrinsically specified to only give rise to upper layer neurons. Moreover, other types of RG, or RG like cells distinct from the

[2] symmetric divisions of RG have been described [62], but are rare and their relevance is unknown (they presumably produce two new RG cells [39])

[3] also known as intermediate progenitor cells or non-surface dividing cells

ones described above have been described. For instance, short neural precursors (SNP) were identified as morphologicaly distinct cells which are in contact with the ventricular surface with their apical process but possess basal processes that terminate in the VZ or sub-ventricular zone (SVZ, see below) rather then elongating to the pial surface [36]. Another type of RG reported are basal RG[4], which lack an apical process [36, 55, 66]. They are rarely found in mice, but more abundant in ferret and human neocortex. However, the link between gyrencephaly and bRG remains uncertain [36].

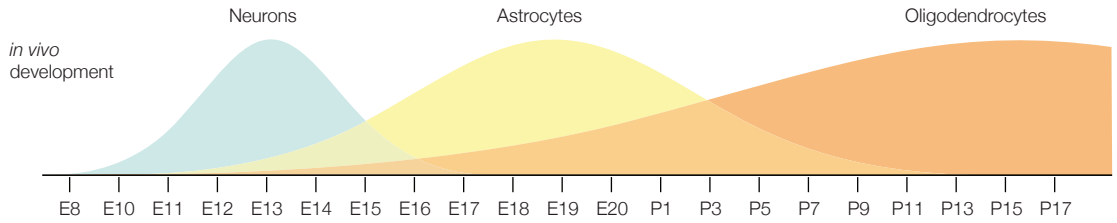

Figure 2: Timing of neuronal and glial development in the neocortex. Modified from Sauvageot and Stiles [75]. The waves of subsequent generation of neurons, astrocytes, and oligodendrocytes are illustrated in correlation to the time of embryonic (E8 – E20 [=birth]) and post-natal (P1 – P17) development.

Early in cortical development, asymmetrical divisions of RG lead to self renewal and generation of a post mitotic neuron. Throughout the majority of neocortical development, however, asymmetric RG division does not produce a post mitotic cell but rather a restricted progenitor cell that can further proliferate before final differentiation. These cells are referred to as intermediate or basal progenitors (IP or BP, respectively). They are characterized by certain morphological and molecular properties. BPs do not extend apical or pial processes to contact the ventricular or pial surface, respectively [48]. After their generation they populate a proliferative zone adjacent to the VZ, the so-called subventricular zone (SVZ). There, BPs proliferate one to two more times via symmetric divisions [48] and then differentiate into post mitotic neurons. This additional expansion of the progenitor pool allows to generate the enormous amounts of neurons populating the neocortex. BPs express many of the same markers as RGs, such as Nestin, but also distinct molecules, such as the T-box transcription factor Tbr2 [23, 37, 77].

Embryonic neural progenitor cells (eNPCs, i.e. RGs and BPs) become more restricted

[4] also called outer or intermediate RG

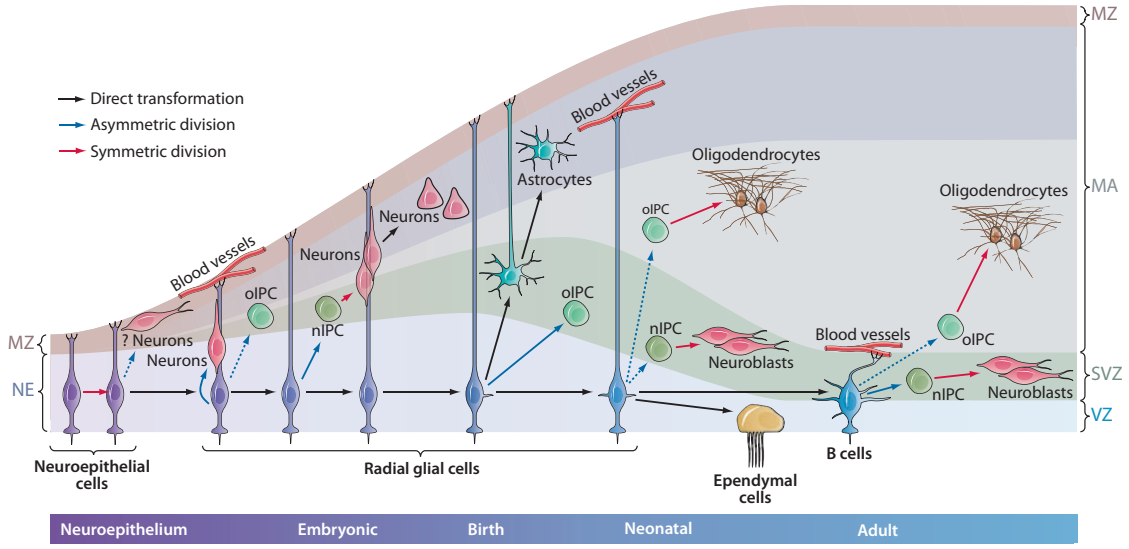

Figure 3: Modes of division of NPCs during neocortical development. Taken from Kriegstein and Alvarez-Buylla [48]. RG can divide symmetrically (red arrows) and asymmetrically (blue arrows), while other progenitors only divide symmetrically. NE = neuroepithelium; MZ = marginal zone; VZ = ventricular zone; SVZ = subventricular zone; MA = mantle zone; oIPC = oligodendrocyte intermediate progenitor cell; nIPC = neuronal intermediate progenitor cell.

as development proceeds. While RGs of the early developing brain are able to produce early and late born neurons (see below), RGs of later stages can only generate late born neurons. This multipotent capacity restricted by time of development was demonstrated with heterotransplant experiments [33]. However, the coexistence of multipotent and clonally more restricted progenitor populations is not excluded by these observations.

The first neurons to be generated during neocortical development form the preplate and differentiate to Cajal-Retzius and subplate neurons (SPN). Following waves of migrating neurons then split the preplate into the marginal zone and subplate. Cajal-Retzius cells form the outer most neuronal layer during development and are required for proper positioning of the following waves of neurons in the cortical plate (CP). The six layers of the CP (layer I – VI) are formed in an inside-out manner, i.e. newly differentiating neurons migrate through already established layers to form new ones on top. Hence, layer VI neurons are early born, while layer II/III neurons are late born. Figure 4 illustrates the development of the neocortex with its six neuronal layers in the CP, as well as other structures. After formation of the prelate, the next wave of neurons (born around E11.5) mainly contains layer VI corticotha-

lamic projection neurons (CThPN), followed by layer V subcerebral projection neurons (SCPN, born around E13.5), and layer IV granule neurons (GN, born around E14.5). Callosal projection neurons (CPN) which start being produced around E12.5 – concurrently with CThPN and SCPN – migrate to deep layers, while those born between E14.5 and E16.5 migrate to superficial cortical layers (see Greig et al. [33] for a review on neocortical projection neuron specification). Newly born neurons use various mechanisms to migrate to their final positions. During early development, they mainly use somal translocation to form the prelate. Later, the majority of neurons migrates along the pial extensions of RGs, that functions as a scaffold for them. During the final positioning neurons disattach from RG processes and again use somal translocation [48].

Beside excitatory neurons generated from RG in the neocortex, GABAergic interneurons generated from RG in the subpallium (ventral telencephalon) also populate the neocortex. Theses neurons arrive in the neocortex via various routes and emerge from distinct locations in the subpallium: First, around E11.5 in the mouse, tangentially migrating cells origin from the medial ganglionic eminences (MGE) and the anterior entopeduncular area (AEP). They migrate superficially to the striatum and invade the cortical marginal zone and subplate [56]. At E12.5 – E14.5, the MGE seems to be the principle source of these cells, and now a superficial, as well as a deep (i.e. closer to the ventricle) route is used by migrating cells to populate both the SVZ / lower intermediate zone (IZ) and the subplate. Later, around E14.5 – E16.5, cells that migrate tangentially into the neocortex seem to derive from both the lateral ganglionic eminences (LGE) and MGE and follow a deep route [56]. GABAergic interneurons in the neocortex are derived from cells that express Dlx genes, and other transcription factors important for subpallium specification, such as Nkx2.1 and Gsh2 [56].

After neurons for all six layers are generated, RG cells start transforming to astrocytes and later oligodendrocyte progenitors [48]. The first astrocytes emerge around E16 in the mouse neocortex, however, the majority is formed just before birth. After the last neurogenic divisions, RG disattach from the ventricular and pial surface and translocate towards the cortical plate. Some astrocytes generated from RG transformation undergo another round of symmetric division before final differentiation and thus represent an astrocyte intermediate progenitor (aINP). Interestingly, it seems like

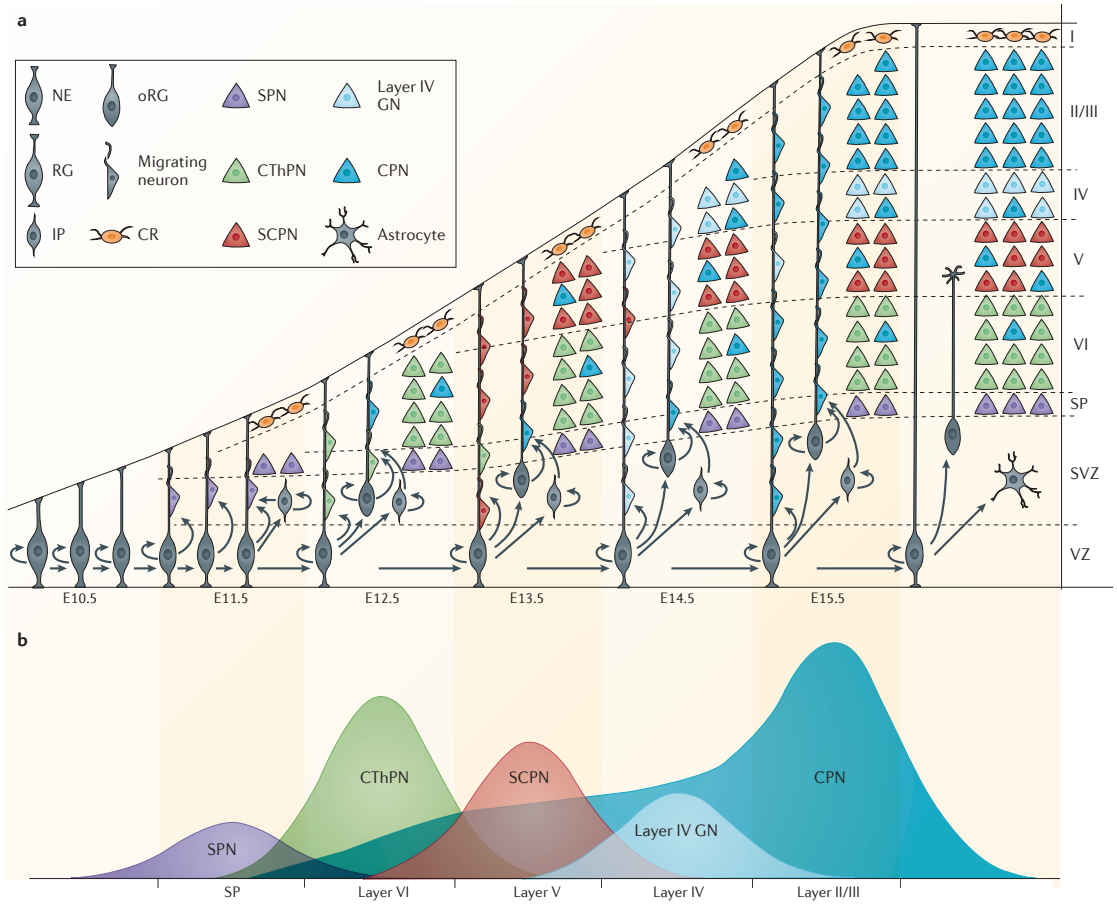

Figure 4: Neuronal subtype development in the neocortex. Modified from Greig et al. [33]. Timed generation of neuronal subtypes by radial glia (RG) and intermediate progenitors (IP) (a). Illustration of main production phases of various neurons (b). CR = Cajal Retzius cells, NE = neuroepethelial cells, RG = radial glia cells, oRG = outer radial glia cells, IP = intermediate progenitor (basal progenitor), SPN = sub plate neuron, CThPN = corticothalamic projection neuron, SCPN = subcerebral projection neuron, CPN = callosal projection neuron

also astrocytes populate the cortex in an inside out manner, similar to neurons (see above) [48]. The first oligodendrocytes arrive in the neocortex around E16 in the mouse. They are produced by Nkx2.1$^+$ precursor cells in the VZ of the medial ganglionic eminences (MGE) in the ventral telencephalon and migrate tangentially into the neocortex, similar to GABAergic neurons. Later, after E18, Emx1$^+$ precursors, presumably in the dorsal cortex itself, produce another wave of oligodendrocytes. Interestingly, most of the early born oligodendrocytes die after birth, leaving mainly Emx1 derived cells in the adult brain. Apart from neurons, astrocytes, and oligodendrocytes, RGs will differentiate to ependymal cells which are lining the ventricles and some RGs will remain in the adult brain to functions as adult neural stem / progenitor cells (see section 1.4.1).

1.3.2 Regulation of cortical development

Over the many decades of studying brain development, many key molecules and regulatory pathways crucial for proper NPC proliferation and differentiation have been identified. A complete review of the major signaling pathway discovered on brain development would be beyond the scope of this thesis. However, a brief summary of the most important and well studied molecules and pathways is given below, with emphasis on molecules known to be connected to ANKHD1 function.

As mentioned above, during early specification of the telencephalon, the main signaling molecules include the fibroblast growth factor (FGF) ligands, Wnts, bone morphogenic proteins (BMPs), and sonic hedgehog (SHH). These molecules are not only expressed in specific centers during telencephalic specification (see 1.3), but also function in other phases of neural progenitor differentiation and brain development. Other secreted molecules known to be involved in neocortical development include epidermal growth factor (EGF), platelet-derived growth factor (PDGF), as well as the interleukin-6 (IL-6) family of cytokines (including leukemia inhibitory factor (LIF) and ciliary neurotrophic factor (CNTF)).

The Notch signaling pathway plays a fundamental role in the regulation of neural progenitor cell development [14]. It is involved in numerous binary fate choices during differentiation of cells in the neocortex. For instance, active Notch signaling in a

cell inhibits differentiation from progenitors to neurons, from oligodendrocyte progenitor cells (OPCs) to oligodendrocytes, and promotes differentiation to astrocytes [54]. In mammals there are four receptors (Notch1–4), and five classical ligands (Delta-like1, 3, 4 and Jagged1, 2), all of which are transmembrane proteins that permit signaling between adjacent cells through direct contact. Upon activation of the Notch receptor a series of proteolytic events eventually release the intracellular domain, allowing it to translocate to the nucleus [54]. There, it associates with transcriptional co-regulators, such as CBF1/RBPjκ and mastermind, to activate gene transcription. Target genes of Notch signaling in the vertebrate nervous system are mainly the basic helix-loop-helix (bHLH) transcriptional repressors hairy and enhancer of split (HES) and HES related (HESR/HEY) family genes (especially Hes 1 and Hes 5) [54].

Basic helix-loop-helix transcription factors (bHLH TFs) are important regulators of brain development. Apart from the aforementioned repressor-type bHLH genes, a plethora of proneuronal bHLH TFs, including Neurogenin 1 and 2 (Ngn1, 2), Achaete scute-like 1 (Ascl1 / Mash1), atonal homolog 1 (Atoh1 / Math1), and hairy and enhancer of split 6 (Hes6), promote and guide differentiation into neurons. These pro neuronal bHLH factors dimerize with ubiquitously expressed bHLH genes, such as E47, and subsequently translocate to the nucleus where they bind to E-box sequences and activate transcription of target genes [44, 100]. Repressor-type bHLH factors inhibit neuronal differentiation in two ways: On one hand they repress transcription of pro neuronal genes by binding to N-box sequences and recruiting co-repressors like Groucho [43]. On the other hand, they dimerize with pro neuronal bHLH factors and thus prevent their transcriptional activity [44]. Recently, the NF-κB pathway was shown to be important for neural progenitor maintenance, at least in part through an antagonistic interaction with the proneuronal bHLH factor Hes6 [57].

Two main signaling pathways have been identified to be crucial for neuronal and glial differentiation: The proneural basic helix-loop-helix (bHLH) neurogenic pathway, and Janus kinase signal transducers and activators of gene transcription (Jak-Stat) gliogenic signaling [16]. As mentioned above, many bHLH factors are regulated directly or indirectly through Notch signaling. In addition, MEK-ERK (mitogen-activated or extra- cellular signal regulated protein kinase kinase and its target extra-

cellular signal regulated protein kinase) signaling promotes generation of neurons during telencephalic development [16]. The JAK-STAT pathway is mainly inactive during early phases of neocortical development, when neurons are generated. Activation of the JAK-STAT pathway is crucial for the switch to gliogenesis. Beside cell intrinsic mechanisms, cytokines acting through the gp130 receptor can activate JAK-STAT signaling.

Moreover, the nonreceptor protein-tyrosine phosphatase SHP2 was shown to be important in neural progenitor proliferation and fate decisions [16]. Interestingly, it can modulate not only the neurogenic (MEK-ERK), but also the gliogenic (gp130-JAK-STAT) signaling pathway by promoting MEK-ERK signaling while simultaneously inhibiting gp130-JAK-STAT signaling, respectively. In SHP2-deficient mice, the number of cells positive for the neuronal marker TuJI are reduced, and an increased in the number of cells positive for the astrocytic marker GFAP was observed [45]. Ke et al. [45] also found that SHP2 deficiency results in decreased proliferation of NPCs in the developing cerebral cortex.

1.4 Neural progenitors in the adult brain

After completion of development, neural progenitors persist in the adult organism. Their activity in the adult brain, however, varies significantly between species. For instance, birds retain RG like cells in their ventricular zones, and these cells proliferate and constantly add new neurons throughout most of the telencephalon [5]. In poikilotherms, widespread adult neurogenesis persists and is associated with constant brain growth [31]. In most animals studied to this day, however, the majority of NPCs are lost at the end of development, and neurogenesis in the adult is restricted to certain regions. In mammals, these regions are the SVZ of the lateral ventricles and the dentate gyrus of the hippocampus (see next section). However, cells with proliferative capacity and the ability to differentiate to certain cells types of the CNS have also been found outside of these regions. For instance, quiescent OPCs – presumably originate from embryonic and adult SVZ progenitors – are found throughout the brain and can be stimulated to divide symmetrically and to differentiate [70].

1.4.1 Adult neurogenesis in mammals

Neurogenesis in mammals was traditionally viewed to only occur during embryonic and perinatal development [60] and therefor no neuronal regeneration to be present in the adult brain. Pioneering work of Altman and colleagues in the 1960s and 70s provided first evidence for newly generated cells in the dentate gyrus of the hippocampus [4]. Following the introduction of the nucleotide analog bromodeoxyuridine (BrdU) as a lineage tracer for proliferating cells, lifelong neurogenesis in almost all mammals examined could be demonstrated [60]. First evidence for adult neurogenesis in humans stems from work by Eriksson et al. [25] in the late 1990s.

In the adult brain of mammals, neurogenesis persists in two regions: the subventricular zone (SVZ) of the lateral ventricles, and the dentate gyrus (DG) of the hippocampus. In both niches more quiescent stem cells give rise to a transit amplifying cell population which in turn produce neuroblasts that migrate to their destinations and differentiate to neurons.

In the SVZ, NPCs produce neuroblasts that migrate along the rostral migratory stream to reach the olfactory bulbs, where they differentiate into interneurons. NPCs in the SVZ are heterogeneous: According to their location in the SVZ they are restricted to give rise to certain neurons (e.g. NPCs in the dorsal SVZ generate superficial granule cells and tyrosine hydroxylase-positive periglomerular cells, while NPCs in the ventral SVZ generate deep granule cells and calbindin-positive periglomerular cells) [40].Transcription factor expression in the various regions of the SVZ resembles that involved in regional specification of the developing brain. Beside neurons, also oligodendrocytes are produced from SVZ NPCs, although to a much lower extend.

In the DG of the hippocampus, NPCs give rise to neurons and astrocytes, but only very few, if any, oligodendrocytes. The radial glia like NPCs are located in the subgranular zone of the DG, bordering the hilus of the hippocampus. They are multipotent [7, 8] and generally give rise to transit amplifying cells that differentiate into neuroblasts and finally dentate granule neurons. New neurons only migrate short distances, settling in the inner granule cell layer of the DG, where they are also functionally integrated (For in depth reviews on adult neurogenesis in the DG see Ming and Song [60], and Bonaguidi et al. [7]). Adult neurogenesis in the DG has been

shown to be important for several brain functions, such as learning and memory [18].

Both intrinsic and extrinsic mechanisms regulate different aspects of adult neurogenesis [60]. Many intrinsic signaling pathways are conserved from embryonic brain development, which is not surprising given the similarities between embryonic and adult NPCs. Extrinsic signals, however, can differ significantly due to the changed environment compared to the embryonic situation. Some of the conserved pathways include Notch, Wnts, BMPs, and SHH signaling. Transcription factors such as Pax6, Tbr2, Sox, or NeuroD are as well conserved and important regulators of adult NPCs function. Signaling mechanisms in adult neurogenesis are reviewed in depth by Faigle and Song [26]. Recent additions to signaling components in adult NPCs include the orphan receptor tailless (TLX) [80] and the tumor necrosis factor receptor superfamily member 6 (TNFRSF6 / Fas / CD95) [15]. Both proteins seem not to be required for NPC function during brain development, and thus represent a distinguishing feature of adult NPCs.

1.4.2 Neural progenitor cells and the origin of brain tumors

In the brain, cancers of many different types can arise following deregulation of cells due to mutations. Gliomas are the most common type of brain tumors, among which glioblastoma multiforme (GBM), are the most devastating and patients have a dismal prognosis.

Until recent years (the late 2000s) somatic mutations in differentiated cells were predominantly perceived as the origin of gliomas. However, in recent years, more and more evidence suggests that neural stem / progenitor cells might be the cells of origin for many tumors in the brain [reviewed in 2, 73, 98]. Adult NPCs use many of the signaling pathways deregulated in cancers. Discussing the cell of origin of brain tumors, it is crucial to discriminate between the cell in which the first oncogenic hit occurs and the cell that eventually has the capacity to develop to a tumor. For instance, an oncogenic hit may occur in a stem cell, but only a certain, more differentiated progenitor might have the ability to transform to a tumor. indeed, using lineage tracing by MADM, Liu et al. [53] have provided evidence for

this theories: They demonstrated that (i) oncogenic hits in progenitor cells are required for tumor initiation, and (ii) only OPCs (that either acquire the oncogenic mutations themselves or inherit them from aNPCs) can form gliomas in a p53 / Nf1 mouse model.

As a complementary *in vitro* approach to assess stem cell features, NPCs can be grown in so called ”neurospheres” in serum-free media supplemented with growth factors. Similarly, cancer cells from GBM patients have been isolated and grown in spheres under serum-free conditions. These sphere-cultures resemble those of ”normal” NPCs in many regards, can act as tumor-initiating cells, and establish tumors that closely resemble the main histologic, cytologic, and architectural features of the human disease, even when challenged through serial transplantation [30]. Taken together, there is strong evidence for a crucial role of aNPC in brain tumor development.

1.5 The Ankyrin repeat and KH domain-containing protein 1 (ANKHD1)

ANKHD1 is a recently discovered protein with important functions in organ development and tumor biology. The protein was first described in Drosophila by Smith et al. [84], where the homolog multiple ankyrin repeats and single KH domain (MASK) has been found to be an important signaling component in photoreceptor differentiation. One year later, the first study describing ANKHD1 in human cells was published by Poulin et al. [65]. The following sections will give an introduction to the protein and summarize findings regarding its functions in normal and neoplastic tissue. Naming of this protein in the literature is inconsistent. Throughout this thesis, and in compliance with the HUGO Gene Nomenclature Committee [90] for human genes, and the International Committee on Standardized Genetic Nomenclature for Mice [58], the protein will be referred to as ANKHD1. The name MASK will be used for the Drosophila protein [27].

1.5.1 Discovery, sequence properties, and structural features

In 2002, Smith et al. [84] identified the hitherto unknown protein MASK in a screen designed to study signaling components of the protein tyrosine phosphatase Cork-

screw (CSW, SHP2 in mammals) in Drosophila melanogaster. Cloning and sequencing revealed an approximately 13kb long open reading frame corresponding to the *mask* gene. The genomic locus of *mask* spans 18kb and encodes for a protein of 4001 amino acids, and a predicted mass of 423 kDa. The MASK protein contains known structural motifs: two blocks of ankyrin repeats and a single KH domain [84]. Both motifs are found in a large number of other proteins.

The ankyrin repeat (ANK) is one of the most common protein sequence motifs. It was discovered in 1987 by Breeden and Nasmyth [9], who reported a 33 residue repeating motif in the two yeast cell-cycle regulators, Swi6p and Cdc10p, and in the Notch and LIN-12 developmental regulators from Drosophila melanogaster and Caenorhabditis elegans [76]. Ankyrin repeats have been discovered in a myriad of proteins with various functions. A sequence homology analysis study, based on the non-redundant SMART protein database, has shown that there are 19276 ankyrin repeat sequences in 3608 proteins [76]. These ankyrin sequences have been detected in organisms ranging from viruses to humans, however most of them were found in eukaryotic proteins, located in both intra- and extracellular compartments. Ankyrin repeat proteins mediate protein–protein interactions and have been shown to be involved in many biological processes, including transcriptional regulation, cytoskeletal organization, modulation of cell cycle progression, cell development, and differentiation [52]. The ANK motif contains certain key residues which are conserved despite the degeneration of other repeating sequences. These patterns of conserved residues ensure structural integrity of the motif. For instance, three glycine residues are conserved at consensus positions 4, 15 and 27, and the characteristic Thr-Pro-Leu-His (TPLH) tetrapeptide motif forms a tight turn and initiates the first alpha-helix of the ANK repeat [76]. Ankyrin repeats exhibit a helix-loop-helix structure. The two alpha-helices are arranged in an anti-parallel fashion, and repeats are connected by beta hairpin motifs that project away from the helices in an nearly 90 degree angle [52].

The K homology (KH) domain was first discovered in – and named after – the heterogeneous nuclear ribonucleoprotein (hnRNP) K by Siomi et al. [83] in 1993. The motif is a conserved sequence of around 70 amino acids. The KH domain can bind RNA or single stranded DNA and is found in a myriad of proteins involved in a wide variety of biological processes, including splicing, transcriptional regulation,

and translational control [95]. All KH domains share a "minimal consensus motif" in their linear sequence, but their three dimensional structure can vary. Two types of KH domains have been described [34]: Type I domains form a beta-alpha-alpha-beta-beta-alpha structure, while type II domains consist of alpha-beta-beta-alpha-alpha-beta modules. All beta strands run anitparallel in type I domains, while two beta-strands run parallel in type II domains. Type I KH domains are usually found in eukaryotes, while type II domains are mostly found in prokaryotes [95]. The binding occurs in a cleft formed between alpha helix 1, alpha helix 2, the highly conserved GXXG loop, and a variable loop. The binding cleft can only accommodate four bases of the binding nucleotide. Proteins often contain multiple KH motifs, which can function independently or cooperatively [95]. However, some proteins only contain a single KH domain, including Mer1p, Sam68, and ANKHD1. Fragile X mental retardation protein (FMRP) contains two KH domains, and loss of function mutations therein have been associated with the fragile X mental retardation syndrome [51].

In addition to the ANK and KH domains, MASK contains several long stretches of glutamine residues and a highly basic region. MASK does not show significant homology in sequence or overall structure to any protein of known function [84].

Orthologs in mice and humans. In 2003, Poulin et al. [65] identified the human and mouse orthologs of MASK. Human ANKHD1 is located on chromosome 5q31.3, and mouse ANKHD1 is found on chromosome 18, in a region syntenic to human 5q31. Both proteins are highly similar to each other, and both contain two blocks of ankyrin repeats (25 repeats in total) and a single KH domain. These domains are strongly conserved compared to MASK, though the overall proteins are shorter in human and mouse. The canonical isoform of human ANKHD1 is translated from a 8139 bp long mRNA (consisting of a 5'-UTR of 60 bp, an ORF of 7629 bp, and a 3'-UTR of 450-bp) [65] and produces a protein of 2542 amino acids in length (mouse: 2548 aa). A schematic illustration of human full length ANKHD1 is shown in Fig. 5.

Several splice variants and isoforms of ANKHD1 have been described or annotated in protein databases. Poulin et al. [65] actually first discovered an interesting variant of ANKHD1, while working on 4E-BP3, a protein important for translational

Figure 5: The human ANKHD1 protein. Ankyrin repeats and KH domain are drawn in dark grey in correct proportion the complete sequence. Numbers indicate amino acid positions.

control, and located just downstream of the *Ankhd1* genomic locus. The authors showed that ANKHD1 and 4E-BP3 loci can produce a single, approximately 8.5 kb long transcript, that codes for a "fusion protein" of those two genes. Moreover, exon B from 4E-BP3 in this fusion protein is translated in an alternative reading frame. The resulting protein was designated MASK-BP3^{ARF} [65]. Both gene fusion and usage of alternative reading frames are rare in humans, and MASK-BP3 its the first instance were both mechanisms are utilized simultaneously. Miles et al. [59] identified two variants of ANKHD1 which both lack the KH domain and are significantly shorter, containing 627 or 435 amino acids. They were shown to bind to the HIV1 viral protein R (Vpr) and hence designated as Vpr-binding ankyrin repeat protein (VBARP) -L or -S, respectively. These variants seem to be involved in cell survival signaling through regulating caspases [59]. Duarte et al. [22] reported yet another splice variant of ANKHD1, which uses an alternative last exon (exon 10A). It is significantly shorter than the full length ANKHD1 and was reported to be upregulated to a higher extend than other splice variants during erythroid differentiation [22]. Finally, the protein database Uniprot [94] lists six isoforms for ANKHD1, one of which corresponds to VARBP-L.

ANKHD1 paralogs. One gene, Ankrd17, has been identified as paralog of ANKHD1 [65, 99]. Ankrd17, also known as gene trap ankyrin repeat (GTAR) [38] and sometimes referred to as MASK2 [74, 81], shows 71% homology to ANKHD1, and seemingly arose by gene duplication of ANKHD1[65]. Ankrd17 has been shown to be important for liver development as well as differentiation of hematopoeitic progenitors, and is essential for vascular integrity during embryogenesis. Homozygous knockouts for Ankrd17 are embryonic lethal at embryonic day 11 (E11) [38].

General expression pattern. ANKHD1 seems to be expressed ubiquitously in human and mouse tissues, though not many tissues have been thoroughly tested in experiments yet. So far, ANKHD1 mRNA expression was reported in several mammalian tissues, including the mouse brain [65]. Data from microarray analyses of differentiating aNPCs suggests that ANKHD1 might be expressed in these cells and regulated during their differentiation (unpublished data from our lab). Moreover, the protein has been detected in some human tissues and cell lines (see sections 4.2 and 4.8 for an in depth discussion of our findings on ANKHD1 expression and comparison to literature).

1.5.2 Known functions of ANKHD1 during development and in adult tissues

Currently, no studies investigating the role of mammalian ANKHD1 during development have been published. However, work in Drosophila shows the involvement of MASK in normal tissue development. Smith et al. [84] investigated many *mask* mutants for their phenotype. They concluded that *mask* is an essential gene because many homozygous and transheterozygous mutant animals die during first instar larval development. Work with non-lethal mutants further revealed that MASK is required for proper photoreceptor differentiation in the eye, as well as cell proliferation and survival. The mutagenesis screen in which *mask* was identified was designed to reveal novel components of receptor tyrosine kinase (RTK) signaling [84]. The authors showed genetic interaction of *mask* and RTK signaling components, such as Sevenless (SEV), corkscrew (CSW), and Ras. Their results suggest that MASK plays a positive role in transducing the signal downstream of receptor tyrosine kinases, such as EGFR. The importance of MASK for proper eye development was recently confirmed with different methods by two other groups [74, 81]. The same studies also revealed that MASK is required for normal wing development, as knockdown of *mask* resulted in smaller wings [74, 81]. Moreover, both studies showed that MASK is a co-factor of, and interacts with, YAP, a signaling component of the Hippo pathway important for tissue growth. This interaction was confirmed in human 293T cells. However, only Sidor et al. [81] could observe translocation of ANKHD1 to the nucleus and DNA binding, and thus a function as nuclear co-factor remains controversial. Given the conservation of the ANK and KH domains in mammals, it is tempting to speculate that ANKHD1 might play an important role in mammalian

organ development.

1.5.3 The role of ANKHD1 in cancer

In 2006, Traina et al. [92] reported a higher expression of ANKHD1 mRNA in primary acute leukemia samples compared to normal hematopoietic cells. Moreover, in the same study, increased levels of ANKHD1 mRNA and protein expression in leukemia cell lines was detected compared to normal hematopoietic cells. The human ortholog to Drosophila CSW, the nonreceptor protein-tyrosine phosphatase SHP2, was shown to be involved in many leukemias and to be overexpressed in many primary leukemia cells and in leukemia cell lines. Given the interaction of CWS and MASK in Drosophila, Traina et al. [92] investigated a possible interaction of SHP2 and ANKHD1. They successfully co-immunoprecipitated the two proteins in K562 and LNCaP cells. The functional relevance of this interaction in acute leukemias, however, remains elusive. In 2012, Dhyani et al. [19] reported that ANKHD1 is highly expressed in multiple myeloma patient cells and cell lines. Knockdown of ANKHD1 inhibited proliferation and delayed S to G2M cell cycle progression [19]. Furthermore, the authors observed an upregulation of cyclin dependent kinase inhibitor p21 – irrespective of the p53 status of the multiple myeloma cell lines – after ANKHD1 knockdown. Finally, low expression of ANKHD1 was correlated with significantly better relapse-free survival in two independent data sets of breast cancer patients [74]. However, the probe used in these data sets recognizes a sequence in the first ankyrin repeat block, and thus it is not clear which variant of ANKHD1 or even if the MASK-BP3 fusion protein are responsible for the correlation. Together, it is tempting to speculate that ANKHD1 plays an cancer promoting role when it is deregulated.

1.6 Aim of this thesis

ANKHD1 seems to be important for the regulation of progenitor cells in various tissues and is presumably expressed in the brain. Moreover, its transcript is preferentially loaded to ribosomes during neuronal differentiation of aNPCs. We thus hypothesized that ANKHD1 is expressed in embryonic and adult NPCs and might be important for their functional regulation. Furthermore, ANKHD1 might be deregulated in brain cancers, similar to the conditions in several leukemias.

The current project aims at elucidating the function of ANKHD1 during mouse neural development and in adult NPCs. First, we will investigate the expression of ANKHD1 in embryonic and adult NPCs, as expression of ANKHD1 in NPCs has not been proven hitherto. Unpublished microarray data from our work already suggests that its mRNA transcripts are present in NPCs. We will investigate mRNA and protein levels in embryonic and adult NPCS in various age groups to clarify its expression patterns.

To elucidate the role of ANKHD1 during neural development, we will use the *in utero* electroporation technique to perform loss- and gain of function experiments in the developing embryo brain *in vivo*. After knockdown or overexpression of ANKHD1 in radial glia cells we will assess how these cells and their progenies, i.e. basal progenitors and neurons, proliferate and differentiate with various methods and markers. Moreover, we will use primary cultures of isolated aNPCs to study the function of ANKHD1 in these cells.

Finally, the influence of ANKHD1 on glioma initiating cells will be assessed. Gliomas presumably originate from mutated NPCs and often have deregulated pathways which are important for NPC maintenance. We will use primary cultures of isolated glioma initiating cells to investigate how deregulated ANKHD1 levels can influence their proliferation phenotype.

2 Materials and Methods

2.1 Materials

2.1.1 Chemicals and reagents

Table 2: Chemicals and reagents

Chemical / reagent / kit	manufacturer
β-glycerophosphate	Sigma
β-mercaptoethanol	Merck
Acid-Phenol:Chloroform	Ambion
Acrylamide solution	Roth
Agarose	Sigma-Aldrich
Ammonium persulphate (APS)	Merck
B27 Supplement	Invitrogen
BCA kit	Thermo Fisher
bFGF	relia tech
Boric acid	Fluka
Brome phenol blue	Merck
Bromo-2-deoxyuridine (BrdU)	Sigma-Aldrich
Complete protease inhibitor	Roche
Diethyl pyrocarbonate (DEPC)	Sigma-Aldrich
dNTP mix (10 mM)	Fermentas
D(+)-Glucose	AppliChem
Dulbeco's Modified Eagles Medium (DMEM)	Invitrogen
DNAse	Roche
Dispase2	Roche
EGF	Promocell
Ethanol	Riedel de Haen
Eukitt (Corbit Balsam)	Hecht
Glycine	Sigma
Hank's balanced salts solution (HBSS)	Invitrogen
Ham's F12	Invitrogen
Heparin Cell Culture Grade	Sigma-Aldrich
HEPES	Sigma-Aldrich
Hoechst 33342	Biotrend
Hydrochloric acid (HCl)	VWR

Continued

Table 2: Chemicals and reagents

Chemical / reagent / kit	manufacturer
Isoflurane	Baxter
Ketavet (100 mg/ml)	Pfizer
L-Glutamine (100x L-Glutamine)	Invitrogen
Magnesium sulfate (MgSO4)	Sigma-Aldrich
mirVana miRNA Extraction Kit	Ambion
Mowiol	Calbiochem
Neurobasal A Medium	Invitrogen
Oligonucleotide primers	MWG
Paraformaldehyde (PFA)	AppliChem
4% Paraformaldehyde in phosphate buffer	Roth
1x PBS (without Mg2+ and Ca2+)	PAA
PCR buffer without MgCl2 (10x)	Applied Biosystems
PCR H2O	Braun
Papain	Sigma-Aldrich
Pellet Paint	Novagen, Merck
Penicillin Streptomycin	Invitrogen
Phenyl methyl sulfonyl fluoride (PMSF)	Sigma
P-nitrophenylphosphate	Merck
Potassium chloride (KCl)	Applichem
Potassium phosphate monobasic (KH2PO4)	Gerbu
Protein A/G PLUS-Agarose beads	Santa Cruz Biotechnology
RNase-free H2O	Ambion
RNeasy Mini Kit	Qiagen
Rompun (2%)	Bayer
Sodium dodecyl sulfate (SDS)	Roth
Sodium acide (NaN3)	Merck
Sodium acetate (C2H3NaO2; RNase free)	Ambion
Sodium chloride (NaCl)	Fluka
Sodium chloride 0.9% sterile (NaCl)	Braun
Sodium dihydrogen phosphate monohydrate (NaH2PO4)	Roth
Sodium fluoride (NaF)	Merck
Sodium hydroxide (NaOH)	Sigma
Sodium orthovanadate	Merck
Sodium phosphate dibasic heptahydrate (Na2HPO4 · 7H2O)	Sigma-Aldrich
Sodium pyrophosphate	Merck
Sodium pyruvate	Invitrogen

Continued

Table 2: Chemicals and reagents

Chemical / reagent / kit	manufacturer
Sodium tetraborate (Borax)	Merck
Subcellular Protein Fractionation Kit for Cultured Cells	Pierce
SuperFrost slides	Roth, Germany
Superscript III First-Strand Synthesis SuperMix	Invitrogen
SYBR® Green PCR Master Mix	Applied-Biosystems
TEMED	Sigma
Tools for mouse surgery	Fine Science Tools
Tris base	Sigma-Aldrich
Triton X-100	Sigma-Aldrich
Trypsin-EDTA (0.05%)	Invitrogen
Tween-20	Merck

2.1.2 Buffers and media

PBS, 20x Dissolve 160 g/l NaCl, 23 g/l Na_2HPO_4, 28.84 g/l NaH_2PO_4, 4 g/l KCl, 4 g/l KH_2PO_4 in H_2O. Adjust pH to 7.4 with HCl.

0.2M monobasic stock solution Dissolve 27,8 g/l NaH_2PO_4 in H_2O.

0.2M dibasic stock solution Dissolve 107,30 g/l $Na_2HPO_4 \cdot 7\,H_2O$ in H_2O.

0.2M Phosphate buffer Combine 69 ml of 0.2M monobasic and 231 ml of 0.2M dibasic stock solutions and adjust volume to 300 ml (pH 7.3) with H_2O.

aNPC / GIC medium Neurobasal A Medium supplemented with B27 Supplement (1x), L-Glutamine (2 mM), Penicillin/Streptomycin (Pen: 100 units/ml; Strep: 100 µg/ml), Heparin (2 µg/ml), bFGF (20 ng/ml), and EGF (20 ng/ml).

PDD-Solution Papain (0.01%), Dispase 2 (0.1%), DNAse (0.01%), MgSO4 (12.4 mM) in HBSS (without $MgCl_2$ and CaCl). The solution is sterile filtered and stored in aliquots at -20°C.

cell lysis buffer 25 mM Tris·HCl pH 8.0, 0.5 mM EDTA, 0.5% Triton X-100, 150 mM NaCl, 1 mM DTT and 1×*Complete Protease Inhbitor Cocktail*

IP wash buffer 25 mM TRIS pH 7.8, 200 mM NaCl, 0.5 % Triton X-100

PBS-Tween 0.1%Tween-20 in PBS.

Sample Buffer 125 mM Tris-HCl (pH 7.4), glycine (200 ml/l), β-mercaptoethanol (100 ml/l), SDS (40 g/l), brome phenol blue (50m g/l).

Running Buffer Tris base (10 g/l), glycine (30.28 g/l), SDS (150 g/l)

Transfer Buffer Tris base (3 g/l), glycine (14.4 g/l), methanol (200 ml/l)

Lower Tris Buffer (4x) Tris base (181 g/l), SDS (4 g/l), 37% HCl (135 ml/l)

Upper Tris Buffer (4x) Tris base (60.6 g/l), SDS (4 g/l)

Running Gel (per 10 ml) 3.5 ml H_2O, 2.5 ml Lower Tris Buffer, 4 ml of 30% Acrylamide, 10 µl TEMED, 100 µl of 10% APS

Stacking Gel (per 10 ml) 6.35 ml H_2O, 2.5 ml Upper Tris Buffer, 1.15 ml of 30% Acrylamide, 10 µl TEMED, 100 µl of 10% APS

Stripping Buffer 75 mM Tris-HCl (pH 6.8), SDS (12 g/l), β-mercaptoethanol (4.68 ml/l)

HBS 150 mM NaCl, 20 mM HEPES, pH 7.4

blocking solution 5% normal donkey serum , 0.1% Triton X-100, 0.5 mg/ml bovine serum albumin in HBS.

hybridization buffer Torula yeast tqRNA (1 mg/ml), Formamid (50%), 1x salt buffer, 10% dextran sulphate solution, 1x Denhardts solution. Mix in respective order and adjust volume with H_2O. Store at -20ºC.

10x salt buffer 114 g/l NaCl, 14.04 g/l Tris HCl, 1.34 g/l Tris Base, 7.8 g/l $Na_2HPO_4 \bullet 2\ H_2O$,7.1 g/l NaH_2PO_4, 18.61 g/l EDTA. Dissolve in H_2O.

100x Denhardts solution 20 mg/ml BSA, 20 mg/ml Ficoll, 20 mg/ml polyvinylpyrollidone. Dissolve in H_2O and store at -20ºC.

Dextrane sulfate solution Dissolve 0.5 g/ml in H_2O, store at 4ºC.

ISH wash solution 1xSSc, 50% form amide, 0.1% Tween20 in water.

5x MAB buffer 58 g/l maleic acid, 43.5 g/l NcCl, 38.5 g/l NaOH in water. Adjust pH to 7.5 and filter sterile.

MABT buffer Dilute 5x MAB buffer to 1x and add 0.1% Tween20.

2% DIG-blocking reagent Dissolve 4 g DIG-block in 200 ml MABT (heating required). Aliquot and store at -20ºC.

ISH staining buffer 100 mM NaCl, 50 mM $MgCl_2$, 100 mM Tris pH 9.5, 0.1% Tween20, and 1 mM (appr.) Levamisol in water (prepare fresh).

FP buffer 5% FCS in PBS.

SFP buffer 0.1% Saponin, 5% FCS in PBS.

2.1.3 Plasmids

The pCAG-YFP plasmid was obtained from Addgene. Human ANKHD1 open reading frame cDNA was purchased from *'Thermo Scientific Open Biosystems ORFeome Collaboration Clones and Collections'* in a pENTR223.1 plasmid and sub-cloned into the pFlag-CMV-D11 plasmid using the gateway cloning system according to the manufacturers instructions. The resulting plasmid was termed pFlag-ANKHD1.

The human ANKHD1 ORF was further sub-cloned into the pCAG-YFP vector to generate the N-terminal tagged fusion protein. Conventional cloning methods (i.e. restriction enzyme digest, T4 polymerase ligation) were used due to lack of gateway compatible recipient vector. First, a new cloning site was inserted at the end of the YFP (removing the stop codon) in the pCAG-YFP plasmid. This new site (MCS2) contains a NotI and downstream XhoI restriction site. The modification was introduced by cutting pCAG-YFP with BsrGI and NotI, and ligating a short sequence of annealed synthesized oligomeres with appropriate 5′ overhangs and containing the required restrictions sites. The NotI site used in this step was removed by altering bases in the oligomers. Next, the ANKHD1 insert was cut out of pENTR223.1 using NotI and SalI restriction sites and inserted into the MCS2 of the newly generated pCAG-YFP plasmid cut with NotI and XhoI. This way ANKHD1 was inserted in frame on the C-terminal side of YFP, generating a fusion protein. This construct is hereafter referred to as pCAG-YFP-ANKHD1.

A C-terminal truncated form of ANKHD1 lacking the KH domain was generated as follows. First, the pFlag-ANKHD1 plasmid was cut with PsyI and SalI to remove the C-terminus containing the KH domain and stop codon. Then synthesized oligomere containing a stop codon was and appropriate 5′ overhangs was inserted and ligated, resulting in the pFlag-ANKHD1-ΔC plasmid.

A summary of all cloned and used plasmids is shown in table 3.

Table 3: Plasmids

Name	Description / source
pCAG-YFP	Addgene
pFlag-CMV-D11	gateway destination vector with N-terminal Flag tag, DKFZ repository
pFlag-ANKHD1	human ANKHD1 cloned into pFlag-CMV-D11
pFlag-ANKHD1-ΔC	truncated ANKHD1 on C-terminus, KH domain missing
pYFP-ANKHD1	human ANKHD1 cloned into pCAG-YFP, generating YFP tagged protein

2.1.4 Antibodies

Primary and secondary antibodies are described in table 4 and 5, respectively.

Table 4: Primary antibodies

Name	Species	Clonality	Manufacturer	Concentration
Actin	goat	polyclonal	Santa Cruz	1:5000 (WB)
Akt	rabbit	polyclonal	Cell signaling	1:1000 (WB)
Ankhd1	rabbit	polyclonal	Sigma	1:1000 (WB), 1:200 (IP)
Erk	rabbit	polyclonal	Santa Cruz	1:1000 (WB)
Flag	mouse	monoclonal	Sigma	1:1000 (WB)
GAPDH	mouse	monoclonal	Santa Cruz	1:1000 (WB)
GFP	chicken	monoclonal	Aves	1:1000 (WB), 1:200 (IP)
p21	mouse	monoclonal	Cell Signaling	1:500 (WB)
pAkt	rabbit	polyclonal	Cell signaling	1:1000 (WB)
pErk	rabbit	polyclonal	Santa Cruz	1:1000 (WB)
Satb2	mouse	monoclonal	Abcam	1:200 (IF)
Tbr2	rabbit	polyclonal	Abcam	1:500 (IF)

Table 5: Secondary antibodies

Name	Manufacturer	concentration
goat anti chicken Alexa 488	Dianova	1:500 (IF)
goat anti rabbit Alexa 568	Dianova	1:500 (IF)
goat anti mouse Alexa 633	Dianova	1:500 (IF)
donkey anti goat HRP conj.	Santa Cruz	1:5000 (WB)
goat anti mouse HRP conj.	Dianova	1:5000 (WB)
goat anti rabbit HRP conj.	Dianova	1:5000 (WB)

2.2 Methods

2.2.1 Animals

Animals were housed in the animal facilities of the German Cancer Research Center (DKFZ) at a twelve-hour dark/light cycle and had free access to food and water. All animal experiments were performed in accordance with institutional guidelines of the German Cancer Research Center and were approved by the Regierungspräsidium Karlsruhe, Germany (G-120/12).

2.2.2 Cell culture

Cell lines. Human embryonic kidney (HEK) 293 and K562 (immortalised myelogenous leukemia line) cells were grown in Dulbecco's Modified Eagle's Medium (high glucose), supplemented with 10% fetal bovine serum, 2 mM Glutamine and antibiotics (Penicillin and Streptomycin, 10,000 U/ml and 10 mg/ml, resp.) at 37 °C and 5% CO_2. Cells were routinely passaged by washing with phosphate-buffered saline (PBS), treatment with 0.05 % Trypsin-EDTA solution for one to two minutes at 37°C and following resuspension in culture medium.

Isolation and culture of aNPCs. For isolation of primary aNPCs, mice were sacrificed and tissue from the SVZ was dissected into ice-cold HBSS supplemented with 1% Penicillin-Streptomycin. Tissue was cut in small pieces with a scalpel and washed three times with HBSS/Pen/Strep. Subsequently tissue was digested in PDD-solution at room temperature for 30 minutes. After digestion, cells were washed three times in DMEM/F12 (50% DMEM, 50% Ham's F12, and 1% L-Glutamine) and subsequently triturated using flame-polished Pasteur pipettes. Cells were afterwards cultured in aNPC medium as neurospheres in 25 cm^2 flasksat 37°C and 5% CO_2. Cells were passaged once to twice weekly.

Isolation and culture of GICs. Patient derived tumor samples were dissociated into single cells and selectively grown for several passages as non-adherent spheroids (tumorspheres) in aNPC/GIC medium. Cell were grown in 25 cm^2 or 75 cm^2 flasks at

37°C and 5% CO_2. For experiments with human recombinant CD95L (T4) treatment, cells were seeded at a density of 1x10^6 cells/well in 6-well culture plates. The cells were then treated with 10 or 40 ng/ml human recombinant CD95L (T4) at indicated time points.

2.2.3 Transient transfection of cultured cells

Electroporations of aNPCs and GICs were performed with the Neon Transfection System. Prior to electroporation, neurospheres or tumorpsheres were dissociated into single cells, counted, resuspended in R buffer to a cell density of 0.5-1x10^6 cells/100 µl, and mixed with siRNA or plasmid DNA. We used ON-TARGETplus SMARTpool siRNAs from Thermo Scientific. Each pool consists of four siRNAs targeting either human *ANKHD1* or non-targeting sequences. The specific sequences are shown in table 6. The following plasmids were used: YFP tagged Ankhd1 plasmid (YFP-Ankhd1), Flag tagged Ankhd1 plasmid (Flag-Ankhd1), or a plasmid with Flag tagged Ankhd1 that lacks the C terminal KH domain (Flag-Ankhd1ΔC). EYFP plasmid was co electroporated to assess electroporation efficiency by flow cytometry. The siRNA was used at a concentration of 0.5 µM, and plasmids at 1 µg / 100 µl reaction. Electroporation conditions were as follows: 1700mA, 20ms, 1 pulse for tumorshperes and 2 pulses (30ms width) of 850V for neurospheres. Electroporated cells were transferred into 6 well plate containing appropriate growth media, and incubated at 37°C, 5%CO2.

Table 6: siRNA target sequences

Description of siRNA	Sequence
human ANKHD1 1	AGAAGGAGCAGACTTACGCACTGTGGATC
human ANKHD1 2	AGAAGGAGCAGACTTACGCACTGTGGATC
human ANKHD1 3	AGAAGGAGCAGACTTACGCACTGTGGATC
human ANKHD1 4	AGAAGGAGCAGACTTACGCACTGTGGATC
mouse ANKHD1 1	CCAAUGGGCCUGCCGAUUU
mouse ANKHD1 2	GUCACAAUCUGUCAUAGGA
mouse ANKHD1 3	GCACGUGGGCACCUCAUAU
mouse ANKHD1 4	GAAUGGUAGCUCCCACUAA
non-targeting sequence 1	UGGUUUACAUGUCGACUAA
non-targeting sequence 2	UGGUUUACAUGUUGUGUGA
non-targeting sequence 3	UGGUUUACAUGUUUUCUGA
non-targeting sequence 4	UGGUUUACAUGUUUUCCUA

2.2.4 *In utero* electroporation

In utero electroporation was carried out as described by Saito [72]. Briefly, timed pregnant C57BL/6 wild type mice were anesthetized with 3% isofluoran / 1.5 vol% O_2, and anesthesia was maintained with 0.5 - 1.5% isofluoran / 1.5 vol% O_2/min. Uterine horns were exposed by midline laparotomy and constantly wetted with warm sterile physiological saline. Embryos were injected with 1 - 2 µl of desired DNA plasmids and / or siRNA mixed with 0.03% Fast Green with the help of heat pulled glass capillaries (bevelled at 30º with an inner diameter of appr. 75-100 µm). Five electric square wave pulses (40V, 50ms duration, 950ms interval) were applied with Tweezertrodes positioned outside of the uterine muscle at approximately 45º respective to the interaural line of the embryo. Uterine horns were replaced within the abdomen and abdominal muscle and skin incisions were closed with sutures. Mice were allowed to recover at 37°C for approximately 15 minutes.

If embryos were used for analysis 24 or 48 hours post *in utero* electroporation, dams were sacrificed and embryos dissected from uterine horns, yolk sac, and amnionic sac, followed by decapitation. Embryo heads were transferred into ice cold PBS and subjected to fixation and cryo-protection (see 2.2.6), or dissection of cortical tissue (see 2.2.5). For studying post natal pups, dams were allowed to give birth (day P0) and pups were sacrificed at P2 by decapitation, without prior perfusion. Heads were then fixed in 4% PFA solution over night before subjected to cryopreservation, cutting and immuno fluorescence staining (see 2.2.6 and 2.2.7).

2.2.5 Dissection of dorsal telencephalic tissue and FACS

Heads of E16.5 embryos were placed in a dish filled with ice-cold HBSS and fixed with needles so that the posterior part touched the bottom of the well and the head was slightly angled to the ventral side. Skin and bone tissue was removed by incisions in a horizontal line above the eyes, followed by pulling away of tissue to the back. Minenges were carefully removed by taking hold of it at the ventrolateral side and slow pulling towards the midline from both sides. The now exposed dorsal telencephalic cortices were dissected, discarding the olfactory bulbs and cortical hem. Tissues from litter-mates were collected in ice-cold eNPC medium and single cell suspension produced by carefully pipetting up and down ten times with a

200 µl pipette. Samples were then subjected to sorting for YFP positive cells with a FACSAria II with a 100 µm nozzle. Cells were sorted into RNA lysis buffer for later isolation of total RNA.

2.2.6 Preparation of cryostat sections from mouse embryo brains

Embryo heads were washed twice with PBS followed by fixation with 4% PFA solution for four hours. PFA was rinsed twice with PBS before incubation in 30% sucrose / PBS overnight or until heads sunk to the bottom of the well. Heads were then shortly put in OCT solution, before placement on specimen disks and fast freezing in the cryostat chamber. Following freezing, 15 µm thick sections in coronal orientation were prepared from the area of interest. Sections were attached to SuperFrost Plus object slides, dried at room temperature for approximately 30 minutes, and stored at -20°C until used for immuno fluorescencestaining.

2.2.7 Immunofluorescence staining on cryostat cut sections

For immunohistochemical analysis, cryostat cut sections were rinsed twice in HBS and then incubated for one hour in blocking solution. Sections were then incubated for two hours at room temperature or over night at 4°C in blocking solution containing primary antibodies (see table 4). Following incubation with primary antibodies, sections were washed in blocking solution twice for five minutes, followed by incubation with the appropriate secondary antibodies (see table 5) and Hoechst 33342 (1:3000) for one hour at room temperature. Sections were then washed twice with blocking solution and three times with PBS, mounted with Fluoromount-G, and allowed to dry at room temperature for 30 minutes. Stained and mounted slides were stored at 4°C in the dark until imaging. Images were acquired with a Leica SP5 confocal microscope at the DKFZ microscopy core facility with a 20x objective and images were processed with Fiji (ImageJ), and Adobe Photoshop software.

2.2.8 Neurosphere cell staining for flow cytometry

Neurospheres were harvested and dissociated with Accutase for three minutes at 37ºC. Cells were washed once with FP buffer, fixed in 4% PFA for five minutes on ice,

followed by blocking and permeabelization with SFP buffer for 30 minutes. Cells were then stained with primary antibodies for 45 minutes on ice, washed twice with SFP buffer, and incubated with secondary antibodies for 30 minutes on ice. Finally, cells were washed twice with FP buffer and resuspendend in 200 µl FP buffer for flow cytometry. Fluorescence data were obtained with a FACSCanto II (BD Biosciences) and analyzed using FlowJo software.

2.2.9 *In situ* hybridization

In situ hybridization was performed with DIG labeled probes as follows. ANKHD1 sense and antisense riboprobes were DIG labeled by *in vitro*transcription of cDNA encoding for their respective sequences, using the DIG RNA Labeling Kit (SP6/T7) from Roche. The riboprobe for ANKHD1 was transcribed from a plasmids containing a sequence covering exons 33 and 34 (see Fig. 7). The sequences used to clone the ANKHD1 fragment used to generate the riboprobe were `5'-CCCAAGCTTAACAGTGC-CAGTCAGGATCG-3'` for the forward primer and `5'-CCCGGATCCTCCAATATGAGGTG-CCCACG-3'` for the reverserse primer.

Cryostat cut sections from E13.5 embryos were hybridized with digoxigenin-labeled riboprobes as follows: Sections were permeabelized with PBS-Tween for 30 minutes at room temperature and pre-hybridized by incubation in hybridization buffer for one hour at 68ºC. DIG labeled probes were diluted 1:500 in hybridization buffer and denatured for 10 minutes at 70ºC, followed by quick cool on ice for two minutes. Sections were incubated with hybridization buffer containing probes i a wet chamber at 68ºC over night. The next day, slides were washed with pre-warmed (68ºC) ISH wash solution for three times 30 minutes, followed by two times 30 minutes washes with MABT buffer, all shaking. Section were blocked with DIG-blocking reagent for one hour at room temperature, followed by anti-DIG antibody (1:2000 in DIG-blocking reagent) incubation for four hours at room temperature, or at 4ºC over night. Sections are then washed four times in MABT and five minutes in staining buffer before incubation with staining buffer containing NBT (4.5µl/ml) and BCIP (3.5µl/ml) in the dark at room temperature or 4ºC, until signal becomes visible. Sections were mounted with Eukitt mounting medium.

2.2.10 EdU incorporation assay

To measure proliferation of cells we used Click-iT® EdU incorporation assays from life technologies. EdU was added to cultured cells at a final concentration of 20 µM for the indicated time, or injected intraperitoneally (1 mg) into dams for 45 minutes. Cells were then fixed and subjected to EdU detection and antibody staining according to the manufacturer's instructions. Briefly, cells were fixed for 15 min with 4% PFA and permeabilized for 30 minutes at room temperature in the dark using a saponin based permeabilisation solution. Cells were then stained with anti-GFP antibody, treated with the Click- iT™-AlexaFluor647 azide, and incubated with Hoechst 33342 to label DNA. Cells were measured in a FACSCanto II and dot blots analyzed with FlowJo software.

2.2.11 Dissection of dentate gyrus tissue from hippocampi of adult mice

C57BL/6 wild type mice were anesthetized with an overdose of Rompun (14 mg/kg bodyweight) and Ketavet (100 mg/kg bodyweight) in 0.9% saline solution and transcardially perfused with 20ml of ice cold HBSS. Subsequently the brain was removed from the head and placed into ice cold DEPC-PBS. The dentate gyrus was dissected from the brain and immediately stored in RNAlater at 4°C until further use.

2.2.12 mRNA extraction from cells and tissue

To isolate RNA from tissues, we used the mirVana™ miRNA Extraction Kit with some modifications. Tissue was transferred from RNAlater into 300 µl Lysis/Binding Buffer and homogenized on ice with a 30G syringe. 30 µl microRNA homogenate additive was added, the sample was shortly mixed, and incubated for 10 minutes on ice. 330 µl of acid-phenol:chloroform was added, samples were mixed for one minute and centrifuged at 13000 rpm for 15 minutes at 4ºC. The upper aqueous phase was transferred into a fresh tube and 1.25 volumes of 100% ethanol were added. Solutions were then applied onto spin columns and centrifuged for 15 seconds at 10000 rpm. Columns were washed with 350 µl microRNA Wash Solution 1. DNA digestion was performed by adding 80 µl digestion mix (10 µl DNAse and

70 µl RDD buffer) onto the column and incubation for 15 minutes at room temperature. Columns were again washed with 350 µl microRNA Wash Solution 1. Next, columns were washed twice with 500 µl microRNA Wash Solution 2/3. To remove residual wash buffer, columns were again centrifuged for one minute at 10000 rpm. 100 µl DEPC-water heated to 95°C were applied on the column followed by centrifugation for one minute at 10000 rpm to elute RNA. In order to concentrate RNA, 10 µl 3M sodium acetate, 2 µl Pellet Paint (Novagen; Merck), and 250 µl 100% Ethanol was added and samples were thoroughly mixed. RNA was precipitated over night at -80°C. The next day, samples were centrifuged for 30 minutes at 10000 rpm and the supernatant was discarded. Samples were washed once with ice cold 80% ethanol and once with 100% ice cold ethanol. Pellets were air dried and resuspended in 20 µl DEPC-water. RNA quality and quantity was assessed with a Nanodrop 2000.

Total mRNA from cells was extracted by using the RNAeasy Plus Mini Kit from Qiagen according to the manufacturer's instructions. The concentration and purity (A260/280 ratios) was analyzed with a Nanodrop 2000.

2.2.13 Quantitative real time PCR (qRT-PCR)

Reverse transcription reaction was performed using the Superscript III First Strand Synthesis SuperMix from Invitrogen according to the manufacturer's instructions. Briefly, 1 µg total RNA in 6 µl water was incubated with 1 µl Annealing Buffer and 1 µl oligo-dTs (50 mM) for 5min at 65°C followed by an incubation on ice for one minute. Subsequently, 10 µl 2x First-Strand Reaction Mix and 2 µl Superscript III/RNaseOUT Enzyme Mix were added and the reaction was incubated at 50°C for 50 minutes. Enzymes were inactivated for five minutes at 85°C and samples were immediately chilled on ice.

Quantitative real-time PCR was performed with Power SYBR® Green PCR Master Mix in a 96 well plate with a ABO 7500 Fast Real-Time PCR System Cycler (Applied-Biosystem). 3.52 µl of the cDNA reaction were mixed with 4.4 µl of forward (1:20) and 4.4 µl of reverse primers (1:20), 19.6 µl water, and 35.04 µl SYBR® Green PCR Master Mix. This reaction was split in three 20 µl aliquots which were pipetted in a 96 well plate to obtain three technical replicates. Primers used for qRT-PCR are listed in table 7, and cycling conditions were as follows: 2 min at 95°C, 10 min at

95°C, followed by 40 cycles of 15 s at 95°C and 60 s at 60°C. Relative levels of gene expression were quantified, using the $2^{-\Delta\Delta CT}$ equation. Melting curve analysis was carried out at the end of each run to check for non-specific amplification.

Table 7: Primers used for qRT-PCR

Primer description	Sequence
mouse ANKHD1 fwd	GCTCCCACTAACATTTTTCACCAG
mouse ANKHD1 rev	CCCAGAGTTCTTCCATAGTCATAG
human ANKHD1 fwd	GGAGAGTTCTCCTGTGAAGTTCTG
human ANKHD1 rev	GTCTCAGCTCCCTCCACCTT
mouse Actin fwd	AGCGTGGCTACAGCTTCACC
mouse Actin rev	TGTCACGCACGATTTCCCT
human GAPDH fwd	CGGTCCTGGTTGCAGGAATA
human GAPDH rev	AGAGCAAGGCAAGAAGGTCC
mouse GAPDH fwd	CCAGTGAGCTTCCCGTTCA
mouse GAPDH rev	GAACATCATCCCTGCATCCA

2.2.14 Cell lysates

Cells were harvested, washed in chilled PBS, and resuspended in cell lysis buffer. Suspensions were incubated on a rotating wheel at 4 °C for 10 to 20 minutes, homogenized using a syringe with a 27G needle, and then centrifuged at 12000 rpm, 4 °C for 5 minutes to remove cell debris. Supernatants were collected (lysates) and stored at -20ºC or used immediately for Western blotting or immunoprecipitation. Protein concentrations were measured with a BCA assay from Pierce.

2.2.15 Co-immunoprecipitation

Protein lysates were prepared as described above and used immediately for immunoprecipitation. One tenth to one-twentieth of each supernatant was saved ('input') while the remaining sample was brought to a volume of 600 µl by adding lysis buffer (without DTT and protease inhibitor). Then 3 µl of an 80 mg/ml bovine serum albumin solution and and 30 µl Protein A/G PLUS-Agarose beads were added together with the appropriate amount of desired antibody, followed by incubation on a rotating wheel at 4 °C overnight. The next day, samples were washed 5 times with wash buffer, beads were resuspended in 30 µl reducing gel loading buffer, incubated

at 95 °C for 5 minutes and either loaded on SDS-polyacrylamide gels immediately or stored at -80 °C.

2.2.16 Sub cellular fractionation

Subcellular fractionation was carried out using the 'Subcellular Protein Fractionation Kit for Cultured Cells' from Pierce, according to the manufacturer's instructions.

2.2.17 Western blotting

Equal amounts of protein samples (25–50 µg) were fractionated on 12 % SDS-polyacrylamide gels or pre-cast 4-20% gradient gels at 180 V for approximately 45 minutes. Proteins were the transferred to nitrocellulose membranes (Biorad Trans-Blot®, 0.45 µm). The gel and the membrane were placed between sheets of absorbent paper and immersed in transfer buffer in a semi-dry blotting chamber. Blotting was performed at 10 V and 150 mA for 1 hour. Following transfer, non-specific binding sites on the nitrocellulose membrane were blocked by incubation with 5% skim milk powder in PBS-Tween (milk/PBST) for one hour. Membranes were incubated with primary antibodies (see table 4) diluted in milk/PBST overnight at 4°C. The next day, membranes were washed with with milk/PBST twice for 10 minutes, followed by incubation with HRP-conjugated secondary antibodies (see table 5) in milk/PBST for one hour at room temperature. Following several thorough washed with PBST, the HRP signal was detected by incubation with Enhanced Chemi Luminescence solution according to the manufacturer's instructions and exposure to Kodak X-Omat films. For removal of antibody complexes from nitrocellulose membranes for reprobing with different antibodies, membranes were incubated with stripping buffer for 30 minutes at 55°C. After thorough washing with PBST, membranes were reprobed as described above.

3 Results

ANKHD1 and its homolog MASK in Drosophila were shown to be important regulators of cell proliferation and differentiation. Published observations regarding ANKHD1 expression as well as unpublished observations in our lab, led us to hypothesize that ANKHD1 might be involved in regulating NPC functions. First, we wanted to characterize ANKHD1 expression in the developing mouse brain and in adult NPCs. Later test its function...

3.1 ANKHD1 expression in the murine brain

Expression of ANKHD1 in the developing mouse brain has not been investigated yet. In adult brain, the only evidence comes from a paper published by Poulin et al. [65] where, alongside various other tissues, brain lysate was used in a quantitative real time PCR experiment and ANKHD1 was detected therein. However, ANKHD1 protein expression in the adult brain has not been described yet. We used quantitative real time PCR, Western blotting and *in situ* hybridization to test for ANKHD1 expression in the developing and adult mouse brain.

First, ANKHD1 mRNA levels in dissected dorsal telencephalic cortices from various embryonic stages were analyzed by quantitative real time PCR. We used primers that specifically detect the full length canonical isoform of ANKHD1 and do not bind to ANKHD1-BP3, a gene-fusion product reported by Poulin et al. [65]. This was achieved by placing the primers at the N-terminus of the protein[5], and including exon 34 (the last exon) which is unique to ANKHD1 (Figure 6A). As shown in Figure 6B, ANKHD1 could be detected as early as E12.5 and in all following embryonic stages tested (E13.5 - E17.5). Levels tended to increase at later stages compared to E12.5. Moreover, ANKHD1 was also found to be expressed in the developing ventral forebrain, i.e. the ganglionic eminences at robust levels (Figure 6C).

We further investigated mRNA expression in the developing forebrain by performing *in situ* hybridization on saggital cryomicrotome cut sections of selected embryonic stages. Again, *in situ* RNA probes were designed to specifically detect the full length canonical isoform. A broad expression of ANKHD1 in the neocortex and ganglionic

[5] All reported isoforms are truncated on the N terminal side, and thus will not be recognized by the designed primers

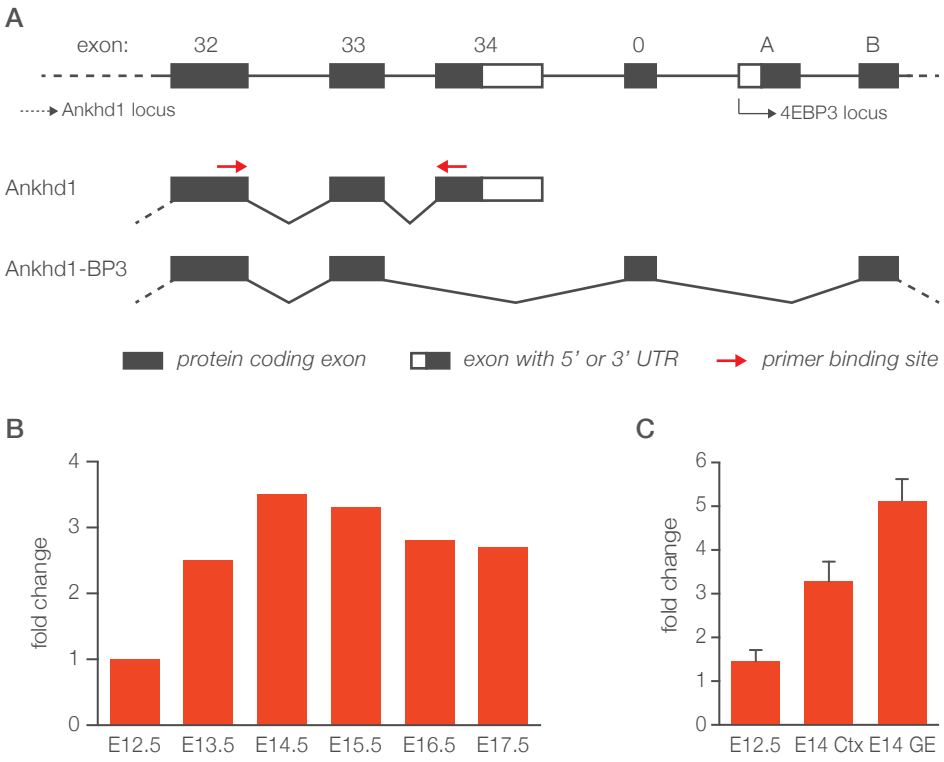

Figure 6: ANKHD1 mRNA is expressed throughout neocortical development. A | Schematic representation of the ANKHD1 gene structure in its genomic locus and positioning of primers for quantitative real time PCR. The last three exons of ANKHD1 (32-34), the intermediate exon 0, and the first two exons of the downstream gene 4E-BP3 are shown on top. Beneath, mRNA transcripts of ANKHD1 and the fusion protein ANKHD1-BP3 are displayed. Red arrows indicate position of primers used for detection of ANKHD1. B | mRNA was prepared from dorsal telencephalic cortices from indicated embryonic stages (E12.5 - E17.5) and tested for ANKHD1 expression with above mentioned primers. Expression values are normalized to the E12.5 data point. C | ANKHD1 mRNA expression in dorsal telencephalic cortices and ganglionic eminences from E14.5 embryos was compared by quantitative real time PCR. Expression values are normalized to one replicate from the E12.5 data point.

eminences was evident at E13.5 (Figure 7A). In the neocortex, strong expression was present in the ventricular and subventricular zones (Figure 7B).

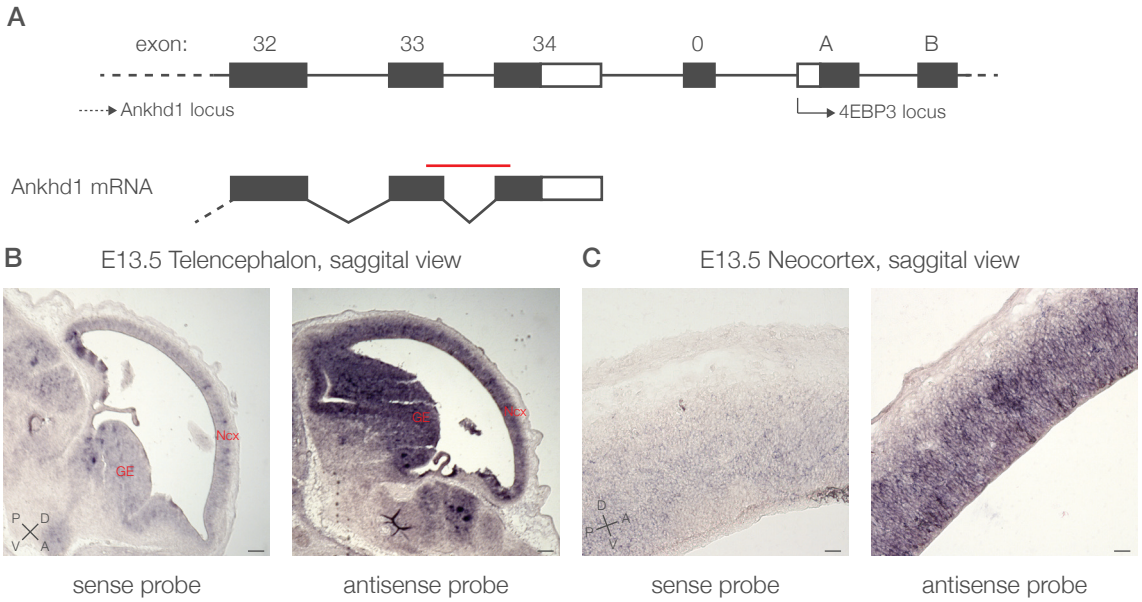

Figure 7: ANKHD1 mRNA expression assessed by *in situ* hybridization. A | Schematic illustration of RNA probe position for ANKHD1 detection by *in situ* hybridization. The probe was designed to span over two exons and include exon 34, which is unique to ANKHD1 (compare with Figure 6). B | 15 µm saggital cryo-cut sections of E13.5. heads were prepared and subjected to *in situ* hybridization. Scale bar= 20 µm. C | Higher magnification of neocortex from images shown in B. Scale bar= 100 µm. Ncx= neocortex, GE= ganglionic eminences, D= dorsal, V= ventral, A= anterior, P= posterior.

To test wether ANKHD1 mRNA is also translated and the protein expressed, we performed Western blot analysis of various embryonic and adult mouse brain samples. At E12.5, only very low levels of ANKHD1 protein could be detected. At all later stages tested (until E17.5), the protein was readily detected. Moreover, in short term cultured primary adult NPCs, strong ANKHD1 expression was observed.

Adult NPC function decreases with aging. To further investigate the expression pattern of ANKHD1 during adulthood, we measured mRNA levels of ANKHD1 in dentate gyri form mice of different age. As seen in Figure 9, ANKHD1 was detected throughout all age time points collected, including in 15 months old mice, and levels did not seem to vary to any significant extent throughout life.

Due to the lack of suitable antibodies, no immuno fluorescence stainings were performed on mouse brain sections. Together, these data suggest that ANKHD1 is ex-

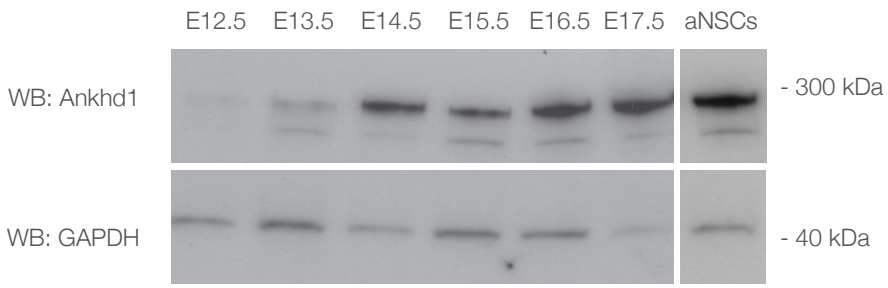

Figure 8: ANKHD1 protein is expressed in embryonic and adult neural progenitor cells. Protein lysates were prepared from either dorsal telencephalic cortices at the indicated embryonic day (E12.5-E17.5), or from short term cultured adult neural progenitor cells. Western blots were tested with antibodies against ANKHD1 (upper row) or GAPDH (lower row).

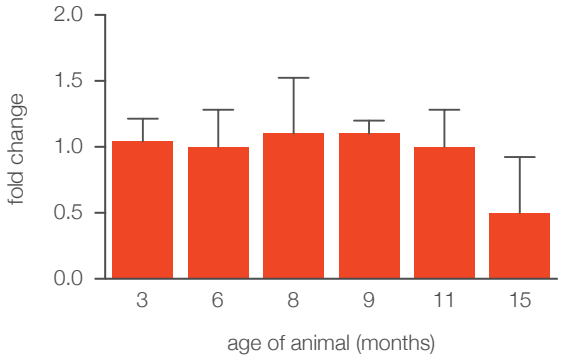

Figure 9: ANKHD1 is expressed in aNPCs throughout life. Total RNA was isolated from dissected dentate gyri from Bl6 mice of different age (3 to 15 months). Samples were subjected to quantitative real-time PCR with ANKHD1 primers. Data were normalized to beta-Actin expression and are displayed as fold change to the first data point (3 month time point). n= at least two for each age.

pressed on RNA and protein level throughout neocortical development and remains present in adult NPCs at high levels.

3.2 ANKHD1 regulates cell cycle progression in adult NPCs

Given the expression of ANKHD1 in adult NPCs and its function in other progenitor cells [84], we hypothesized that it may be involved in aNPC proliferation and differentiation. We first sought to investigate the effect of ANKHD1 on NPC proliferation. Because no knockout mice or cells are available, we used siRNA directed against ANKHD1 to knock it down through transient transfection of cells. Adult NPCs were isolated from Bl6 mice and cultured as neurospheres in serum free media. 48 hours after knockdown of ANKHD1 with siRNA, cells were treated with EdU for 45 minutes. Subsequently the samples were subjected to immunofluorescence staining for flow cytometry with anti GFP antibody (detection of transfected cells) and detection of EdU via a copper catalyzed covalent reaction between an fluorophor coupled azide and the ethynyl moiety of EdU (Figure 10). Interestingly, the number of cells that incorporated EdU was increased by approximately 50% when ANKHD1 was knocked down compared to cells transfected with non-targeting siRNA (Figure 10B-C), indicating that ANKHD1 might be involved in negative regulation of cell proliferation.

Next, we tested if knockdown of ANKHD1 in cultured aNPCs inhibited differentiation in addition to increasing proliferation. When grown under ”stem cell” conditions as neurospheres, only very few cells will be able to differentiate. However, after withdrawal of EGF and FGF growth factors, cells differentiate and express markers of post mitotic neurons (such as β-III-tubulin). Cultured NPCs were transfected with either ANKHD1 or non-targeting siRNA and grown under differentiating conditions for six days. As seen in Figure 11, the amount of β-III-tubulin positive cells amongst all transfected cells was decreased when ANKHD1 was knocked down. Conversely, the proportion of β-III-tubulin positive cells increased when human ANKHD1 was overexpressed. Human full length ANKHD1 was used for overexpression experiments because mouse ANKHD1 has not been cloned by us or others, including commercial providers, yet. Due to the high similarity between human and mouse ANKHD1 we hypothesized that those two proteins might be interchangeable (see

1.5 and 3.3.4). However, only few cells could be measured because electroporation was very inefficient (due to the large size of full-length ANKHD1). Together, this data suggest that knockdown of ANKHD1 can promote proliferation of aNPCs *in vitro* and inhibit their differentiation.

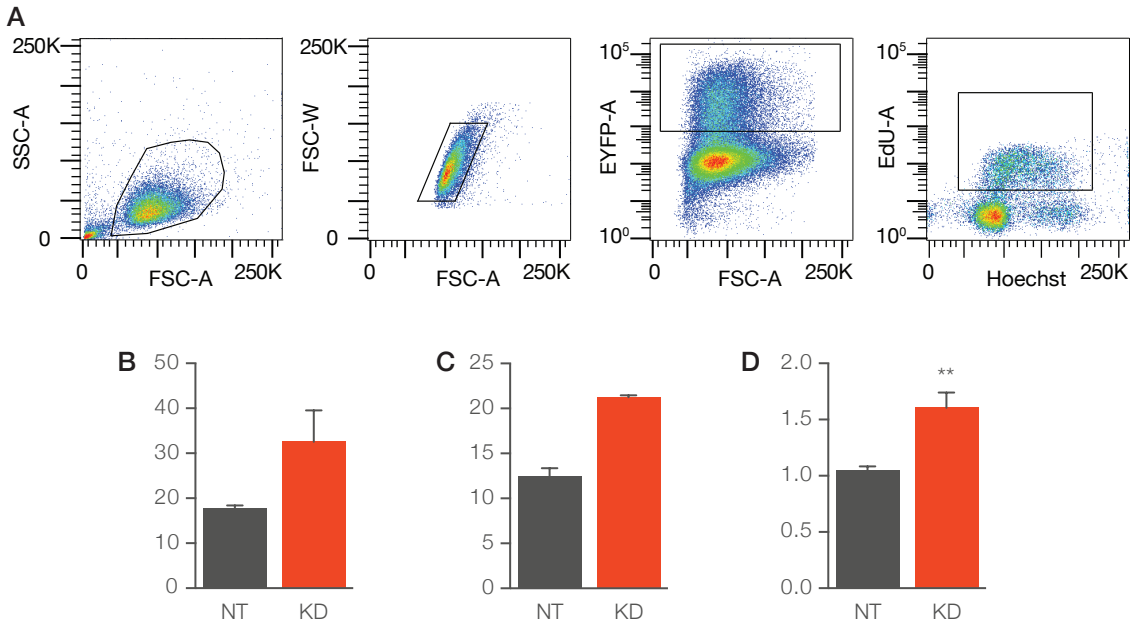

Figure 10: ANKHD1 knockdown promotes proliferation of aNPCs *in vitro*. Low passage aNPCs were electroporated with a YFP plasmid and siRNA targeted against ANKHD1 (KD) or non-targeting control siRNA (NT). 48 hours later cells were treated with 10 µM EdU for 30 (B) or 45 (C) minutes followed by immuno fluorescence staining and EdU detection. A | Representative flow cytometry dot plots and gating strategy shown for a control sample. First the living cell population was selected and doublets excluded, followed by gating on YFP positive cells and subsequently EdU positive cells. Number of EdU positive cells amongst all YFP positive cells was measured. B | Percentage of EdU^+ cells amongst all YFP^+ cells after 30 minutes of EdU treatment. C | Percentage of EdU^+ cells amongst all YFP^+ cells after 45 minutes of EdU treatment. D | Relative increase in number of of EdU+ cells of B and C combined. n=4 (2 each for 30' and 45' treatment), **p<0.05, unpaired Student's t-test.

3.3 ANKHD1 regulates proliferation during cortical development

We observed ANKHD1 expression in the developing neocortex and other proliferating regions of the brain (see Figures 6-8). The role of ANKHD1 in the developing brain has not been studied yet. In fact, it has not been studied in any other tissue during mammalian development so far. Knockout mice, that would provide great insight into the role of ANKHD1 during development, are not available yet. The drosophila homolog of ANKHD1, MASK, has been reported to be important

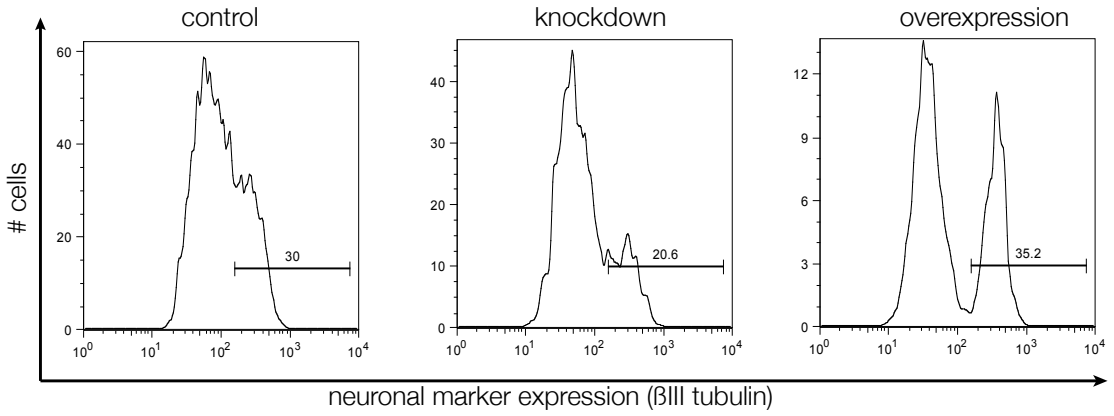

Figure 11: ANKHD1 promotes differentiation of aNPCs *in vitro*. Low passage aNPCs were electroporated with a YFP plasmid and siRNA targeted against ANKHD1 (knockdown) or non-targeting control siRNA (control), or with pCAG-YFP-ANKHD1. Six days later cells were stained with GFP and β-III-tubulin antibodies and analyzed by flow cytometry.

for photoreceptor progenitor proliferation and differentiation during development. Moreover some MASK mutants are embryonic lethal [84]. Based on our expression data and functional roles of ANKHD1 in progenitor cells of other organisms, we hypothesized that it might play an important role during murine brain development. Thus, we next set out to investigate the role of ANKHD1 in murine embryonic neural progenitor cells (eNPCs).

3.3.1 Knockdown of ANKHD1 increases proliferation of eNPCs

Despite the lack of knockout mice, eNPC function can be studied *in vivo* by utilizing the *in utero* electroporation technique to specifically target radial glia cells: Uterine horns of anesthetized dams are exposed, followed by DNA or RNA injection into the lateral ventricle and electroporation with forceps type electrodes (see methods for details). We knocked down ANKHD1 in radial glia of E13.5 and E14.5 mice and measured EdU incorporation into eNPCs 48 hours later. Illustration of the experimental layout and representative dot plots from flow cytometry analysis are shown in Figure 12 A and B, respectively. Strikingly, the number of progenitor cells that incorporated EdU was markedly increased from 5.6% ± 0.2 to 12.4% ± 0.45 (E13.5, Figure 12 C) and 5.8% ± 0.7 to 9.7% ± 0.9 (E14.5, Figure 12 C) in ANKHD1 knockdown samples. Note that the rather low number of cells incorporating EdU is due to the fact that YFP positive post mitotic cells (i.e. immature neurons generated

from labeled progenitors) were not excluded from the analysis. These cells account for approximately 55% of all labeled cells. Together with a rather short EdU pulse time of three hours the measured numbers are reasonable and comparable to data obtained in other publications. Due to lack of suitable antibodies we confirmed knockdown of ANKHD1 in electroporated brains by qRT-PCR. Tissue around electroporated area was dissected 48 hours post IUE and sorted for YFP positive cells (3–4 embryos were pooled for each sample). Total RNA was isolated and tested with primers recognizing ANKHD1. Knockdown of ANKHD1 was at least 40 – 60%. Primes used showed some degree of self-annealing and thus actual ANKHD1 knockdown probably was even more efficient.

3.3.2 The apical and basal progenitor pool is expanded after ANKHD1 knockdown

The increased EdU incorporation could be a consequence of altered radial glia cell behavior, changes in basal progenitor proliferation and / or differentiation, or both. To gain further insight into the expanding progenitor pool, we next performed *in utero* electroporation of E14.5 embryos followed by immuno fluorescencestaining of sections for the basal progenitor marker Tbr2 and the neuronal marker Satb2 (Figure 13A). By using marker expression and location information (see Figure 13 E), radial glia, basal progenitors, and post-mitotic neurons can be distinguished. Interestingly, in ANKHD1 knockdown samples the number of radial glia cells was increased from 12.49 ± 0.83 to 17.17 ± 3.05 (Fig. 13B) and the number of basal progenitor cells was increased from 30.56% ± 1.03 to 39.14% ± 2.25 (Fig. 13C). The number neurons generated from transfected radial glia cells during the observation period decreased from 56.95% ± 0.36 to 43.70% ± 3.68 (Fig. 13D). This data suggest that ANKHD1 is required for normal progenitor proliferation and differentiation.

3.3.3 Overexpression of human ANKHD1 promotes differentiation into neurons

We hypothesized that overexpression ANKHD1 would increase differentiation of NPCs. To test this hypothesis we overexpressed human ANKHD1 in eNPCs. The

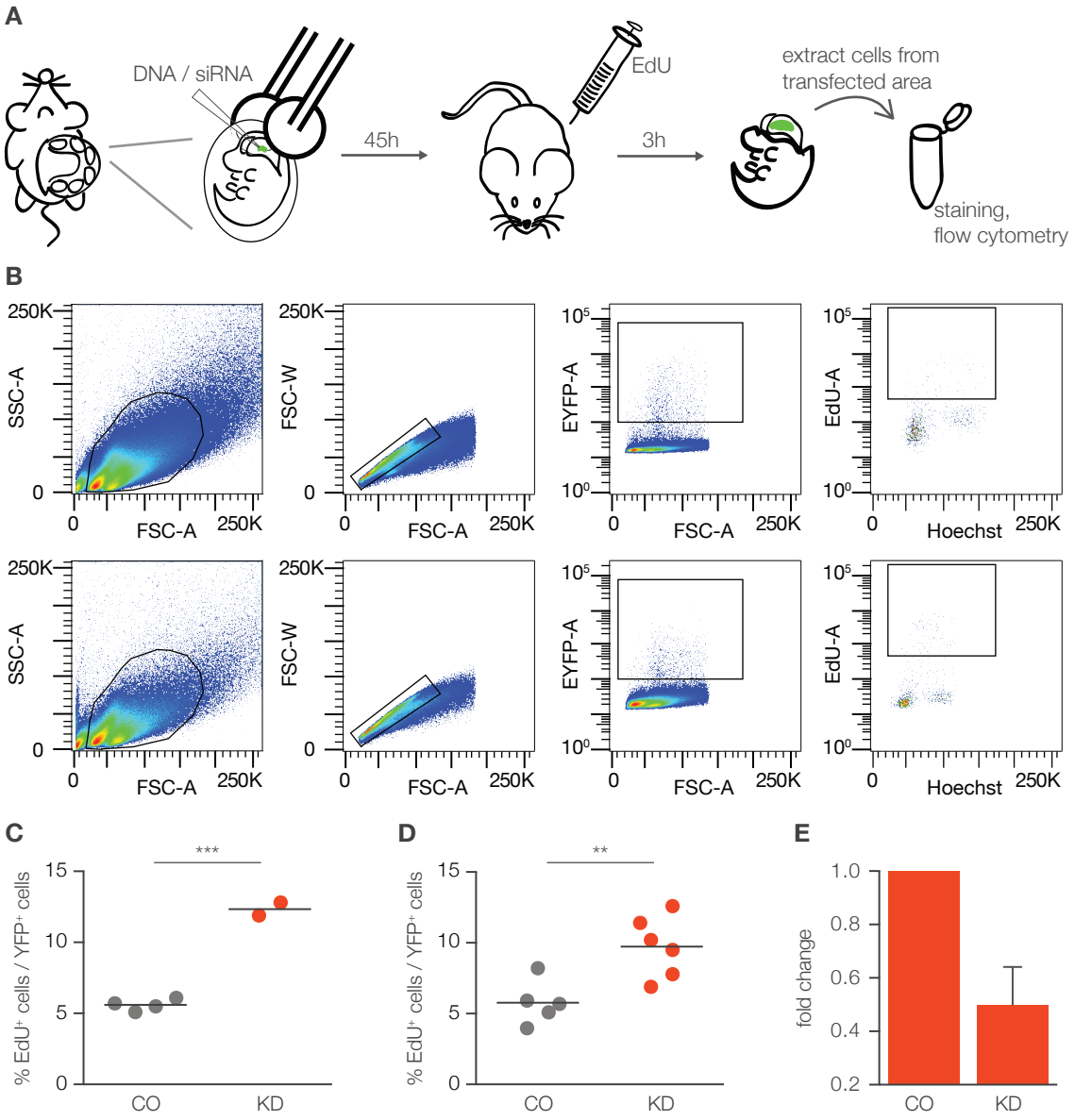

Figure 12: ANKHD1 knockdown promotes eNPC proliferation *in vivo*. A | Schematic illustration of *in utero* electroporation and subsequent analysis. B | Representative flow cytometry dot plots and gating strategy of a control (upper row) and ANKHD1 knockdown (lower row) sample. First the living cell population was selected and doublets excluded, followed by gating on YFP positive cells and subsequently EdU positive cells. Number of EdU positive cells amongst all YFP positive cells was measured. C | E13.5 embryos were electroporated with either pCAG-YFP and non-targeting siRNA (CO) or pCAG-YFP and siRNA against ANKHD1 (KD). Dams were injected i.p. with 1 mg EdU 45 hours later and sacrificed 3 hours after EdU injections. n=4 for CO and 2 for KD from two litters. Data are presented as mean and individual values, ***p<0.001, unpaired Student's t-test. D | Same as in C, but here E14.5 embryos were electroporated. n=5 for CO and 6 for KD, from two litters. Data are presented as mean and individual values, **p<0.01, unpaired Student's t-test. E | Knockdown of ANKHD1 was confirmed by qRT-PCR. Embryos were electroporated as in C and D. 48 hours later tissue around electroporated area was isolated and sorted for YFP positive cells. Total RNA was isolated from these cells and tested for ANKHD1 expression. n=2 (3–4 embryos pooled per sample). Expression values are normalized to controls.

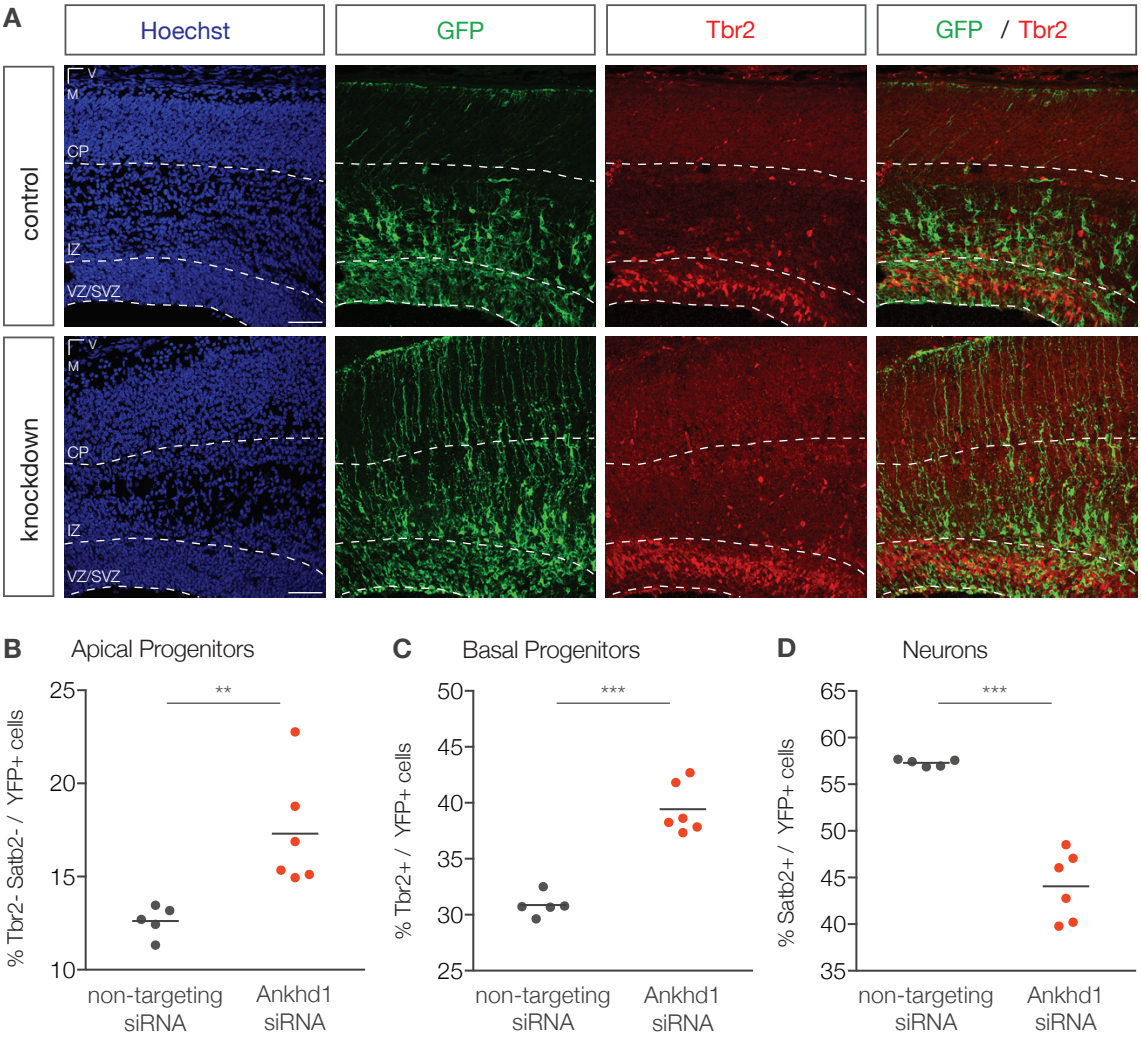

E

phenotype	marker	location
radial glia (RG)	Pax6+, Tbr2-, Satb2-	ventricular zone, subventricular zone
basal progenitor (BP)	Pax6+, Tbr2+, Satb2-	subventricular zone
neuron (N)	Pax6-, Tbr2-, Satb2+	intermediate zone, cortical plate

Figure 13: ANKHD1 knockdown promotes apical and basal progenitor proliferation *in vivo*. A | Representative images of E16.5 neocortex sections 48 hours after *in utero* electroporation. Control (upper panels) and ANKHD1 knockdown samples (lower panels) were stained for YFP (middle-left panels), and Tbr2 (middle-right panels). Merged images are shown in panels on the right and nuclei were counter-stained with Hoechst (left panels). VZ= ventricular zone, SVZ=subventricular zone, IZ=intermediate zone, CP=cortical plate, V=ventral, M=medial. Scale bar=50 µm. B-D | Percentage of radial glia cells (B), basal progenitor cells (C), and neurons (D) amongst all transfected cells in embryos electroporated with non-targeting siRNA (CO) or siRNA against ANKHD1 (KD). n=5 embryos for CO and n=6 embryos for KD from four different litters; total number of cells counted: n=1007 for CO and n=1010 for KD. **p<0.01, ***p<0.001, two-way ANOVA. E | Discrimination of RG, BPs, and neurons is based on marker expression and location.

human and mouse homologs of ANKHD1 are vey similar. Both the ankyrin domains and the KH domain are highly conserved in sequence and position (see 1.5 for details). We have obtained a human cDNA clone from genecopedia and subcloned it to suitable expression vectors in order to study overexpression phenotypes in NPCs.

We overexpressed human ANKHD1 in the neocortex of E14.5 embryos via *in utero* electroporation and compared phenotypes 48 hours later (Fig 14). Interestingly, ectopic expression of ANKHD1 led to increased differentiation into neurons compared to controls. More cells with immature neuron morphology were located in the intermediate zone and cortical plate compared to controls, and fewer cells were found in the VZ/SVZ (compare upper and middle row in Fig. 14). Moreover, when we overexpressed a truncated form of ANKHD1 that is missing the KH domain (ANKHD1-ΔC), differentiation to neurons was reverted to normal levels (Fig. 14, last row).

3.3.4 Overexpression of human ANKHD1 rescues knockdown phenotype

Overexpression of human ANKHD1 led to converse effects compared to knockdown conditions (compare Fig. 13 and Fig. 14). We thus wondered if we could rescue the ANKHD1 knockdown phenotype by simultaneously overexpressing human ANKHD1. We co-electroporated mouse ANKHD1 siRNA and a human ANKHD1 overexpression plasmid in E14.5 embryos and analyzed them 48 hours later (Fig. 15). Co-electroporation of human ANKHD1 could revert progenitor populations close to control levels and partially rescue differentiation into neurons.

3.4 ANKHD1 sub-cellular localization and interaction partners

3.4.1 ANKHD1 can localize to the nucleus in NPCs

The mechanisms by which ANKHD1 functions are largely unknown. ANKHD1 was shown to interact with the Hippo pathway component YAP in various cell lines [74, 81], and to be partly required for YAP activity. However, if they shuttle to the nucleus together and if ANKHD1 has a function in the nucleus remains controversial.

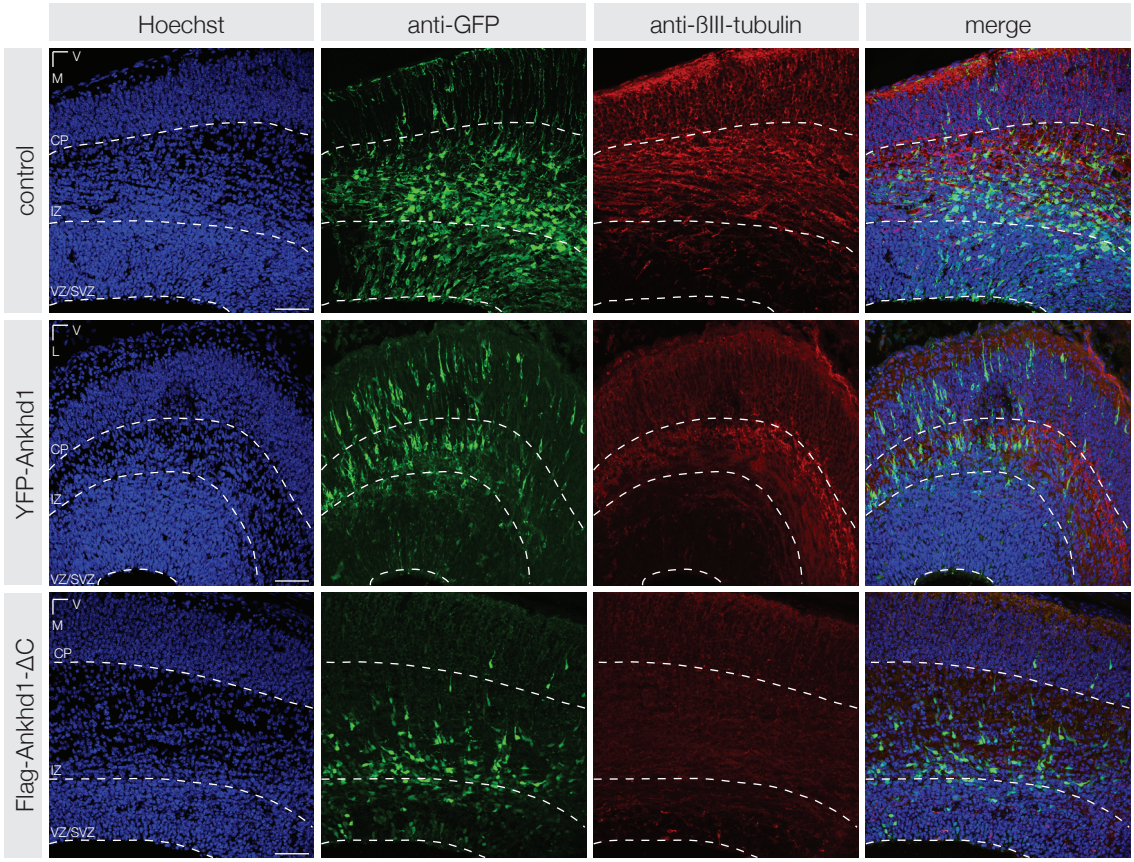

Figure 14: ANKHD1 overexpression promotes differentiation *in vivo*. Representative images of E16.5 neocortex sections 48 hours after *in utero* electroporation. Control (YFP, upper row), ANKHD1 overexpression (YFP-hANKHD1, middle row) and c-terminal truncated ANKHD1 overexpression (Flag-ANKHD1-ΔC, lower row) were stained for GFP or Flag (middle-left panels) and β-III-tubulin (middle-right panels). Merged images are shown in panels on the right; nuclei were counter stained with Hoechst (left panels). VZ= ventricular zone, SVZ=subventricular zone, IZ=intermediate zone, CP=cortical plate, V=ventral, L=lateral, M=medial. Scale bar=50 µm.

We first analyzed the mouse ANKHD1 for a nuclear localization and nuclear export signal (NLS and NES, resp.).Using the protein predict platform [71], a stretch from position 1458 to 1477 was identified as potential NLS (Figure 16A). The sequence is `KREKRKEKRKKKKEEQKRK`, and it is highly conserved across species (100% in those tested, Figure 16B). This sequence is also 100% identical in the only paralog of ANKHD1, Ankrd17—which has been shown to locate to the nucleus. Furthermore, we performed nuclear fractionation of aNPCs lysates and tested for ANKHD1 abundance within them. The majority of the protein is localized in the cytoplasm, however, ANKHD1 can be clearly detected in the nucleus as well. Due to lack of suitable antibodies, we were unable to test for localization of endogenous ANKHD1

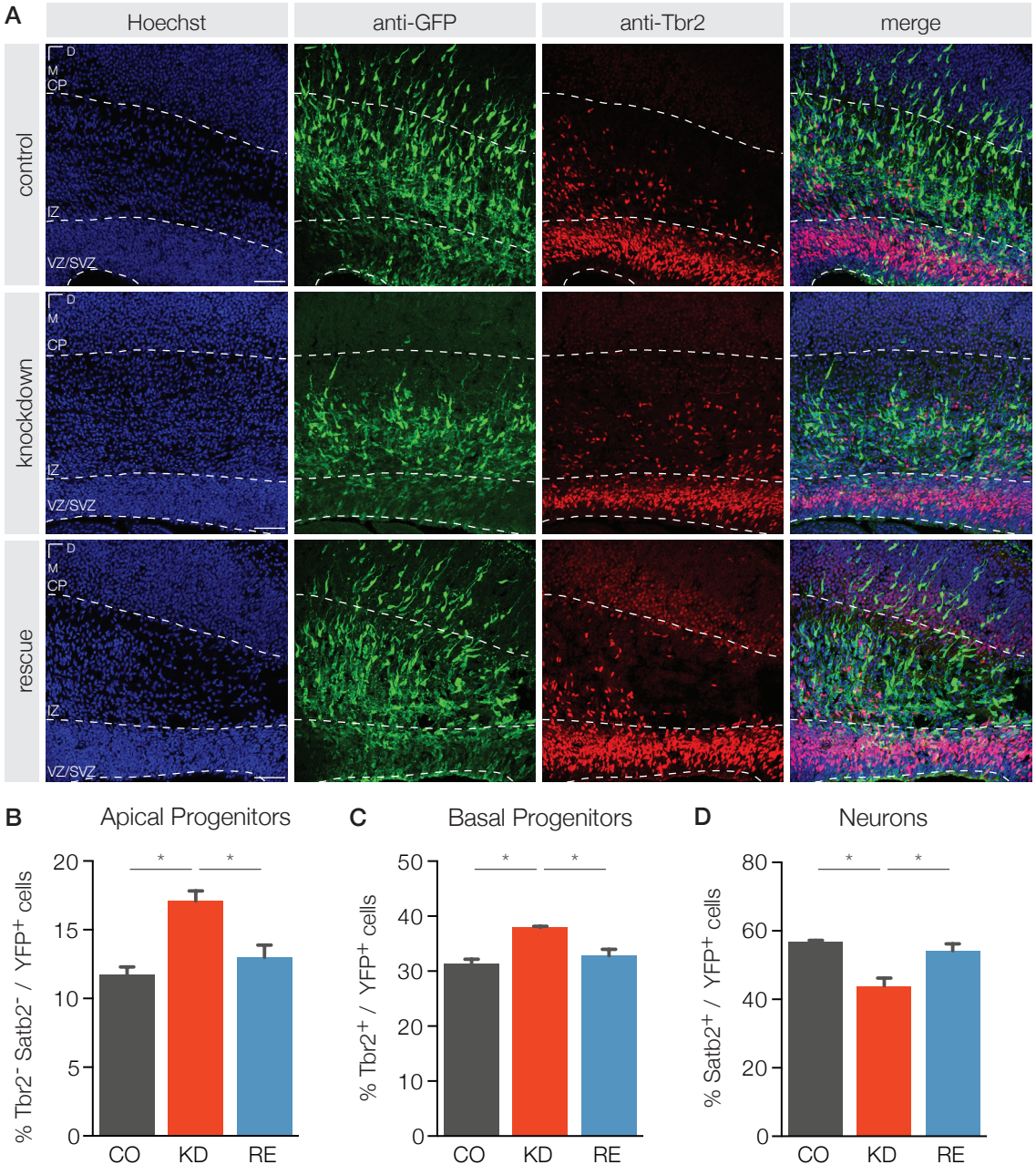

Figure 15: Overexpression of human ANKHD1 rescues knockdown phenotype. **A** | Representative images of E16.5 coronal neocortex sections 48 hours after *in utero* electroporation. Control (upper panels) and ANKHD1 knockdown samples (lower panels) were stained for YFP (middle-left panel), and Tbr2 (middle-right panel). Merged images are shown in panels on the right and nuclei were counter stained with Hoechst (left panels). VZ= ventricular zone, SVZ=subventricular zone, IZ=intermediate zone, CP=cortical plate, D=dorsal, M=medial. Scale bar=50 µm. **B-D** | Percentage of radial glia cells (B), basal progenitor cells (C), and neurons (D) amongst all transfected cells in samples electroporated with non-targeting siRNA (CO), siRNA against ANKHD1 (KD), or siRNA against ANKHD1 together with pCAG-YFP-hANKHD1 (RE). n=2 embryos from two different litters; total number of cells counted: n=482 for CO, n=621 for KD, and n=481 for RE, *p<0.05, two-way ANOVA.

on tissue sections. Notably, when we overexpressed YFP tagged ANKHD1 in eNPCs *in vivo*, we observed it mainly in the cytoplasm, but also in the nucleus, similar to the fractionation experiments. Both Sansores-Garcia et al. [74] and Sidor et al. [81] showed that ANKHD1 can interact with YAP, and Sidor et al. [81] suggested that ANKHD1 and YAP might translocated to the nucleus together. While YAP expression in the developing brain is rather low, the other known effector of the Hippo pathway in mammals, TAZ (or WWRP1) is highly expressed in the ventricular and sub ventricular zones during neocortical development. We first tested if ANKHD1 interacts with YAP in eNPC by isolating E13.5. dorsal telencephalic cortices and performing co-immunoprecipitation experiments. So far, we were not able to detect an interaction of YAP and ANKHD1 in eNPCs. A possible interaction with TAZ has not been tested yet. Together, our observations suggest that ANKHD1 can localize to the nucleus in eNPCs, although its predominant location seems to be in the cytoplasm. Moreover, if ANKHD1 interacts with the Hippo pathway in NPCs as well remains elusive.

3.4.2 ANKHD1 does not interact with SHP2 to promote NPC proliferation

It was previously reported that ANKHD1 can interact with the tyrosine-protein phosphatase SHP2 (PTPN11) in the human leukemia cell line K562. SHP2 is known to be important during brain development, controlling the switch from neurogenesis to gliogenesis and promoting proliferation of NPCs. Hence, we hypothesized that ANKHD1 might interact with SHP2 in embryonic NPCs as well, and at least partially function via the SHP2 signaling pathways. We performed co-immunoprecipitation with both ANKHD1 and SHP2 antibodies to test their interaction in freshly isolated dorsal telenchephalic cortices from E13.5 embryos. As shown in Figure 17, we could not observe interaction between the two proteins, independent of which antibody was used to perform the immunoprecipitation.[6]

[6] N.B.: We were unable to reproduce interaction of ANKHD1 and SHP2 in K562 cells (data not shown).

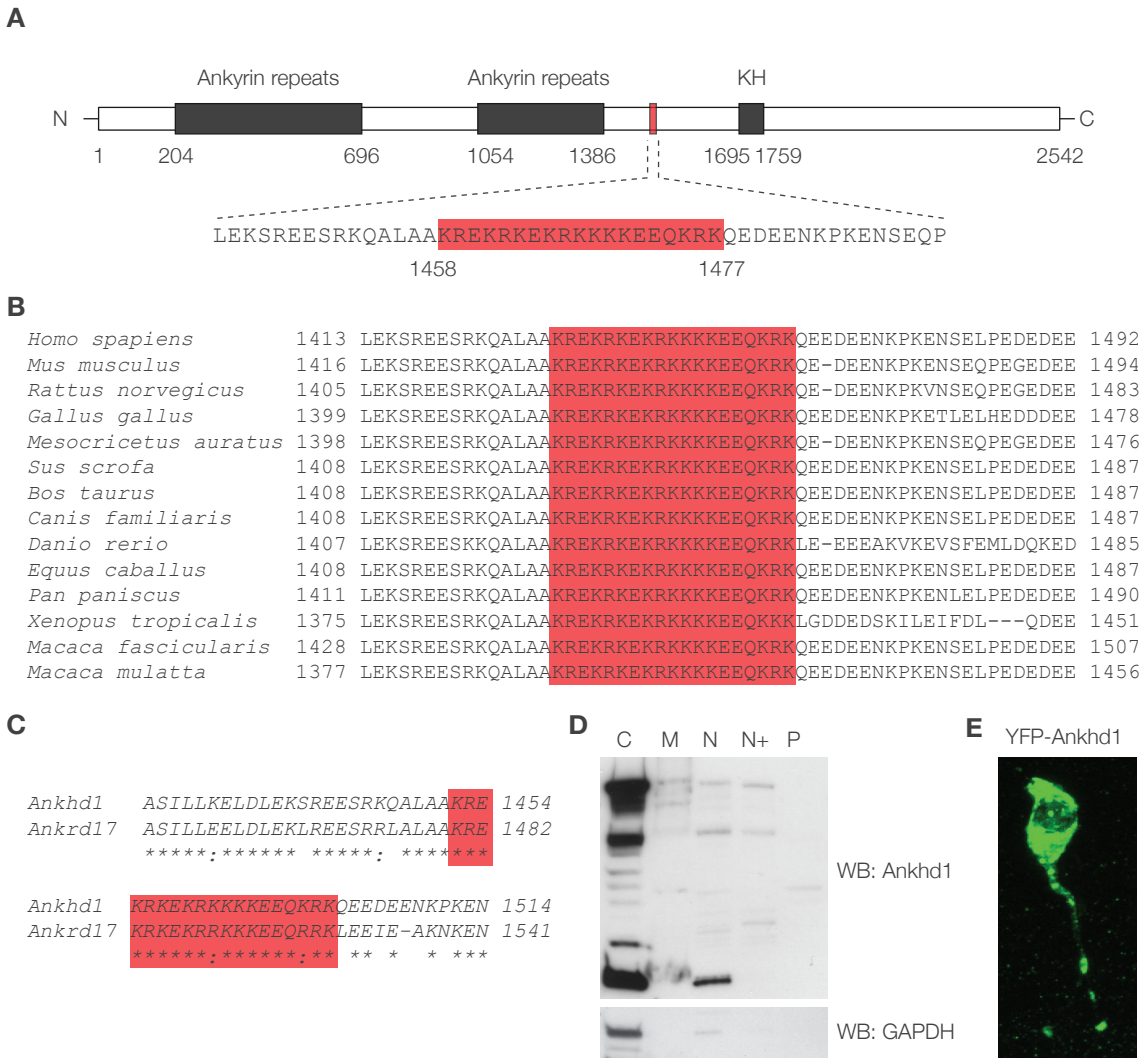

Figure 16: ANKHD1 contains a putative NLS and can localize to the nucleus. A | Putative nuclear localization signal (NLS) in human ANKHD1. NLS highlighted as identified by prediction with preditprotein.org [71] and ELM [20]. B | Protein sequence alignment of ANKHD1 from various species. Aligned with COBALT. Accession numbers of shown species: Homo sapiens (NP_060217.1), Mus musculus (NP_780584.2), Rattus norvegicus (NP_001190982.1), Gallus gallus (NP_001191026.1), Mesocricetus auratus (XP_005069288.1), Sus scrofa (NP_001190196.1), Bos taurus (XP_005209554.1), Canis familiaris (NP_001191024.1), Danio rerio (NP_001186697.1), Equus caballus (NP_001191034.1), Pan paniscus (XP_003829227.1), Xenopus tropicalis (NP_001191021.1), Macaca fascicularis (XP_005558028.1), Macaca mulatta (XP_002804593.1). C | Alignment of human ANKHD1 and its paralog Ankrd17 with Clustal Omega, accession numbers: ANKHD1, see above, Ankrd17: NP_115593.3. D | Western Blot of sub-cellular fractions of aNPCs. C = cytoplasmic extract, M = membrane extract, N = nuclear extract, N+ = chromatin-bound extract, P = pellet extract. E | pCAG-YFP-ANKHD1 was overexpressed via *in utero* electroporation in E14.5 neocortex. Cryomicrotome sections were prepared 48 hours later and stained with GFP antibody.

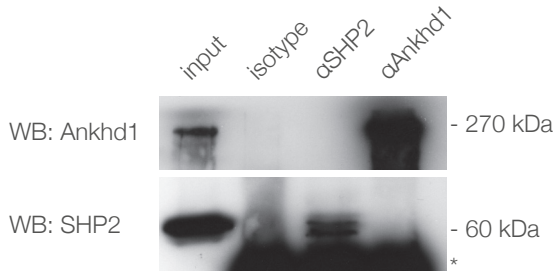

Figure 17: ANKHD1 does not interact with SHP2. Dorsal cortices of E13.5 embryos were dissected, followed by cell lysis and immunoprecipitation with either ANKHD1 antibody (lane 4), SHP2 antibody (lane 3), or an isotope control antibody (lane 2). 5% of total cell lysate were kept as input sample (lane 1). *heavy chain IgG from antibodies used for immunoprecipitation.

3.5 Role of ANKHD1 in glioma initiating cells

Gliobastoma multiforme is likely to origin from neural progenitor cells in the brain (see 1.4.2). Based on our observations regarding ANKHD1 effects on proliferation in neural progenitor cells, we wanted to investigate ANKHD1 levels in various glioma initiating cell (GIC) cultures, and elucidate if ANKHD1 is also involved in proliferation control of these cells.

3.5.1 ANKHD1 is expressed in glioma initiating cells

First, we tested ANKHD1 expression in various GIC cultures (we received GBM samples from two different hospitals and denote them GBM or NMA, depending on their source, see 2.2.2 for details) by Western blotting. ANKHD1 was detected in all cultures in varying amounts. All samples had a stronger expression than a human brain parenchyma control lysate.[7] ANKHD1 has various shorter isoforms (see introduction). Five main bands were detected in all GIC samples with the polyclonal ANKHD1 antibody used, and all five of these bands were affected by knockdown with siRNA designed against ANKHD1(see Figure 23). The ratio of the canonical isoform to smaller products did vary from sample to sample but was usually stable for a given GIC culture over time. Notably, very little full length ANKHD1 was detected in GBM 14 (not shown) and 39 (see Figure 18, lane 7). One sample, GBM 29, displayed two bands larger than the full length protein. These bands are of unknown

[7] A more suitable control to compare expression levels would be human adult neural stem cells which, however, were not available

identity; they might, however, represent the ANKHD1-BP3 fusion protein described by Poulin et al. [65]. These data suggest that ANKHD1 is either generally highly expressed in GBM or enriched in GICs.

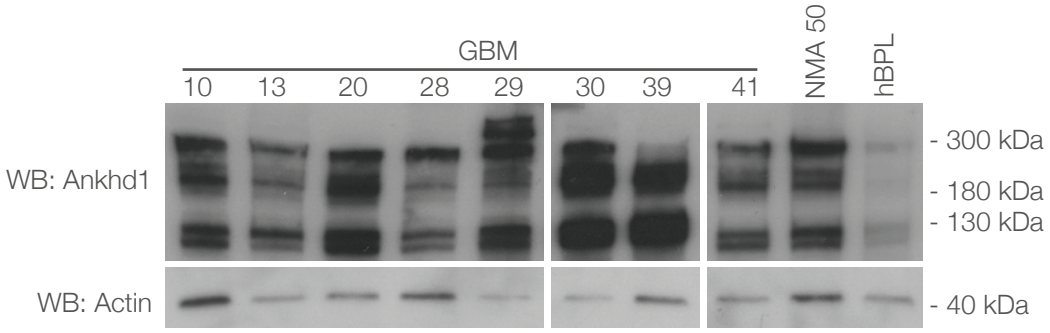

Figure 18: ANKHD1 expression in GBM Various GIC cultures were tested for ANKHD1 expression. Total lysates were prepared and tested with antibodies against ANKHD1 (upper panels) or beta-Actin (lower panels). All five bands in upper levels detect ANKHD1: the largest is representing the canonical isoform, while the others are other isoforms or break down products. The very large band in GBM 29 is of unknown origin. hBPL= human brain parenchyma lysate.

3.5.2 Overexpression of ANKHD1 increases proliferation of cultured glioma initiating cells

Next, we tested if knockdown or overexpression of ANKHD1 had similar effect on proliferation of GICs as observed for murine NPCs. We have chosen two different GIC cultures (GBM 13 and 30) for following experiments. Cells were transfected by electroporation, either with siRNA targeting human ANKHD1 together with a pCAG-YFP plasmid, non-targeting siRNA with pCAG-YFP, or a YFP-ANKHD1 plasmid under the control of a CAG promoter. Knockdown and overexpression were checked by quantitative real-time PCR (see Figure 20B and D) and also confirmed by Western blotting (see Figure 23 for an example). To determine the effect of ANKHD1 knockdown or overexpression on GIC proliferation, EdU incorporation was measured by flow cytometry 72 hours after electroporation. Flow cytometry dot plots and gating strategies for representative samples are shown in Figure 19. Interestingly, other then in murine NPCs, knockdown of ANKHD1 did not have an effect on GIC proliferation in any of the two cultures tested (Figure 20 A and C; GBM13: control = 10.90% ± 0.70, knockdown = 13.35% ± 1.55; GBM30: control = 6.72%± 2.02, knockdown = 9.68% ± 0.63). However, compared to control samples, overexpression markedly

increased EdU incorporation in both GBM 13 (10.90% ± 0.70 vs. 33.15% ± 0.45) and GBM 30 (6.72% ± 2.02 vs. 27.55% ± 0.15). These results suggest that ANKHD1 promotes cell proliferation in GICs.

3.5.3 ANKHD1 regulates p21 levels in glioma initiating cells

It was previously reported that ANKHD1 can promote proliferation of multiple myeloma cells and regulate expression levels of the cyclin dependent kinase inhibitor p21. To test if ANKHD1 has an influence on p21 expression levels in GICs, we performed knockdown and overexpression experiments in GBM 13 cells and examined p21 levels via Western blotting. Compared to cells transfected with non-targeting siRNA, knockdown of ANKHD1 led to an moderate increase of p21 (Figure 21, third lane). Conversely, overexpression of pCAG-YFP-ANKHD1 slightly reduced p21 expression levels (Figure 21, fourth lane). These data suggest ANKHD1 is able to modulate p21 expression, which, in turn, may contribute to the proliferation effects described above.

3.5.4 Akt and Erk activation is not influenced by ANKHD1 levels

Tumor cells often exhibit aberrant signaling in pathways involved in growth and proliferation such as Akt and Erk. Moreover, our lab and others have previously shown that CD95 can promote tumor growth and invasion by regulating Akt and Erk pathways [47]. We wanted to test if ANKHD1 modifies Akt or Erk levels to fulfill its function in GICs and if CD95 driven activation of Akt or inhibition of Erk is blocked or enhanced by ANKHD1. First, we measured if CD95 activation with T4 ligand had any effects on ANKHD1 expression levels. GBM 13 or GBM 30 cells were either left untreated or incubated with T4 for 24 and 48 hours. As shown in Figure 22, ANKHD1 levels did not change to any greater extend after CD95 activation in any of the two tested GIC cultures, independent of the T4 concentration used. Next, we tested if ANKHD1 can interfere with CD95 promoted activation of Akt or inhibition of Erk, and if ANKHD1 by itself had any effect on Akt or Erk phosphorylation. To this end, GBM 13 or GBM 30 cells were first electroporated with non-targeting siRNA or siRNA targeted against ANKHD1. 72 hours later, cells were either left untreated or treated with T4 ligand for 15 or 30 minutes, followed by

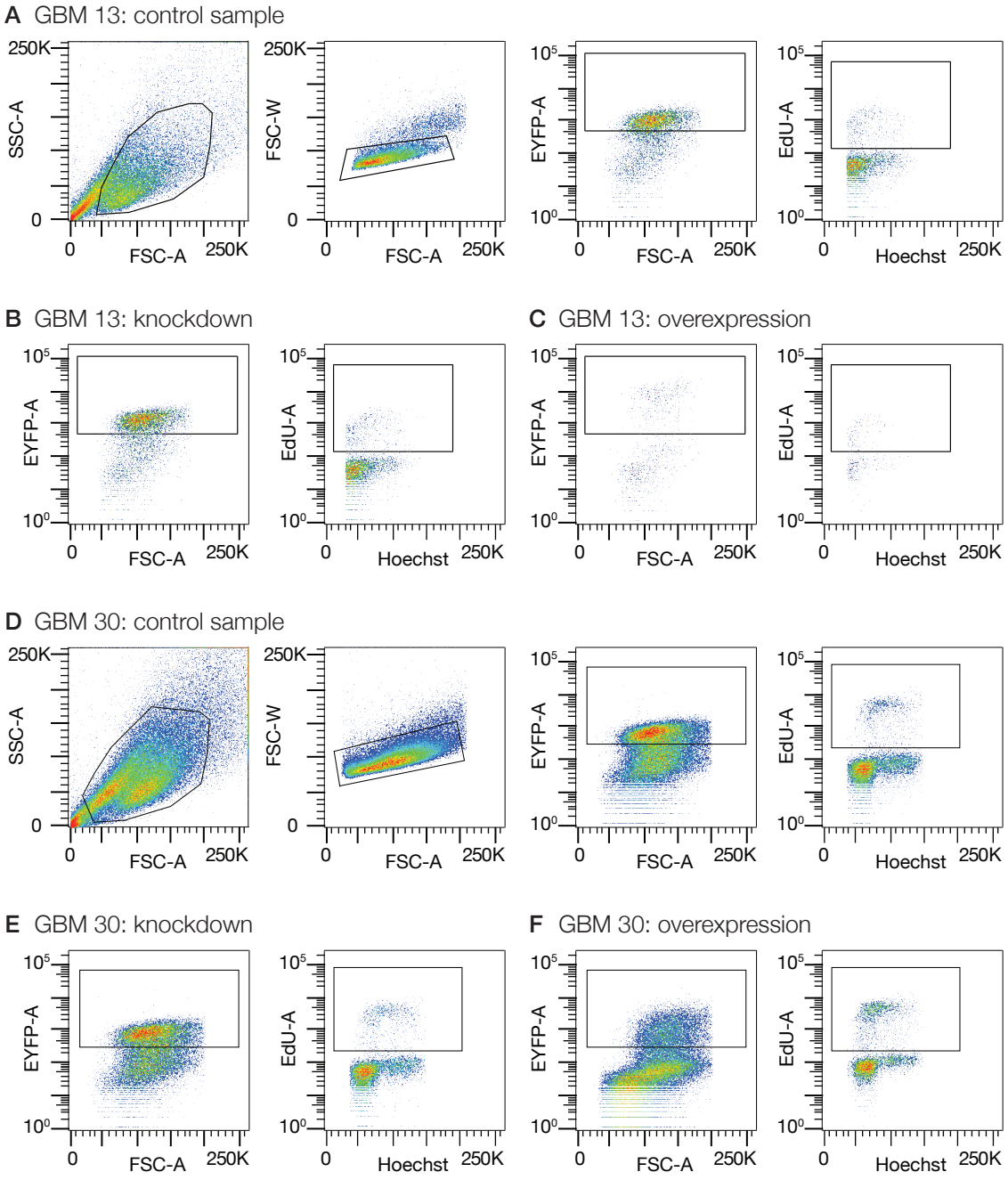

Figure 19: Flow cytometry dot plots and gating strategy of GIC samples tested for EdU incorporation. A | GBM 13 cells electroporated with non-targeting siRNA and pCAG-YFP were first broadly gated for living cells (left panel), followed by doublet exclusion (middle left panel), and exclusion of sub-G1 DNA content events (not shown). Finally YFP positive (middle right panel) and EdU positive (right panel) cells were identified. YFP and EdU gates were set against negative controls. B | YFP (left panel) and EdU (right panel) positive populations in GBM13 cells electroporated with siRNA against ANKHD1 and pCAG-YFP. C | YFP (left panel) and EdU (right panel) positive populations in GBM13 cells electroporated with pCAG-YFP-ANKHD1. D-F | Same as A-C but for GBM 30 cells.

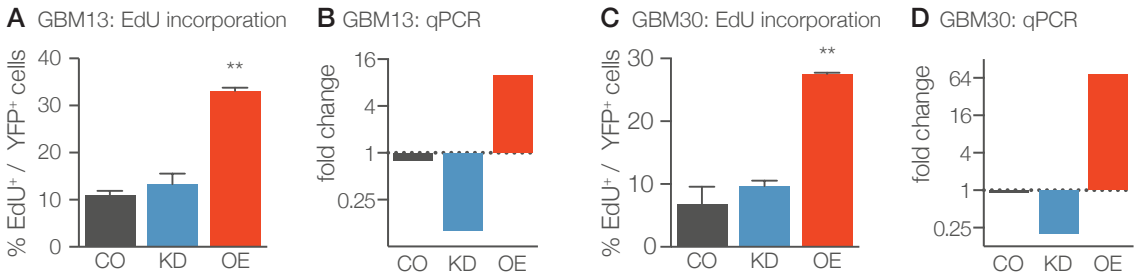

Figure 20: ANKHD1 overexpression promotes GIC proliferation *in vitro*. A+C | GBM 13 (A) or GBM 30 (C) cells were electroporated with either pCAG-YFP together with non-targeting siRNA (CO), pCAG-YFP together with siRNA targeting ANKHD1 (KD), or pCAG-YFP-ANKHD1 (OE). 72h later cells were treated with 20μM EdU for 60 minutes, followed by fixation and staining for EdU, YFP and DNA content. EdU incorporation amongst YFP positive cells was measured by flow cytometry as described in Fig. 19. Data are presented as mean ± s.d., n=2, one-way ANOVA, **p < 0.01. B+D | Knockdown and overexpression of ANKHD1 was confirmed by qRT-PCR.

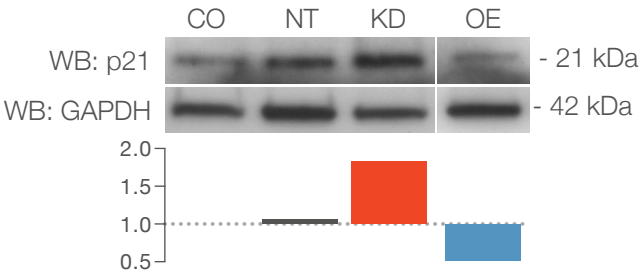

Figure 21: ANKHD1 regulates p21 expression levels in GBM 13. GBM 13 cells were either left untreated, or electroporated with pCAG-YFP together with non-targeting siRNA (NT), pCAG-YFP together with siRNA targeting ANKHD1 (KD), or pCAG-YFP-ANKHD1 (OE). 72h later cells were harvested and lysed, followed by Western blotting for GAPDH (loading control, upper lane), and p21 (lower lane). Changes of p21 expression levels in lanes 2 - 4 relative to untreated cells (lane 1) are shown below each lane.

cell lysate preparation and Western blotting for phosphorylated and total Akt protein (pAkt and tAkt, respectively), as well as phosphorylated and total Erk protein (pErk and tErk, resp.). Contrary to previous reports, Akt activation was not observed in GBM 13 or GBM 30 cells following stimulation with 10 ng/ml T4 (Figure 23 A and B, lanes 1-3) or 40 ng/ml T4 (Figure 23 C and D, lanes 1-3). Moreover, Erk phosphorylation and expression levels were seemingly not affected by T4 ligand treatment in GBM 13 or GBM 30 cells. Knockdown of ANKHD1 strongly decreased its protein levels in both GBM 13 and 30 cells (Figure 23 A-D, lanes 3-6), but did not influence Akt and Erk phosphorylation and expression (compare lane 4 to lanes 1-3 in each panel). Furthermore, knockdown of ANKHD1 did not influence phosphorylation and expression levels of Akt or Erk in CD95 activated samples (Figure 23 A-D, lanes 5 and 6). Together, this data suggest that ANKHD1 does not influence Akt and Erk phosphorylation or expression in GICs.

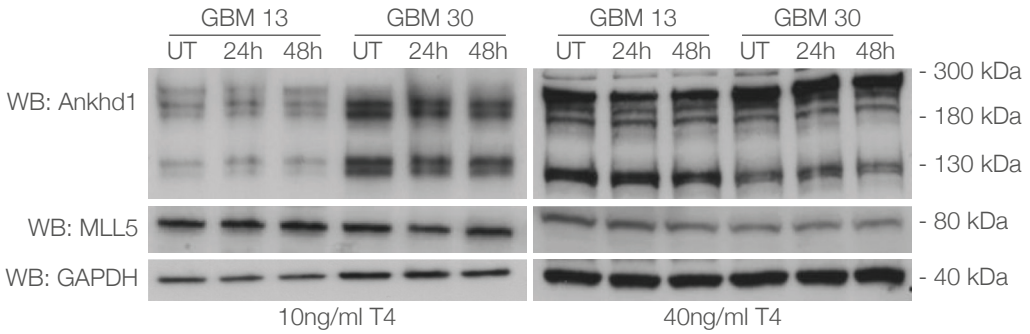

Figure 22: ANKHD1 expression levels are not influenced by CD95 activation in GICs. GBM 13 and 30 cells were left untreated (UT), or were treated with 10 ng/ml (left panel) or 40 ng/ml (right panel) T4 for 24 or 48 hours before preparation of cell lysates and Western blotting. Membranes were then tested with the indicated antibodies.

Together, the presented data suggest that ANKHD1 is highly expressed in most of the tested GIC cultures and that high ANKHD1 levels might contribute to the cells' proliferation properties. Moreover, this function might, at least partially, be dependent on influencing p21 protein levels, while Akt and Erk signaling pathways seem to be unaffected by ANKHD1.

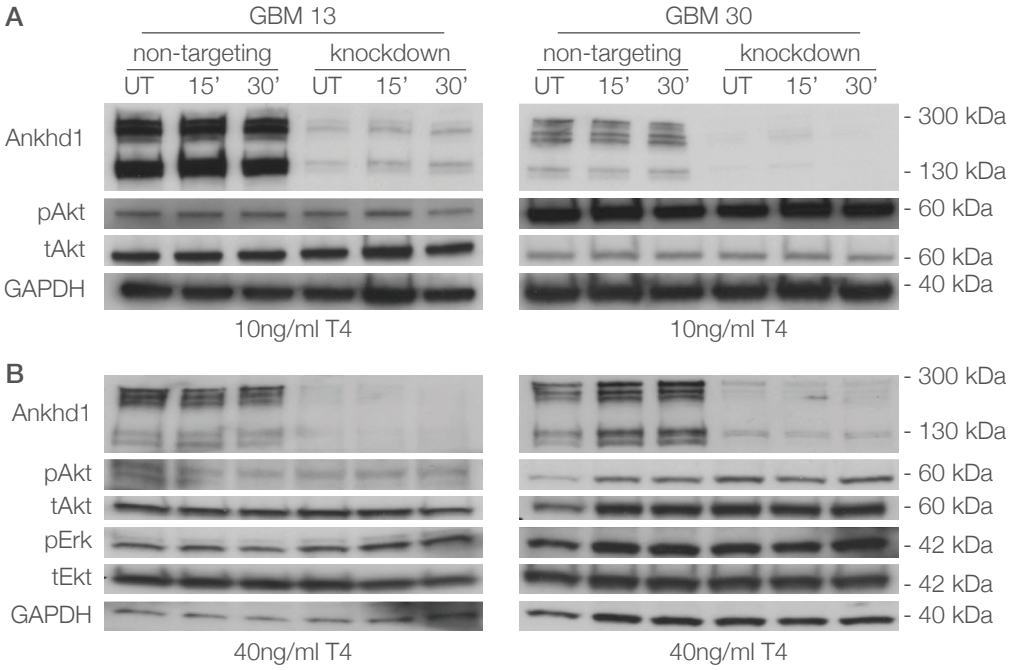

Figure 23: Akt and Erk activity is not influenced by ANKHD1 knockdown. A | GBM 13 (A) or GBM 30 (B) cells were electroporated with pCAG-YFP together with non-targeting siRNA (CO), or pCAG-YFP together with siRNA targeting ANKHD1 (KD). 72h later cells were treated with 10 ng/ml T4 for 15 or 30 minutes, or left untreated (UT), followed by cell lysis and Western blotting. Membranes were tested with the indicated antibodies. B | Same as in A, but with 40 ng/ml T4 treatment and including testing for tErk and pErk as indicated.

4 Discussion

The brain is a very complex organ that evolved to carry out all the higher cognitive functions – such as reasoning, planning, emotions, and problem solving – which are so central to what we are. The main structure involved in these functions is the neocortex. It is part of the dorsal forebrain which underwent a tremendous expansion in humans. It is a seemingly impossible task to try to comprehend its full inner workings—from the generation of billions of brain cells to the hundreds of billions of connections that are formed between them. And yet, step by step we make great progress in understanding this extraordinary organ. We have come a long way since the discovery of the neuron as such by Jan Evangelista Purkinje in the 1830s and the fundamental work on brain anatomy by Santiago Ramón y Cajal. However, despite the many thousands of researchers committed to study the brain, we have yet to solve the puzzle of fully comprehending the brain.

Many of the known diseases of the brain are directly connected to malfunctions of neural progenitor cells (NPCs). For instance, neurodevelopmental disorders are often caused by de-regulated proliferation and differentiation behavior of NPCs during brain development, and the cells of origin of many cancers in the adult brain are thought to be NPCs. Understanding how these cells are regulated in the healthy organism is crucial for the development of treatment strategies for the diseased brain.

The work presented in this thesis aims to add to our understanding of how normal and neoplastic NPCs are regulated. We investigated the role of ANKHD1 in NPCs, hitherto without a described function in these cells. We have shown that ANKHD1 is expressed in NPCs of the developing and adult brain. Furthermore, we demonstrated by loss and gain of function approaches that ANKHD1 is important for regulation of embryonic and adult NPCs. Knockdown of ANKHD1 caused increased proliferation and inhibited differentiation in NPCs. ANKHD1 does not seem to bind to SHP2 to control proliferation and differentiation in eNPCs but might interact with the Hippo pathway components instead.

Interestingly, in cultured glioma initiating cells (GICs), overexpression of ANKHD1 promoted proliferation, while knockdown showed no pronounced effect. Akt and Erk signaling seemed to be unaffected by ANKHD1 knockdown in GICs, while p21 protein expression was slightly increased.

Together, our data suggest that ANKHD1 is expressed in embryonic and adult NPCs and is an important regulator of their proliferation and differentiation behavior.

4.1 The ANKHD1 gene across species

ANKHD1 is a recently discovered and still poorly studied protein. It has first been described in Drosophila melanogaster [84] and shortly later in mammals, including humans [65]. Comparison of the human ANKHD1 gene sequence with genomes from other organisms[8] revealed that genes homolog to ANKHD1 can be found in many different species, belonging to various animal classes. Genes with more than 80% sequence identity to ANKHD1 include species in the classes of *Insecta*, *Aves*, *Reptilia*, *Bivalvia*, *Anthozoa*, and *Amphibia*. The gene duplication event that led to the emergence of the ANKHD1 paralog ANKRD17 occurred in vertebrates. The relation between the two proteins is poorly studied and it is unclear if they can compensate for each other in some organisms or tissues. In mice, knockout of ANKRD17 has severe effects [38] suggesting that gene compensation of these two proteins is unlikely in mammals. Furthermore, we have compared sequences stretches of particular interest within the ANKHD1 gene – such as the putative nuclear localization signal – and found them to be highly conserved among all mammals tested and even across species of other animal classes. Hence, ANKHD1 is an evolutionary old protein conserved across many species, suggesting that it might have a pivotal function in most organisms of the animal kingdom.

4.2 ANKHD1 expression in the mammalian brain and other tissues

Expression of ANKHD1 has been experimentally proven in only a few tissues so far. In Drosophila, the ANKHD1 homolog MASK was found to be expressed ubiquitously during development [84]. Similarly, ANKHD1 seems to be expressed ubiquitously in mammals. Expression of ANKHD1 mRNA in mammalian tissues was first reported by Poulin et al. [65] in 2003. The authors described ANKHD1 mRNA levels determined by qRT-PCR in the brain, eye, spleen, lung, liver, smooth muscle, kidney, testis, prostate, and uterus of mice. They also tested expression of the ANKHD1 4EBP3 fusion protein (mMASK-BP3) in the same tissues. Expression of ANKHD1

[8] using databases and tools provided by Ensembl [24] and UniGene [93]

was highest in brain and eyes. MASK-BP3 expression was barely detectable in the brain, and a bit lower than ANKHD1 in the eye, while it was strongly expressed in tissues where ANKHD1 levels were lower, such as in the kidney and testis. Thus, expression of these two transcripts is not mutually exclusive but it seems that one or the other are preferably expressed in a given tissue. The dominant transcript in the mouse brain seems to be ANKHD1. The authors did not discriminate between different brain structures in their qRT-PCR analyses. We found very robust expression levels of both ANKHD1 mRNA and protein in short term cultured aNPCs, as well as ANKHD1 mRNA in the hippocampus of adult mice throughout life. Together, these data suggest that ANKHD1 is robustly expressed in the adult mouse brain. Due to the lack of suitable antibodies or reporter mice, a more detailed study of ANKHD1 expression in the brain is not feasible. It would be of interest to reveal if ANKHD1 is expressed in all cells of the brain, and if expression levels are similar between cells. A role of ANKHD1 seems to be in proliferation control, and if it is expressed in post mitotic cells as well it would be intriguing to study if in these cells ANKHD1 is involved in maintaining a non-proliferative state or has different functions.

Poulin et al. [65] also studied ANKHD1 expression by Northern blotting in human tissues, including heart, brain, placenta, skeletal muscle, and pancreas. They found no, or only very little expression of ANKHD1 in the brain. However, it is not clear which part of the brain the sample was taken from, and in which condition the specimen was. Contrary to this finding, immunohistological images from the Human Protein Atlas database [91] do indicate ANKHD1 expression in the adult human brain. Images of histological sections of the cortex show a strong signal in neuronal cells. Expression is also observable in other brain areas and tissues. There are two limitations to this dataset: (i) these data were not validated, and (ii) the antibody used can also detect the MASK-BP3 fusion protein. Since Poulin et al. [65] did not detect MASK-BP3 in their human brain sample either, it is not clear to which extend ANKHD1 is expressed in the human brain. More detailed qRT-PCR expression studies and validation of the human-protein-atlas data with the same antibody, but if possible also with one that specifically recognizes ANKHD1 and not MASK-BP3, are needed to clarify expression patterns in the human brain.

Expression of ANKHD1 in the developing mammalian brain has not been demonstrated so far. As mentioned above, MASK is expressed ubiquitously during Droso-

phila development, including the brain. Databases such as the Allen Brain Atlas of the developing mouse brain [3] or the EMAP project [89] do not yet include data on ANKHD1. We have shown for the first time that ANKHD1 is expressed in the developing mammalian brain. We have used qRT-PCR, *in situ* hybridization, and Western blotting to investigate ANKHD1 expression in the developing forebrain. For qRT-PCR detection of ANKHD1 we dissected the complete dorsal telencephalon (without skin and meninges layers) from various embryonic stages, from which we then isolated mRNA. This means that all cell types present in the tissue at the time were included in the analysis. For early stages (E12.5) the neocortical tissue consist mainly of radial glia (RG), and some early born neurons. Very few other types of progenitors are present. During mid-embryonic stages the proportion of RG is reduced and many basal progenitors (BPs) and neurons are present. With ongoing development more differentiated glia cells are added. Therefore we could not distinguish the cell type(s) that express ANKHD1 in the developing cortex. Because we detected ANKHD1 expression from the early stages on (i.e. E12.5), it is likely that it is expressed in eNPCs. We next performed *in situ* hybridization experiments to analyze ANKHD1 in more detail. We found broad expression of ANKHD1 at E13.5, including in the ventricular and subventricular zones. Together, these data strongly suggest that ANKHD1 is expressed in eNPCs. Finally, we could show that the ANKHD1 protein is indeed translated during neocortical development by Western blotting. Due to lack of suitable antibodies, ANKHD1 expression could not have been investigated in more detail on mouse brain sections. It would be of interest to see if ANKHD1 in the brain is truly ubiquitous and of similar intensity in different cell types.

4.3 The function of ANKHD1 during mammalian brain development

Thus far, only studies performed in Drosophila have shown a function for ANKHD1 in progenitor cells during development, and no studies regarding brain development have been conducted. Smith et al. [84] showed that MASK is essential for early embryogenesis, since most MASK loss-of-function mutants are embryonic lethal, and that it is later required for normal proliferation and differentiation of photoreceptor progenitor cells. Sansores-Garcia et al. [74] and Sidor et al. [81] observed a significant reduction of eye and wing size in mask null or knockdown mutants.

We have shown that ANKHD1 is expressed in embryonic and adult NPCs of mice. To elucidate its function in these cells we performed several *in vitro* and *in vivo* loss- and gain-of-function experiments in embryonic and adult NPCs.

ANKHD1 knockout mice would be of great value to study the function of ANKHD1 during development but are unfortunately not available yet. Transient manipulation in dissociated primary cultures of eNPCs can provide good insights into possible functions but does not resemble the *in vivo* situation and hence might not be sufficient to draw solid conclusions. In order to study ANKHD1 function in the developing mammalian brain *in vivo*, we used the *in utero* electroporation technique. With this technique it is possible to specifically manipulate RG cells in the developing brain [88] and to follow their daughter cells. The manipulation via *in utero* electroporation is spatially restricted to the injection site and the region were electrodes are applied. For instance, the dorsal pallium can be targeted without affecting the ventral pallium, and thus tangentially migrating cells invading the neocortex (see 1.3.1) will not influence and be mixed up with locally produced, radially migrating daughter cells of RG. Importantly, not all cells in the electroporated area will be transfected and thus the study of cell extrinsic effects might be limited. Compared to knockout mice, *in utero* electroporation has several advantages (e.g. it allows to overcome compensatory mechanisms of gene redundancy, different brain regions can be targeted, combinatorial knockdown of two or more genes may be easily performed, etc.) but also a few disadvantages (e.g. the special equipment required, and difficulties for studying early development). Reiner et al. [67] compared observations in knockout mice and knockdown via *in utero* electroporation with the doublecortin superfamily as example. The authors described how using *in utero* electroporation might overcome compensatory mechanisms of gene redundancy in the doublecortin superfamily and thus better information could have been obtained from single gene knockdown experiments compared to single gene knockout mice, which did not show obvious phenotypes in this case. The *in utero* electroporation method is often utilized in studies of mammalian brain development and has proven to be reliable, despite of some cases in which conflicting results were produced compared to knockout mice [67].

First, we wanted to investigate the effects of ANKHD1 knockdown on developing cells in the neocortex. We used a pool of four siRNAs directed against mouse

ANKHD1 to knock it down in RG of E13.5 or E14.5 embryos. We then analyzed transfected cells 48 hours later with various methods. The 48 hour time window between *in utero* electroporation and analysis is long enough to allow knockdown of the protein and generation of several daughter cells, but still short enough to neglect dilution and degradation effects of electoporated plasmids or siRNA. We first analyzed transfected cells for EdU incorporation by flow cytometry to measure cell proliferation. Interestingly, we observed that proliferation of NPCs was increased in cells with knock down of ANKHD1. We then analyzed ANKHD1 knockdown cells on cryosections with markers for RG, BPs, and neurons. The proportion of both, RG and BPs was increased, while the number of newly born neurons was decreased in ANKHD1 knockdown cells. These data suggest that knockdown of ANKHD1 promotes proliferation and inhibits differentiation to neurons. In Drosophila photoreceptor progenitors, loss of MASK similarly leads to a lower number of differentiated cells. However, the authors did not observe more proliferation, they rather suggested that apoptosis is increased. Sansores-Garcia et al. [74] and Sidor et al. [81] demonstrated that loss of mask leads to smaller organs. This suggests that loss of ANKHD1 would rather promote differentiation than inhibiting it, generating insufficient numbers of differentiated cells. However, it is also possible that cells without ANKHD1 initially fail to differentiate and thus are kept in a proliferative state. Some of these cells might differentiate eventually, other which later fail to differentiate still, might die and thus lead to smaller organs in the end. We did not measure apoptosis here, however, total cell numbers between knockdown and control conditions did not seem to be different, suggesting that apoptosis does not play a big role, at least in early stages after ANKHD1 knockdown. In mice, ANKHD1 might play an active role in promoting proliferation and thus initially inhibiting differentiation. Control of proliferation and differentiation are tightly coupled and thus it is often not possible to distinguish if a protein is required only for one of these processes or both. Some differences in Drosophila MASK and mouse ANKHD1 might of course exist due to differences in the two proteins: While the ankyrin and KH domains are well conserved, other parts differ significantly. No functional domains have been annotated apart from the ankyrin and KH domains, but they still might be pivotal for the function of the protein. Moreover, MASK is 1500 amino acids longer than ANKHD1. How this additional residues contribute to the function of the protein is not known.

Co-labeling of electroplated cells with markers for RG, BPs, and neurons revealed that both RG and BP pools were expanded. We used expression of the transcription factor Tbr2 to distinguish RG from BP cells. Tbr2 was shown to be exclusively expressed in BPs [23], and hitherto remains the only reliable marker to distinguish BP from RG, beside some morphological characteristics. Interestingly, the number of apical and basal progenitors was increased, while the number of neurons was decreased after ANKHD1 knockdown. These data suggest that ANKHD1 has a function in RG cells. ANKHD1 could promote the asymmetric division of a RG cell that leads to the generation of a neuron and RG. After knockdown of ANKHD1, RG cells might self-renew and generate a BP rather than a neuron. However, the relative increase of RG cells might be explained by a blocked differentiation to both neurons and BPs, or a switch form asymmetric to symmetric division of RG cells.

The expansion of BP cells after knockdown of ANKHD1 was more prominent then the increase in RG cells. As mentioned above, this effect can be explained in part by RG cells that shift to producing a BP rather than a neuron. A second possibility is that BPs undergo additional rounds of divisions instead of differentiating to neurons. Cell cycle exit is tightly coordinated with the initiation of differentiation [64]. We have observed a strong decrease in the number of produced neurons when ANKHD1 was knocked down. A shift of asymmetric RG division from neurons to BPs is most likely not sufficient to explain the decrease in neurons. Especially because at this time of development, the main neurogenic phase, most RG division already produce BPs, and RG to neuron division are less frequent. A change in RG differentiation mode without affecting differentiation of BPs into neurons would not lead to the observed extend of neuron production decrease. Moreover, we measured a strong increase in EdU incorporation, again suggesting that BPs undergo additional rounds of divisions instead of differentiation. Together, our data suggest that it is less likely that expansion of BPs and decrease in neurons is solely due to RG cells division behavior and rather a significant contribution comes from enhanced BP proliferation and inhibited differentiation of BPs to neurons.

Apart from RG and BP cells, some other progenitor cell types have been described (see introduction). However, these cells are not very abundant, poorly studied and molecular markers for their identification are lacking. Hence, we did not further investigate if, e.g. basal RG or SNPs are more affected by ANKHD1 knockdown

than RGs or BPs.

The number of neurons was reduced in ANKHD1 knockdown cells 48 hours post *in utero* electroporation. Apart from a complete blockade of differentiation, it might be that it is only delayed. Indeed, when we compared P2 brains, we did not notice an apparent difference in the number of neurons reaching the cortical plate. However, knockdown of ANKHD1 was only transient and thus its effect might be diluted and less apparent at later stages. More detailed analyses of post natal brains and usage of long term knockdown / knockout strategies are necessary to unravel the complete effect of loss of ANKHD1 in differentiating neurons. We did not observe misexpression of markers in areas were they are usually not present, i.e. neuronal markers in the VZ or SVZ or an expansion of the SVZ (Tbr2 positive cells). The additional BPs we observed after KD of ANKHD1 were all accumulating in their appropriate location (the SVZ). This suggests that migration of proliferating and differentiating cells is not affected by ANKHD1.

Conversly, when we overexpressed human ANKHD1 in eNPCs, more cells differentiated into neurons. As mentioned before, human and mouse ANKHD1 are very similar and probably can substitute each other. After we found that human ANKHD1 is able to promote differentiation in mouse eNPCs, we hypothesized that overexpression of ANKHD1 might rescue the knockdown phenotype we observed. Indeed, simultaneous knockdown of mouse ANKHD1 and overexpression of human ANKHD1 reverted proliferation and differentiation rates close to control levels. A partial rescue is not surprising, especially because overexpression of ANKHD1 is quite inefficient due to its size. Together, these data suggest that knockdown of ANKHD1 leads to an expansion in the RG and BP pool and thereby inhibits differentiation into neurons.

4.4 The role of ANKHD1 in adult NPCs

We have found that ANKHD1 is expressed in isolated adult NPCs. Expression patterns through the adult brain have not been examined in more detail due to lack of suitable antibodies. We are currently generating a reporter mouse that will allow detailed analysis of ANKHD1 expression patterns.

To investigate if ANKHD1 might play a similar role in aNPCs as in eNPCs we performed *in vitro* proliferation and differentiation assays. We used aNPCs isolated from the SVZ of adult mice which were then cultured in serum free media as neuroshperes. Cells isolated and cultured this way were shown to retain aNPC characteristics (e.g. differentiation to neurons, astrocytes, and oligodendrocytes) and can be transplanted into the adult mouse brain, where they engraft, survive and produce differentiated cells [29, 68].

Knockdown of ANKHD1 in aNPCs similarly led to an increase in EdU incorporation as in eNPCs. Moreover, knockdown of ANKHD1 in an aNPC differentiation assay caused fewer neurons to form. Conversely, overexpression of ANKHD1 resulted in more differentiated neurons. These data suggest that ANKHD1 might have conserved functions in aNPCs. However, *in vivo* experiments will be needed to fully understand the role of ANKHD1 in aNPCs. For instance, virus mediated knockdown of ANKHD1 in aNPCs of the SVZ could be utilized to verify proliferation and differentiation phenotypes observed *in vitro*. Furthermore, conditional knockout (cKO) mice for ANKHD1 will allow detailed analysis of phenotypes associated with loss of ANKHD1 in aNPCs.

Conserved functions of genes in embryonic brain development and adult NPCs are not surprising and have been studied extensively. For instance, the Notch signaling pathway was shown to be crucial for "stem cell" maintenance, similar to the role in RG cells during embryonic development. However, due to the very different environment that aNPCs face, also additional and / or alternative functions for proteins known from development have been described. For instance, Wnt signaling Examples? at least refs. Future work *in vivo* will shed more light into the functions of ANKHD1 in the adult brain.

4.5 Involvement of ANKHD1 in GBM

GBM presumably originates form progenitor cells in the brain. However, exactly which kind of progenitor cell might be the cell of origin is currently under debate. Apparently these progenitors might be oligodendrocyte progenitor cells (OPCs) rather than aNPCs. Of note, OPCs develop from embryonic or adult NPCs (see introduction). It is, however, important to distinguish the cells that acquire and propagate

relevant oncogenic hits and those cells that are in the right environment and state that permits cancers to develop [87]. Independent of the debate over which cells exactly have the capabilities to form tumors, it has become clear in recent years that NPCs are involved in this process. Thus, signaling pathways and components relevant in NPCs are often found to be de-regulated in GBM and display interesting targets for treatment strategies.

ANKHD1 was suggested to be involved in cancer biology of solid and suspension tumors [92, 74]. It was shown that ANKHD1 is overexpressed in acute leukemias [92], can contribute to cell cycle progression in multiple myeloma cells [19], and that low levels of ANKHD1 are beneficial for relapse-free survival of breast cancer patients [74]. We have identified ANKHD1 as regulator of NPC proliferation and thus wanted to investigate if it is invovled in GBM biology as well, similar to other cancer types described above.

We obtained surgical specimens of GBM resections which were subsequently cultured in serum free conditions to enrich for ″cancer stem cells″ or ″glioma initiating cells″ (GICs). These cells were shown to form tumors when injected orthotopically into immune-comprimised mice, and – to a certain extend – resemble the primary tumor phenotype [82]. These phenotypic features include the differentiation to various cell types and the invasive nature of GBM. Moreover, serial transplantation of these cells suggest that it is indeed a population capable of tumor initiation and sustainable tumor growth.

We used these GICs to gain first insights into the role of ANKHD1 in GBM. First, we examined ANKHD1 expression in various GIC samples. Indeed, ANKHD1 was expressed in all GIC samples tested. Levels of expression varied significantly between samples, and tended to increase with passages of cultures (not quantified observations). All expression levels measured were higher compared to a human brain parenchyma lysate control. The precise origin (i.e. what part of the brain) of the sample is unknown and more control samples of defined origin are need to clarify expression of ANKHD1 in adult human brain. Especially a sample of human adult neural progenitor cells would be the ideal control sample to compare expression levels too. Nonetheless, elevated ANKHD1 levels in other cancers have been described. Traina et al. [92] reported that ANKHD1 is overexpressed in leukemias. The group determined levels of acute lymphoblastic leukemias and acute myeloid

leukemias by qRT-PCR and compared them to normal hematopoeitic cells. Most of the 38 leukemia samples had elevated mRNA levels, but it is not clear if the protein levels are similarly elevated. The same group later reported elevated ANKHD1 mRNA levels in multiple myeloma [19]. Notably, all of the establishes leukemia cell lines Traina et al. [92] and Dhyani et al. [19] tested showed strong ANKHD1 expression by Western blotting. We have also observed ANKHD1 to be highly expressed in established cancer cell lines, including K562 and HEK 293 cells. It is not clear if this high levels on cancer cell lines are related to the fact that the cells are of a cancerous origin, or rather have to do with culturing conditions and cell cell contact (see below). Finally, Sansores-Garcia et al. [74] compared expression data from breast cancer patients and found that ANKHD1 expression is heterogenous in these samples, and more importantly that low ANKHD1 levels correlated with better relapse free survival.

Functional roles of ANKHD1 in tumors are poorly studied. Dhyani et al. [19] have shown that knockdown of ANKHD1 in multiple myeloma cells inhibited their proliferation and G1 to S phase transition of the cell cycle. In NPCs, we found that knockdown of ANKHD1 rather leads to higher proliferation rates and that overexpression favors differentiation of cells. Therefore it was of interest to test the influence of ANKHD1 on proliferation of GBM cells. Surprisingly, proliferation was increased significantly when we overexpressed ANKHD1 in GICs. We did not observe significant effects on proliferation after ANKHD1 knockdown in the same samples. While these results are consistent with published findings, our observations in embryonic and adult NPCs suggest an opposing function for ANKHD1. Though this finding is quite puzzling, opposing roles for a molecule in normal and neoplastic cells have been reported before [101]. Interestingly, we did not measure less proliferation when ANKHD1 was knocked down in GICs. Possibly the present culture conditions (including growth factors EGF and bFGF) are sufficient to sustain growth with lower ANKHD1 levels. The two GIC samples that we used for knockdown and overexpression experiments displayed robust expression of ANKHD1 and knockdown with siRNA was very efficient in both of them. Despite the high expression of ANKHD1 in these two GIC samples, overexpression further increased mRNA levels five to ten fold. Apparently, further increase of ANKHD1 expression still could enhance proliferation.

Together, our findings support that ANKHD1 might be highly expressed in many GBM cells and promote their proliferation, similar to its function in leukemia cells. Further work, especially *in vivo*, will be needed to elucidate the function of ANKHD1 in GBM.

4.6 Controversy in functions of ANKHD1 in NPCs and GICs

As mentioned above, we observed opposing effects of ANKHD1 in NPCs and GICs. While in NPCs ANKHD1 seems to inhibit proliferation and promote differentiation, we actually observed stronger proliferation of GICs in which ANKHD1 was overexpressed. How this varying outcomes are established is not clear. However, similar cases have been reported for other proteins before, or are evident from studying the literature [49, 79, 101].

For instance, blockage of the transmembrane receptor integrinα6 was shown to have different outcomes in aNPCs and GICs. Disruption of integrinα6 function *in vivo* caused SVZ aNPCs to move away from blood vessels and stimulated their proliferation [79]. On the other hand, blocking the laminin–integrinα6 interaction in GICs reduced proliferation and tumorsphere formation capacity, and increased cell death [49]. These different outcomes could be due to altered requirements for niche interactions of aNPCs and GICs. The precise mechanism underlying this behavior remains elusive.

Another examples for such paradox behavior is found in the E2F transcription factors. E2F–1 to 5 can regulate human telomerase reverse transcriptase (TERT) gene expression by binding to its promoter. TERT is the catalytic subunit of telomerase, which is active in cells with high proliferative potential, such as stem cells. Won et al. [101] have shown that all five isoforms of E2F activate hTERT transcription in normal human somatic cells. In tumor cells, however, E2F–1 to 3 (but not 4 and 5) repressed TERT expression. Here again, the precise molecular mechanisms causing this opposing behavior are not known.

Thus, it is plausible to assume that ANKHD1 indeed exhibits opposing roles in NPCs and GICs, similar to the above mentioned examples. It is currently unknown if protein binding via the ankyrin repeats or RNA binding via the KH domain are differentially required for ANKHD1's opposing functions. It will be of high interest

to elucidate the precise pathways and molecules involved in ANKHD1 function in both NPCs and GICs.

4.7 Signaling mechanism of ANKHD1

Published data as well as our own work suggests that ANKHD1 functions in proliferation control of cells. How this function is executed in the cell is largely unknown. Work in Drosophila [84] and leukemia cells [92] revealed that ANKHD1 can interact with the protein tyrosine phosphatase SHP2 genetically and physically, respectively. SHP2 is known to be crucial for proliferation and differentiation of embryonic NPCs. Not only does it influence NPC proliferation through Akt and Bmi pathways, it is also important for the timed switch from neurogenesis to gliogenesis through Erk and Jak/Stat pathways. Thus, it was very intriguing to hypothesize that ANKHD1 might interact with SHP2 in murine NPCs to control proliferation and differentiation. To test this hypothesis, we tried to co-immunoprecipitate SHP2 with ANKHD1 from lysates of E13.5 NPCs. Both proteins were readily detectable in the lysate and could be immunoprecipitated with their respective antibodies. Unfortunately, we could not co-immunoprecipitate (co-IP) the two proteins in NPC lysates. Either the co-IP in NPCs is technically not feasible with endogenous proteins, or they simply do not interact in these cells. Notably, we also failed to repeat the co-IP published in K562 cells. Co-IP with one of the proteins overexpressed and tagged might provide further insight, but will not prove the interaction of endogenous proteins.

Recently, Sansores-Garcia et al. [74] and Sidor et al. [81] have shown that ANKHD1 can interact with the Hippo pathway effector protein YAP in Drosophila and HEK293 cells. The Hippo pathway is important for cell growth and proliferation, and is often deregulated in cancer. Less is known about its role in NPCs, though some publications reported expression of the downstream effectors YAP/TAZ in chicken and murine NPCs and their function in proliferation control during neural development [11, 50]. We started to investigate if ANKHD1 interacts with Hippo pathway components during neocortical development. We could not find an interaction between YAP and ANKHD1 in eNPCs. Currently, the interaction with TAZ is being probed. Sidor et al. [81] suggested that ANKHD1 might translocate to the nucleus together with YAP. Before this study was published, we have independently found a possible

nuclear localization signal (NLS) located behind the second ankyrin repeat domain. Sidor et al. [81] seem to locate the NLS at a similar position, though they do not further comment on the exact sequence or validation of it. The predominant localization of ANKHD1 in mouse NPCs seems to be in the cytosol, although we could observe small amounts of it in the nucleus by sub-cellular fractionation and subsequent Western blotting, as well as imaging of overexpressed YFP-ANKHD1 in eNPCs *in vivo*. Even if only small amounts of ANKHD1 should shuttle to the nucleus, they still might be functional relevant. Indeed, Sidor et al. [81] were able to identify ANKHD1 in a DNA pulldown experiment with a sequence of the YAP target gene *diap1*. However, Sansores-Garcia et al. [74], who all investigated the ANKHD1 - YAP interaction, did not observe a YAP dependent recruitment of ANKHD1 to the nucleus or its presence in complexes binding to DNA. Thus the significance and function of ANKHD1 in the nucleus remains elusive and has to further investigated in the future.

Dhyani et al. [19] suggested that ANKHD1 might control cell cycle progression by regulating expression levels of the cyclin dependent kinase inhibitor p21. It inhibits the activity of cyclin dependent kinase (CDK) 1, -CDK2, and CDK4/6 complexes thus regulating cell cycle progression at G1 and S phase. P21 mediates growth arrest and cell senescence. We observed that knockdown of ANKHD1 increased levels of p21 protein in GIC cultures, while overexpression slightly decreased its levels. This effect is similar to that reported in multiple myeloma cells by Dhyani et al. [19]. However, the measured change is also quite small and it is unclear if it is sufficient to be solely responsible for the observed effects on cell proliferation.

Important signaling components of survival and proliferation in GBM include Akt and Erk. It was shown previously that external signals, e.g. via the CD95 receptor, can stimulate GBM proliferation by increasing phospho-Akt and / or phospho-Erk levels [47]. We tested if knockdown of ANKHD1 influenced Akt or Erk levels or phosphorylation in addition to modulating p21 levels in GICs. However, we failed to observe changes in Akt or Erk total or phosphorylation levels following knockdown of ANKHD1, independent of previous activation of the CD95 pathway. As mentioned above, knockdown of ANKHD1 in these cells did not have a significant influence on proliferation, which might at least in part explain why Akt and Erk pathways are unaffected.

Interacting proteins probably bind to ANKHD1 via its ankyrin repeats. Additionally, ANKHD1 also contains a type I KH domain that can bind single stranded DNA or RNA (see 1.5). Indeed, experimental evidence suggests that ANKHD1 is a RNA binding protein: Castello et al. [12] reported ANKHD1 as a mRNA binding protein identified in a mRNA interactome screen ([13]). Hitherto, it is unknown which mRNAs and possible other RNA species are bound by ANKHD1, or if its function in NPCs is based on its RNA binding ability. We have cloned a mutated form of ANKHD1 that lacks the KH domain (ANKHD1-ΔKH). Unlike *in utero* overexpression of full length ANKHD1, ANKHD1-ΔKH seemingly failed to promote differentiation of developing neocortical neurons. More detailed work is needed to elucidate the function of the KH domain in ANKHD1 during NPC proliferation and differentiation. It will be crucial to identify the RNAs bound to ANKHD1 via cross-linking immunoprecipitation (CLIP) and subsequent sequencing of bound RNA (CLIP-Seq). These experiments are extremely challenging and will first have to be performed with cell lines were plenty of cell material can be generated for use in CLIP experiments.

Signaling cascades and transcription factors are well studied in neural development, but only few roles for RNAs in this process have been described so far. For instance, overexpression of microRNA-92b causes a reduction in Tbr2 positive BPs and proliferation [63], and microRNA-7a regulates Pax6 to control spatial origin of forebrain dopaminergic neurons [17]. If ANKHD1 is involved in microRNA biology or only functions by interacting with mRNA remains elusive.

4.8 Conclusive remarks

ANKHD1 is a poorly studied protein in mammals and other organisms. The scientific evidence so far, including our work, points to important functions during organ development as well as tumor biology. However, much work is needed to understand the role of ANKHD1 in various tissues and cancers.

ANKHD1 seems to be expressed in most, if not all tissues and most cell types within tissues. These cell types include proliferating as well as post mitotic cells. Functions for ANKHD1 have been described only in proliferating cells so far. While it becomes more and more evident that ANKHD1 is important for proliferation and differentiation control, the precise functions remain largely elusive and might be

cell type specific and context dependent. For instance, knockdown of ANKHD1 can have different effects on normal and neoplastic cells.

The expression of ANKHD1 in differentiated, post mitotic cells raises the question about its function in these cells. One explanation is that ANKHD1 is required for cell cycle exit and maintenance of a non-proliferative state. Our own data presented in this thesis suggest that ANKHD1 might be upregulated during the course of differentiation from progenitors to neurons, and thus promote neurogenesis. Elevated levels of ANKHD1 in newly differentiated neurons might then help to establish their neuronal identity. Such a function, however, contradicts observations in cancer cells (including our own findings in GICs), where high ANKHD1 levels seem to be beneficial for tumor proliferation. It is of course not unlikely that ANKHD1 exerts completely different functions in post-mitotic cells. Indeed, other molecules, including the well studied Notch receptor, are expressed in both proliferating and differentiated cells and have different function in these two cell types. For instance, additional to its well described function in progenitor cells, Notch is also essentialls for synaptic plasticity in some hippocampal neurons [1]. No such diverging functions for ANKHD1 in post-mitotic cells have been published yet. However, a collaborating group has observed that overexpression of ANKHD1 in neurons in Drosophila brains causes a pronounced axonal outgrowth phenotype.[9] This suggests that ANKHD1 might be involved in axonal growth in development and / or regeneration and would represent a cell proliferation independent function for ANKHD1 in post-mitotic cells.

Another intriguing function, though mostly speculative at this point, involves a role of ANKHD1 in cell density sensing. This hypothesis stems from comparing expression patterns in suspension cells, tissues, and cell cultures (of suspension or monolayer grown cells). A search in the Human Protein Atlas database [91], revealed that 45 out of the 47 testes cell lines were classified as having a strong ANKHD1 expression, with the other two displaying a moderate[10] expression level. Moreover, the database contains expression data on various leukemia samples as well as peripheral blood monocyte cells, all of which are classified as stong ANKHD1-expressing. Experimental evidence for high ANKHD1 in these cell types is also present [19, 92].

[9] unpublished data, personal communication Bassem A. Hassan
[10] Four staining intensities are classified: negative, weak, moderate, and strong

In contrast, expression in solid tissues seems to be much more heterogenous. However, because most of these data come from automated procedures and no experimental work was done in most cases, these data need to be interpreted with caution and validation will be necessary to draw solid conclusions. Still, it is intriguing to speculate that ANKHD1 expression might be differentially regulated in suspension cells and solid tissues, and that it thus might have a function in a signaling cascade related to cell density detection / mechanical sensing of the cell environment. ANKHD1 might thus be involved in sensing organs size / tissue growth, similar to the function of the Hippo pathway.

In this study, we have provided evidence for expression of ANKHD1 in the developing mammalian brain as well as in adult NPCs. We showed that a primary function of ANKHD1 in NPCs is proliferation and differentiation control, consistent with functions described in other cell types. Moreover, de-regulation of ANKHD1 in neoplastic cells leads to increased proliferation. The signaling mechanisms are still largely unknown, but might involve Hippo pathway components, interaction with SHP2, and regulation of p21 expression levels. Future work with reporter and (conditional) knockout mice will help to elucidate the role and signaling mechanisms of this still very mysterious, yet seemingly very important protein.

References

[1] Alberi L, Liu S, Wang Y, Badie R, Smith-Hicks C, Wu J, Pierfelice TJ, Abazyan B, Mattson MP, Kuhl D, Pletnikov M, Worley PF, and Gaiano N. Activity-induced Notch signaling in neurons requires Arc/Arg3.1 and is essential for synaptic plasticity in hippocampal networks. *Neuron*, 69(3):437–444, 2011.

[2] Alcantara Llaguno SR, Chen J, and Parada LF. Signaling in malignant astrocytomas: role of neural stem cells and its therapeutic implications. *Clinical cancer research : an official journal of the American Association for Cancer Research*, 15(23):7124–7129, 2009.

[3] Allen Developing Mouse Brain Atlas. ©2012 Allen Institute for Brain Science. `http://developingmouse.brain-map.org`. 2012.

[4] Altman J and Das GD. Autoradiographic and histological evidence of postnatal hippocampal neurogenesis in rats. *The Journal of comparative neurology*, 124(3):319–335, 1965.

[5] Alvarez-Buylla A, García-Verdugo JM, Mateo AS, and Merchant-Larios H. Primary neural precursors and intermitotic nuclear migration in the ventricular zone of adult canaries. *The Journal of neuroscience : the official journal of the Society for Neuroscience*, 18(3):1020–1037, 1998.

[6] Azevedo FAC, Carvalho LRB, Grinberg LT, Farfel JM, Ferretti REL, Leite REP, Jacob Filho W, Lent R, and Herculano-Houzel S. Equal numbers of neuronal and nonneuronal cells make the human brain an isometrically scaled-up primate brain. *The Journal of comparative neurology*, 513(5):532–541, 2009.

[7] Bonaguidi MA, Song J, Ming GL, and Song H. A unifying hypothesis on mammalian neural stem cell properties in the adult hippocampus. *Current Opinion in Neurobiology*, 2012.

[8] Bonaguidi MA, Wheeler MA, Shapiro JS, Stadel RP, Sun GJ, Ming GL, and Song H. In vivo clonal analysis reveals self-renewing and multipotent adult neural stem cell characteristics. *Cell*, 145(7):1142–1155, 2011.

[9] Breeden L and Nasmyth K. Similarity between cell-cycle genes of budding yeast and fission yeast and the Notch gene of Drosophila. *Nature*, 329(6140):651–654, 1987.

[10] Campbell K and Götz M. Radial glia: multi-purpose cells for vertebrate brain development. *Trends in neurosciences*, 25(5):235–238, 2002.

[11] Cao X, Pfaff SL, and Gage FH. YAP regulates neural progenitor cell number via the TEA domain transcription factor. *Genes & development*, 22(23):3320–3334, 2008.

[12] Castello A, Fischer B, Eichelbaum K, Horos R, Beckmann BM, Strein C, Davey NE, Humphreys DT, Preiss T, Steinmetz LM, Krijgsveld J, and Hentze MW. Insights into RNA Biology from an Atlas of Mammalian mRNA-Binding Proteins. *Cell*, 149(6):1393–1406, 2012.

[13] Castello A, Horos R, Strein C, Fischer B, Eichelbaum K, Steinmetz LM, Krijgsveld J, and Hentze MW. System-wide identification of RNA-binding proteins by interactome capture. *Nature Protocols*, 8(3):491–500, 2013.

[14] Corbin JG, Gaiano N, Juliano SL, Poluch S, Stancik E, and Haydar TF. Regulation of neural progenitor cell development in the nervous system. *Journal of Neurochemistry*, 106(6):2272–2287, 2008.

[15] Corsini NS, Sancho-Martinez I, Laudenklos S, Glagow D, Kumar S, Letellier E, Koch P, Teodorczyk M, Kleber S, Klussmann S, Wiestler B, Brüstle O, Mueller W, Gieffers C, Hill O, Thiemann M, Seedorf M, Gretz N, Sprengel R, Celikel T, and Martin-Villalba A. The death receptor CD95 activates adult neural stem cells for working memory formation and brain repair. *Cell stem cell*, 5(2):178–190, 2009.

[16] Coskun V, Zhao J, and Sun YE. Neurons or glia? Can SHP2 know it all? *Science's STKE : signal transduction knowledge environment*, 2007(410):pe58, 2007.

[17] de Chevigny A, Coré N, Follert P, Gaudin M, Barbry P, Béclin C, and Cremer H. miR-7a regulation of Pax6 controls spatial origin of forebrain dopaminergic neurons. *Nature Neuroscience*, 15(8):1120–1126, 2012.

[18] Deng W, Aimone JB, and Gage FH. New neurons and new memories: how does adult hippocampal neurogenesis affect learning and memory? *Nature Reviews Neuroscience*, 11(5):339–350, 2010.

[19] Dhyani A, Duarte ASS, Machado-Neto JA, Favaro P, Ortega MM, and Olalla Saad ST. ANKHDI regulates cell cycle progression and proliferation in multiple myeloma cells. *FEBS Letters*, 2012.

[20] Dinkel H, Van Roey K, Michael S, Davey NE, Weatheritt RJ, Born D, Speck T, Krüger D, Grebnev G, Kuban M, Strumillo M, Uyar B, Budd A, Altenberg B, Seiler M, Chemes LB, Glavina J, Sánchez IE, Diella F, and Gibson TJ. The eukaryotic linear motif resource ELM: 10 years and counting. *Nucleic acids research*, 2013.

[21] Drachman D. Do we have brain to spare? *Neurology*, Jun 28;64(12):2004–5, 2005.

[22] Duarte AdSS, Traina F, Favaro PMB, Bassères DS, de Carvalho IC, Medina SdS, Costa FF, and Saad STO. Characterisation of a new splice variant of MASK-BP3(ARF) and MASK human genes, and their expression patterns during haematopoietic cell differentiation. *Gene*, 363:113–122, 2005.

[23] Englund C, Fink A, Lau C, Pham D, Daza RAM, Bulfone A, Kowalczyk T, and Hevner RF. Pax6, Tbr2, and Tbr1 are expressed sequentially by radial glia, intermediate progenitor cells, and postmitotic neurons in developing neocortex. *The Journal of neuroscience : the official journal of the Society for Neuroscience*, 25(1):247–251, 2005.

[24] Ensembl. `http://www.ensembl.org`. 2013.

[25] Eriksson PS, Perfilieva E, Björk-Eriksson T, Alborn AM, Nordborg C, Peterson DA, and Gage FH. Neurogenesis in the adult human hippocampus. *Nature Medicine*, 4(11):1313–1317, 1998.

[26] Faigle R and Song H. Signaling mechanisms regulating adult neural stem cells and neurogenesis. *Biochimica et biophysica acta*, 2012.

[27] Flybase. `http://flybase.org/static_pages/docs/nomenclature/nomenclature3.html`. 2013.

[28] Franco SJ, Gil-Sanz C, Martinez-Garay I, Espinosa A, Harkins-Perry SR, Ramos C, and Müller U. Fate-Restricted Neural Progenitors in the Mammalian Cerebral Cortex. *Science (New York, NY)*, 337(6095):746–749, 2012.

[29] Gage FH, Coates PW, Palmer TD, Kuhn HG, Fisher LJ, Suhonen JO, Peterson DA, Suhr ST, and Ray J. Survival and differentiation of adult neuronal progenitor cells transplanted to the adult brain. *Proceedings of the National Academy of Sciences of the United States of America*, 92(25):11879–11883, 1995.

[30] Galli R. Isolation and Characterization of Tumorigenic, Stem-like Neural Precursors from Human Glioblastoma. *Cancer research*, 64(19):7011–7021, 2004.

[31] Garcia-Verdugo JM, Ferrón S, Flames N, Collado L, Desfilis E, and Font E. The proliferative ventricular zone in adult vertebrates: a comparative study using reptiles, birds, and mammals. *Brain research bulletin*, 57(6):765–775, 2002.

[32] Gould E, Tanapat P, Hastings N, and Shors T. Neurogenesis in adulthood: a possible role in learning. *Trends in cognitive sciences*, 3(5):186–192, 1999.

[33] Greig LC, Woodworth MB, Galazo MJ, Padmanabhan H, and Macklis JD. Molecular logic of neocortical projection neuron specification, development and diversity. *Nature Reviews Neuroscience*, 14(11):755–769, 2013.

[34] Grishin NV. KH domain: one motif, two folds. *Nucleic acids research*, 29(3):638–643, 2001.

[35] Götz M and Sommer L. Cortical development: the art of generating cell diversity. *Development (Cambridge, England)*, 132(15):3327–3332, 2005.

[36] Hevner RF and Haydar TF. The (Not Necessarily) Convoluted Role of Basal Radial Glia in Cortical Neurogenesis. *Cerebral cortex (New York, NY : 1991)*, 22(2):465–468, 2012.

[37] Hodge RD, Kowalczyk TD, Wolf SA, Encinas JM, Rippey C, Enikolopov G, Kempermann G, and Hevner RF. Intermediate progenitors in adult hippocampal neurogenesis: Tbr2 expression and coordinate regulation of neuronal out-

put. *The Journal of neuroscience : the official journal of the Society for Neuroscience*, 28(14):3707–3717, 2008.

[38] Hou SC, Chan LW, Chou YC, Su CY, Chen X, Shih YL, Tsai PC, Shen CKJ, and Yan YT. Ankrd17, an ubiquitously expressed ankyrin factor, is essential for the vascular integrity during embryogenesis. *FEBS Letters*, 583(17):2765–2771, 2009.

[39] Huttner WB and Kosodo Y. Symmetric versus asymmetric cell division during neurogenesis in the developing vertebrate central nervous system. *Current protocols in cell biology / editorial board, Juan S Bonifacino [et al]*, 17(6):648–657, 2005.

[40] Ihrie RA and Alvarez-Buylla A. Lake-front property: a unique germinal niche by the lateral ventricles of the adult brain. *Neuron*, 70(4):674–686, 2011.

[41] Iwata T and Hevner RF. Fibroblast growth factor signaling in development of the cerebral cortex. *Development, growth & differentiation*, 51(3):299–323, 2009.

[42] Jacobson S and Marcus EM. Neuroanatomy for the Neuroscientist. Springer, 2011. ISBN 9781441996534.

[43] Kageyama R, Ohtsuka T, Hatakeyama J, and Ohsawa R. Roles of bHLH genes in neural stem cell differentiation. *Experimental cell research*, 306(2):343–348, 2005.

[44] Kageyama R, Ohtsuka T, and Kobayashi T. Roles of Hes genes in neural development. *Development, growth & differentiation*, 50 Suppl 1:S97–103, 2008.

[45] Ke Y, Zhang EE, Hagihara K, Wu D, Pang Y, Klein R, Curran T, Ranscht B, and Feng GS. Deletion of Shp2 in the brain leads to defective proliferation and differentiation in neural stem cells and early postnatal lethality. *Molecular and Cellular Biology*, 27(19):6706–6717, 2007.

[46] Kim CFB, Jackson EL, Woolfenden AE, Lawrence S, Babar I, Vogel S, Crowley D, Bronson RT, and Jacks T. Identification of bronchioalveolar stem cells in normal lung and lung cancer. *Cell*, 121(6):823–835, 2005.

[47] Kleber S, Sancho-Martinez I, Wiestler B, Beisel A, Gieffers C, Hill O, Thiemann M, Mueller W, Sykora J, Kuhn A, Schreglmann N, Letellier E, Zuliani C, Klussmann S, Teodorczyk M, Gröne HJ, Ganten TM, Sültmann H, Tüttenberg J, von Deimling A, Regnier-Vigouroux A, Herold-Mende C, and Martin-Villalba A. Yes and PI3K bind CD95 to signal invasion of glioblastoma. *Cancer cell*, 13(3):235–248, 2008.

[48] Kriegstein AR and Alvarez-Buylla A. The Glial Nature of Embryonic and Adult Neural Stem Cells. *Annual Review of Neuroscience*, 32:149–184, 2009.

[49] Lathia JD, Gallagher J, Heddleston JM, Wang J, Eyler CE, Macswords J, Wu Q, Vasanji A, McLendon RE, Hjelmeland AB, and Rich JN. Integrin alpha 6 regulates glioblastoma stem cells. *Cell stem cell*, 6(5):421–432, 2010.

[50] Lavado A, He Y, Paré J, Neale G, Olson EN, Giovannini M, and Cao X. Tumor suppressor Nf2 limits expansion of the neural progenitor pool by inhibiting Yap/Taz transcriptional coactivators. *devbiologistsorg*, 2013.

[51] Lewis HA, Musunuru K, Jensen KB, Edo C, Chen H, Darnell RB, and Burley SK. Sequence-specific RNA binding by a Nova KH domain: implications for paraneoplastic disease and the fragile X syndrome. *Cell*, 100(3):323–332, 2000.

[52] Li J, Mahajan A, and Tsai MD. Ankyrin repeat: a unique motif mediating protein-protein interactions. *Biochemistry*, 45(51):15168–15178, 2006.

[53] Liu C, Sage JC, Miller MR, Verhaak RGW, Hippenmeyer S, Vogel H, Foreman O, Bronson RT, Nishiyama A, Luo L, and Zong H. Mosaic analysis with double markers reveals tumor cell of origin in glioma. *Cell*, 146(2):209–221, 2011.

[54] Louvi A and Artavanis-Tsakonas S. Notch signalling in vertebrate neural development. *Nature Reviews Neuroscience*, 7(2):93–102, 2006.

[55] Martínez-Cerdeño V, Noctor SC, and Kriegstein AR. The role of intermediate progenitor cells in the evolutionary expansion of the cerebral cortex. *Cerebral cortex (New York, NY : 1991)*, 16 Suppl 1:i152–61, 2006.

[56] Marín O and Rubenstein JL. A long, remarkable journey: tangential migration in the telencephalon. *Nature Reviews Neuroscience*, 2(11):780–790, 2001.

[57] Methot L, Hermann R, Tang Y, Lo R, Al-Jehani H, Jhas S, Svoboda D, Slack RS, Barker PA, and Stifani S. Interaction and antagonistic roles of NF-κB and Hes6 in the regulation of cortical neurogenesis. *Molecular and Cellular Biology*, 33(14):2797–2808, 2013.

[58] MGI. `http://www.informatics.jax.org/mgihome/nomen/index.shtml`. 2013.

[59] Miles MC, Janket ML, Wheeler EDA, Chattopadhyay A, Majumder B, Dericco J, Schafer EA, and Ayyavoo V. Molecular and functional characterization of a novel splice variant of ANKHD1 that lacks the KH domain and its role in cell survival and apoptosis. *The FEBS journal*, 272(16):4091–4102, 2005.

[60] Ming GL and Song H. Adult neurogenesis in the Mammalian brain: significant answers and significant questions. *Neuron*, 70(4):687–702, 2011.

[61] Nakafuku M GA. Neurogenesis in the Damaged Mammalian Brain. Elsevier Ltd, 2011.

[62] Noctor SC, Martínez-Cerdeño V, Ivic L, and Kriegstein AR. Cortical neurons arise in symmetric and asymmetric division zones and migrate through specific phases. *Nature Neuroscience*, 7(2):136–144, 2004.

[63] Nowakowski TJ, Fotaki V, Pollock A, Sun T, Pratt T, and Price DJ. MicroRNA-92b regulates the development of intermediate cortical progenitors in embryonic mouse brain. *Proceedings of the National Academy of Sciences*, 110(17):7056–7061, 2013.

[64] Oshikawa M, Okada K, Nakajima K, and Ajioka I. Cortical excitatory neurons become protected from cell division during neurogenesis in an Rb family-dependent manner. *Development (Cambridge, England)*, 140(11):2310–2320, 2013.

[65] Poulin F, Brueschke A, and Sonenberg N. Gene fusion and overlapping reading frames in the mammalian genes for 4E-BP3 and MASK. *The Journal of biological chemistry*, 278(52):52290–52297, 2003.

[66] Reillo I, De Juan Romero C, García-Cabezas M , and Borrell V. A role for intermediate radial glia in the tangential expansion of the mammalian

cerebral cortex. *Cerebral cortex (New York, NY : 1991)*, 21(7):1674–1694, 2011.

[67] Reiner O, Gorelik A, and Greenman R. Use of RNA Interference by In Utero Electroporation to Study Cortical Development: The Example of the Doublecortin Superfamily. *Genes*, 3(4):759–778, 2012.

[68] Reynolds BA and Weiss S. Generation of neurons and astrocytes from isolated cells of the adult mammalian central nervous system. *Science (New York, NY)*, 255(5052):1707–1710, 1992.

[69] Rezai-Zadeh K, Gate D, and Town T. CNS infiltration of peripheral immune cells: D-Day for neurodegenerative disease? *Journal of neuroimmune pharmacology : the official journal of the Society on NeuroImmune Pharmacology*, 4(4):462–475, 2009.

[70] Rivers LE, Young KM, Rizzi M, Jamen F, Psachoulia K, Wade A, Kessaris N, and Richardson WD. PDGFRA/NG2 glia generate myelinating oligodendrocytes and piriform projection neurons in adult mice. *Nature Neuroscience*, 11(12):1392–1401, 2008.

[71] Rost B, Yachdav G, and Liu J. The PredictProtein server. *Nucleic acids research*, 32(Web Server issue):W321–6, 2004.

[72] Saito T. In vivo electroporation in the embryonic mouse central nervous system. *Nature Protocols*, 1(3):1552–1558, 2006.

[73] Sanai N, Alvarez-Buylla A, and Berger MS. Neural stem cells and the origin of gliomas. *The New England journal of medicine*, 353(8):811–822, 2005.

[74] Sansores-Garcia L, Atkins M, Moya IM, Shahmoradgoli M, Tao C, Mills GB, and Halder G. Mask Is Required for the Activity of the Hippo Pathway Effector Yki/YAP. *Current biology : CB*, 23(3):229–235, 2013.

[75] Sauvageot CM and Stiles CD. Molecular mechanisms controlling cortical gliogenesis. *Current Opinion in Neurobiology*, 12(3):244–249, 2002.

[76] Sedgwick SG and Smerdon SJ. The ankyrin repeat: a diversity of interactions on a common structural framework. *Trends in Biochemical Sciences*, 24(8):311–316, 1999.

[77] Sessa A, Mao Ca, Hadjantonakis AK, Klein WH, and Broccoli V. Tbr2 Directs Conversion of Radial Glia into Basal Precursors and Guides Neuronal Amplification by Indirect Neurogenesis in the Developing Neocortex. *Neuron*, 60(1):56–69, 2008.

[78] Shen Q, Wang Y, Dimos JT, Fasano CA, Phoenix TN, Lemischka IR, Ivanova NB, Stifani S, Morrisey EE, and Temple S. The timing of cortical neurogenesis is encoded within lineages of individual progenitor cells. *Nature Neuroscience*, 9(6):743–751, 2006.

[79] Shen Q, Wang Y, Kokovay E, Lin G, Chuang SM, Goderie SK, Roysam B, and Temple S. Adult SVZ stem cells lie in a vascular niche: a quantitative analysis of niche cell-cell interactions. *Cell stem cell*, 3(3):289–300, 2008.

[80] Shi Y, Chichung Lie D, Taupin P, Nakashima K, Ray J, Yu RT, Gage FH, and Evans RM. Expression and function of orphan nuclear receptor TLX in adult neural stem cells. *Nature*, 427(6969):78–83, 2004.

[81] Sidor CM, Brain R, and Thompson BJ. Mask Proteins Are Cofactors of Yorkie/YAP in the Hippo Pathway. *Current biology : CB*, 23(3):223–228, 2013.

[82] Singh SK, Hawkins C, Clarke ID, Squire JA, Bayani J, Hide T, Henkelman RM, Cusimano MD, and Dirks PB. Identification of human brain tumour initiating cells. *Nature cell biology*, 432(7015):396–401, 2004.

[83] Siomi H, Matunis MJ, Michael WM, and Dreyfuss G. The pre-mRNA binding K protein contains a novel evolutionarily conserved motif. *Nucleic acids research*, 21(5):1193–1198, 1993.

[84] Smith RK, Carroll PM, Allard JD, and Simon MA. MASK, a large ankyrin repeat and KH domain-containing protein involved in Drosophila receptor tyrosine kinase signaling. *Development (Cambridge, England)*, 129(1):71–82, 2002.

[85] Stiles J. The Fundamentals of Brain Development. Integrating Nature and Nurture. Harvard University Press, 2008. ISBN 9780674026742.

[86] Stiles J and Jernigan TL. The Basics of Brain Development. *Neuropsychology Review*, 20(4):327–348, 2010.

[87] Sukhdeo K, Hambardzumyan D, and Rich JN. Glioma development: where did it all go wrong? *Cell*, 146(2):187–188, 2011.

[88] Tabata H and Nakajima K. Efficient in utero gene transfer system to the developing mouse brain using electroporation: visualization of neuronal migration in the developing cortex. *Neuroscience*, 103(4):865–872, 2001.

[89] The e-Mouse Atlas Project. `http://www.emouseatlas.org/emap/home.html`. 2013.

[90] The HUGO Gene Nomenclature Committee. `http://www.genenames.org`. 2013.

[91] The Human Protein Atlas. `http://www.proteinatlas.org`. 2013.

[92] Traina F, Favaro PMB, Medina SdS, Duarte AdSS, Winnischofer SMB, Costa FF, and Saad STO. ANKHD1, ankyrin repeat and KH domain containing 1, is overexpressed in acute leukemias and is associated with SHP2 in K562 cells. *Biochimica et biophysica acta*, 1762(9):828–834, 2006.

[93] UniGene N. `http://www.ncbi.nlm.nih.gov/unigene/`. 2013.

[94] UniProt Consortium. Update on activities at the Universal Protein Resource (UniProt) in 2013. *Nucleic acids research*, 41(Database issue):D43–7, 2013.

[95] Valverde R, Edwards L, and Regan L. Structure and function of KH domains. *The FEBS journal*, 275(11):2712–2726, 2008.

[96] van Praag H, Kempermann G, and Gage FH. Running increases cell proliferation and neurogenesis in the adult mouse dentate gyrus. *Nature Neuroscience*, 2(3):266–270, 1999.

[97] Vescovi AL, Reynolds BA, Fraser DD, and Weiss S. bFGF regulates the proliferative fate of unipotent (neuronal) and bipotent (neuronal/astroglial) EGF-generated CNS progenitor cells. *Neuron*, 11(5):951–966, 1993.

[98] Visvader JE. Cells of origin in cancer. *Nature*, 469(7330):314–322, 2011.

[99] Watt AJ, Jones EA, Ure JM, Peddie D, Wilson DI, and Forrester LM. A gene trap integration provides an early in situ marker for hepatic specification of the foregut endoderm. *Mechanisms of development*, 100(2):205–215, 2001.

[100] Wilkinson G, Dennis D, and Schuurmans C. NEUROSCIENCE FOREFRONT REVIEWPRONEURAL GENES IN NEOCORTICAL DEVELOPMENT. *Neuroscience*, 253(C):256–273, 2013.

[101] Won J, YIM J, and Kim TK. Opposing regulatory roles of E2F in human telomerase reverse transcriptase (hTERT) gene expression in human tumor and normal somatic cells. *The FASEB journal : official publication of the Federation of American Societies for Experimental Biology*, 16(14):1943–1945, 2002.